PREPARATION, CHARACTERIZATION AND UTILIZATION OF
PALLADIUM DOPED PAN-BASED ACTIVATED CARBON FIBERS

by

SERKAN BAŞ

Submitted to the Graduate School of
Engineering and Natural Sciences in partial fulfillment of
the requirements for the degree of
Master of Science

Sabancı University
2005

PREPARATION, CHARACTERIZATION AND UTILIZATION OF
PALLADIUM DOPED PAN-BASED ACTIVATED CARBON FIBERS

by

Serkan Baş

APPROVED BY:

Prof. Dr. Yuda Yürüm   (Thesis Supervisor)   ....

Prof. Dr. Ferhat Yardım   ....

Assoc. Prof. Dr. Yusuf Menceloğlu   ....

Assist. Prof. Dr. Gürsel Sönmez   ....

Assist. Prof. Dr. Melih Papila

DATE OF APPROVAL: 22.07.2005

ii

ACKNOWLEDGEMENT

TABLE OF CONTENTS

LIST OF FIGURES

LIST OF TABLES

ABSTRACT

Wet-spun poly (acrylonitrile) fibers were stabilized at 200 ^{o}C for 1, 2, 3, 4, 5 hours and 300 ^{o}C for 0.5, 1, 2 hours under an air atmosphere. Carbon fibers were investigated in terms of functional groups at the surface and surface area changes at different carbonization temperatures, 500°C, 600°C, 700°C, 800°C, 900 ^{o}C, 1000 ^{o}C. After this, all carbon fibers were chemically activated with aluminium chloride ($AlCl_3$) and carbon dioxide (CO_2). Fourier Transformation Infrared Spectra and Scanning Electron Microscopy images of the chemically activated carbon fibers were measured to highlight possible changes on the surface. The highest surface area was obtained for the carbon fibers that was stabilized at 300°C for and carbonized at 600°C as 135.68 m^{2}/g. Activation of fibers increased the surface area of fibers activated at 800°C under a CO_2 atmosphere for 0.5 and 1 hour. After the activation of fiber at 800°C for 0.5 and 1 hour and at 900°C for 1 hour and with $AlCl_3$/Et_2O, the highest surface area was obtained for the carbon fiber stabilized at 300°C, carbonized at 800°C and activated for 1hour as 189.60 m^{2}/g. Non-activated CFs had microporous surface which was converted to macroporous surface after activation by CO_2. However, longer activation times created more ordered graphitic layers.

FT-IR spectra of almost all samples showed two major peaks near ~1200cm^{-1} and ~1600cm^{-1} that belonged to =C-H and -C=C-, respectively. Although some fibers contains –C-N groups these groups vanished after activation.

After 5%Pd (by wt) was loaded by $NaBH_4$ reduction method onto carbon fibers carbonized at 800°C and stabilized at 300°C for 1 hour, cyclohexane was dehydrogenated in micro-autoclaves at 350°C in a differential scanning calorimeter system. Two main endothermic peaks were observed in DSC thermograms until 350°C. Chemical compounds produced after dehydrogenation experiments over 5%Pd/CF were analyzed in GC-MS. Cyclohexene, 1-methyl-cyclopentene, 1,3,5-trimethylbenzene, 3-methylcyclohexene, decanal, 1-hexanol were some of the compounds observed.

ÖZET

Yaş çekim sistemi ile üretilmiş poli (akrilonitril) fiberler 200 ^{o}C' de 1, 2, 3, 4, 5'er saat ve 300 ^{o}C'de 0.5, 1, 2'şer saat hava ortamında okside edildi. 500, 600, 700, 800, 900, 1000 ^{o}C'de azot gazlı ortamda karbonize edilen PAN fiberlerin yüzey alanları, grafit içerikleri ve yüzeyde yer alan fonksiyonel gruplar Fourier Transform İnfrared spektrokopisi, taramalı electron mikroskopisi ile incelendi. Bundan sonra bütün karbon fiber örnekleri aluminyum kloritle ve karbon dioksit aktive edildi. Aktivasyon sonrası gene yüzeyde yer olabilecek olası fonksiyonel gruplar ve yüzey alanı gruplar sırasıyla Fourier Transform İnfrared spektrokopisi, taramalı electron mikroskopisi, ve BET yöntemi ile incelendi. BET yöntemi ile en yüksek yüzey alanı 300°C'de okside edilmiş ve 600°C'de karbonize edilmiş karbon fiber örneklerinde 135.68 m^2/g olarak elde edildi. Bununla birlikte bu yüzey alanı 300°C'de okside edilmiş ve 800°C'de karbon dioksitli ortamda aktive edilmiş fiber örneğinin yüzey alanı 189.60 m^2/g olarak ölçüldü. Bunun yanında alanı 300°C'de okside edilmiş ve 900°C'de karbon dioksitli ortamda ve AlCl$_3$/Et$_2$O komposuzyonunda aktive edilmiş fiber yüzey alanları 54.50 ve 117.42 m^2/g'a düştü.

FT-İR analizinde karbon fiber örneklerinin yüzeyinde özellikle iki ana pik analiz edildi. Bunlar ~1200cm^{-1} and ~1600cm^{-1} gibi dalga sayılarında =C-H and -C=C- gibi fonksiyonel gruplardı. Bazı karbon fiberlerde gozlenen –C-N pikinin aktivasyon sonrası kaybolduğu görüldü.

NaBH$_4$ aracılığıyla kütlece %5 oranında Pd yüklenmiş 800°C karbonize edilmiş ve 300°C'de 1 saat süresince okside edilmiş karbon fiber örneği siklohekzan bileşiğinin dehirojenasyonunda kullanıldı. Bir DSC aletinde 350°C'ye kadar ısıtılmaya programlanmış olan mikro-otoklavlarda reaksiyon sonunda ortaya çıkmış bileşikler GC-MS yardımıyla incelendi. Siklohekzen, 1-metil-siklopenten, 1,3,5-trimetilbenzen, 3-metilsiklohekzen, dekanal, 1-hekzanol gibi kimyasallara rastlandı.

CHAPTER 1. INTRODUCTION

Carbon fibers (CF) are attractive materials that are arising from their high thermal and load resistance. Alternatively, they have lower density relative to the steel. These superior properties make them to be used in high variety of applications from construction to electronics. Carbon fiber reinforced composite materials are increasingly used instead of metals when weight ratio is critical. Carbon fiber contributes strength through its ligaments. Especially these materials are used in aircraft, advanced sport materials, thermal management. Its intrinsic properties enable it to be tailored as both insulator and conductor for heat and electricity [1-2].

Organic polymers such as poly(acrylonitrile), pitch, cellulose, rayon etc. are used as starting material to produce carbon fibers. Production of carbon fibers has a few steps. Stabilization at 200-300°C is the first step by applying stress onto materials to prevent shrinkage of these starting materials. Then this step is followed by carbonization at 1000-2500°C. In the second step volatile substances like H_2 and N_2 evolve. Finally produced carbon fibers contain 92% carbon. Carbon fibers are usually woven into sheets, tubes and then embedded with epoxy resin in industrial applications.

Among superior properties of carbon fibers, they are resistant materials to stretching and compressing. Carbon fibers are also inert materials. The properties enable them to be used in many applications from tennis racket to biomaterials to be used as hip and knee substitutes. These applications are due to their higher load capacity. Carbon fibers are formed from disordered graphitic layers. Especially, points around fracture are heavily in base of graphite. Main difference of graphite and carbon fiber is their crystalline extent. Graphite is formed from hexagonal cubic unit cells. However, carbon fiber is an amorphous material that contains disordered graphitic layers. Nevertheless, a small portion of carbon fiber is out of graphite. Carbon fiber is mainly formed from ribbons of carbon atoms parallel to the axis of carbon fiber. Carbon fiber has a chaotic structure inside out of ribbons hairpin-like ribbon carbon fibers and graphitic layers. This chaotic structure makes carbon fiber so strong that has 220 GPa Young's Moduli. Since sliding over of folded layers (Figure 1.1) is so hard that renders material resistance to higher strength and compression. [3]
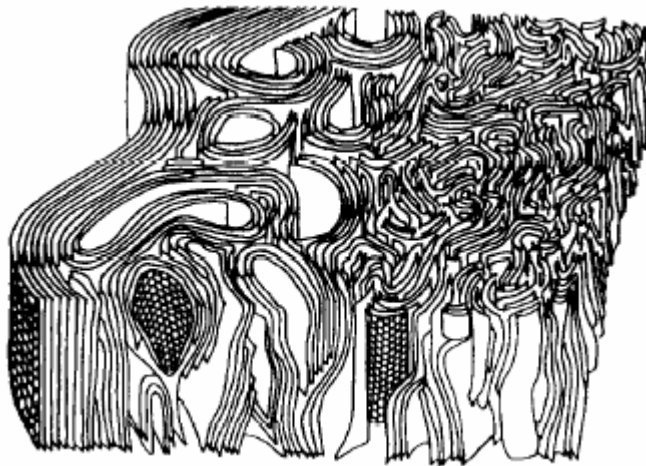
Figure 1.1. Microstructure of carbon fiber [3].

Activated carbon fibers (ACF) are much more new generation but their utilization areas have almost passed carbon fibers'. This study focuses on the activation time and type relationship of activated carbon fibers with surface morphology change.

Research Objectives

Activated carbon fibers have applications especially to be used as catalyst supports, capacitors, electrodes in electrolysis, environmental applications, i.e. adsorption of heavy metals and hazardous organic molecules. Materials of surface of these materials can be modified with different substances. By means of this process ACFs draw gradually growing interest from both industry and science.

In this study, carbon fibers were produced at different carbonization times from wet-spun PAN fibers, stabilized at different activation time in ambient media. All fibers were analyzed with BET, SEM, and FT-IR techniques. It was aimed to modify the surface of the fiber with aluminium chloride ($AlCl_3$) and carbon dioxide (CO_2) and to highlight functional groups on the surface, surface area change, change in percentage of graphitic layers.

This study was useful to understand the mechanism of carbonization of the PAN fibers. It highlights how carbonization temperature affects percentage of the graphitic layers, changes in the functional groups. After the highest surface area was obtained, optimum activation and carbonization process of wet-spun PAN fibers will be determined for the most convenient industrial method. Activation of carbon fibers with aluminium chloride ($AlCl_3$) and carbon dioxide (CO_2) is another query in this study. In fact, the surface area obtained after

chemical activation is more important since final area is dramatically determined after activation. It is aimed to see also how activation affect surface area and functional groups on the surface. The activation might cause different orientations of graphitic layers that may result in different percentage of surface area changes.

CHAPTER 2. BACKGROUND

2.1. Activated Carbon Fibers

2.1.1. Brief Introduction on Activated Carbon Fibers

Activated carbon fibers (ACF) have been growing interest of scientists due to their versatile applications ranging from adsorbents for industrial organic wastes to materials used in electronics. ACFs are a comparatively modern type of porous carbon material with a number of important advantages: ACFs show a high apparent specific surface area, normally in the range of 1500–3000 m^2/g, and a high adsorption capacity, as well as very high rates of adsorption from the gas and liquid-phases [4]. The adsorption capacity of ACFs depends on many kinds of factors, such as raw materials, activation process, the nature of pore structure, and the surface functionality ([5-7]. Studies show that ACFs can be used in capacitors because of their porous structures, catalyst supports. This is due to big surface areas of activated carbon fibers which can be observed as nano-, meso- and micropores. ACFs are amorphous materials consisting of graphitic layers. Kaneko found that 3 or 4 graphitic layers existed in each microcrystal of ACFs [8-9]. In these materials effectivity is determined according to their microstructure since adsorption or reactivity coefficients primarily depend on pore volume, size and chemical structure. Microstructure is controlled by carbonization during graphitic layer stacking. Therefore stabilizationand carbonization are the most important criteria to specify the qualification of ACFs. In addition to this non-ordered structure and heteroatoms in ACF make this material very interesting [10].

2.1.2. Synthesis of Carbon Fibers

Activated carbon fibers (ACFs) are generally prepared from polyacrylonitrile (PAN) fibers, cellulose fibers, phenolic fibers, and pitch fibers by chemical or physical activation [11-12]. PAN is industrially produced by wet or dry spinning methods. It contains semicrystalline atactic polymer partially composed of orthorhombic unit cells. Even 30% of crystallinity is reported that gives 3.3 Å distance between layers (d) in XRD characterization [13].

Production of PAN-based ACFs includes three steps: stabilization of PAN at relatively lower temperatures about 250°C in ambient media, carbonization of PAN precursors at higher temperatures like 1000°C, then activation of these carbonized fibers by water, carbon dioxide, air or various inorganic chemicals such as sodium or potassium hydroxide, zinc chloride [14]. The cyano-groups in PAN are cross-linked to each other through weaker π bonds during carbonization and nitrogen content decreases, finally graphitic layers are formed. Donnet et al. [9] showed that external surface of the fibers is more crystalline than interior part of the fiber. For the stabilization of PAN several mechanisms were offered in the literature. These might be (a) heteroaromatic cyclic structure, (b) polyimine cyclic structure, (c) polyenamine cyclic structure, (d) propagation crosslink, (e) intermolecular nitrile crosslink, (f) azomethine crosslink, (g) conjugated polyene. Lactam, ketone, nitrone and lacton structures were observed during stabilization in the previous studies [13].

Possible mechanism was offered given below during carbon fiber production;
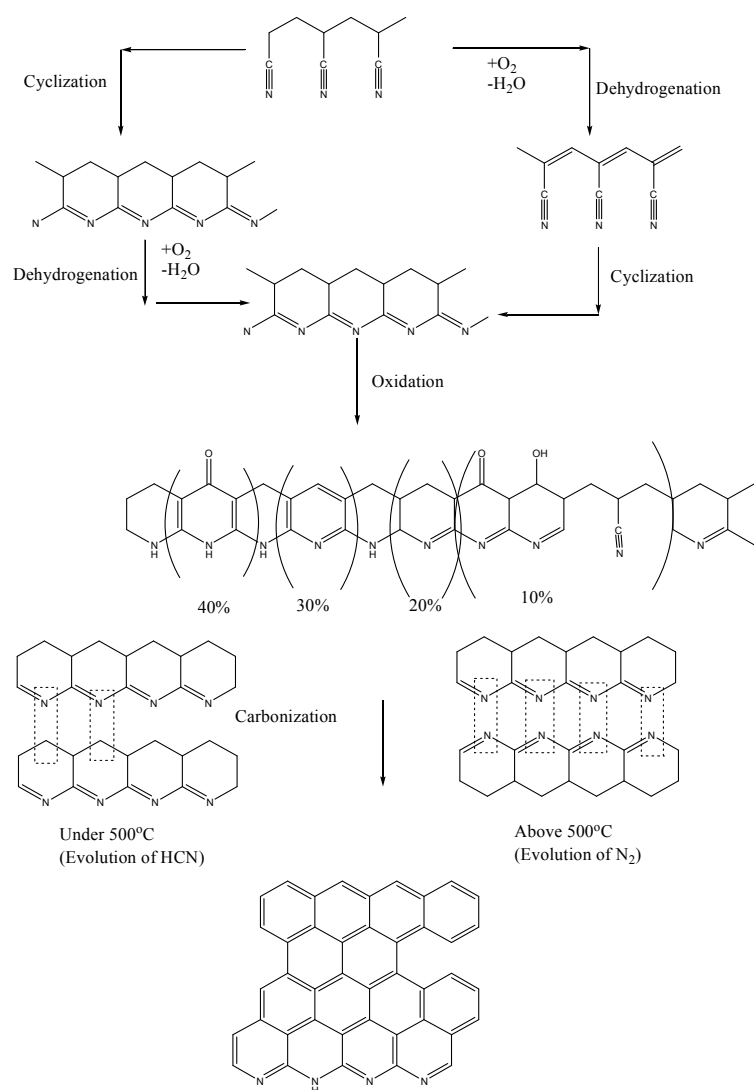
Figure 2.1. General mechanism for PAN stabilization and carbonization [16].

2.2. Structure of Activated Carbon Fibers

Activated carbon fibers are composed of disordered graphitic structures. ACFs contain high percentage of pores in the size of 6 to 21Å. These pores consequently are connected to the surface. Brasquet et al. [17] explained that micropores were slit-shaped and connected to the external surface which render ACFs to be used as catalyst support and influential adsorbents. Pores are formed during the activation process. Pore size and distribution are affected by activation type, time and temperature. Ryu et al. [18] proposed pores are intercrystalline or intracrystalline voids that are between each microcrystalline disordered graphitic layers. This reveals that surface area of the ACFs increases with short-range order and small thickness of each microcrystalline structure. Pore sizes decreased from 31 Å to 19 Å after steam activation rate increased 0.4 to 2.0 ml/min. However, surface area of materials increased three times [18]. Interaction of π systems with water, as well as with cations, draws interest in terms of considerable fundamental and practical interest. Although carbon materials have more hydrophobic character than clay and zeolites, they can be used effectively as adsorbents to remove organic, inorganic acids and bases. Fortunately, it is possible to modify the surface with acidic oxygen functional groups [19].

Ryu et al. [18] showed that activated PAN-based carbon fibers have >1 nm supermicropores and <0.7 nm ultramicropores when were carbonized at $1000^{o}C$ and then activated by CO_2 and water. Pore size and pore distrubition increase while activation time increases [19]. Activation process affects surface chemistry and morphology of fibers. It causes a decrease in the percentage of nitrogen while oxygen content of the materials increases as well as this carbon structure of the fibers damaged. The decrease in the diameter of the fiber indicates etching and removal of some amount of carbon fiber (Figure 2.3). Physical activation time and intensity increases the surface area. Nitrogen content of the external surface is lower than nitrogen level of internal structure as it was shown by X-ray Photoelectron Spectroscopy. However, carbon content increases from core to external surface [14].
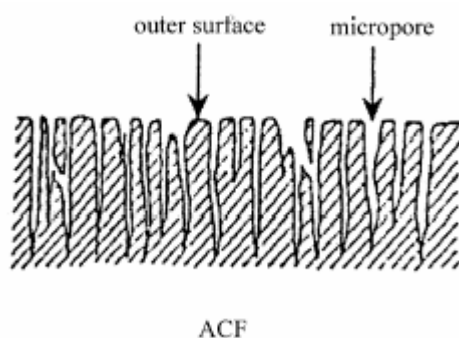
Figure 2.2. Cross-section area of Activated Carbon Fiber [8].

Activated carbon fibers are used as catalyst support materials with a growing interest. They have larger pore volumes even than zeolites have. In addition to this they can be modified via post-modification processes like physical and chemical activation methods [20]. Additionally, mesoporosity of the materials can be shaped by pre-impregnation of some compounds like boric and phosphoric acid. Apart form zeolites they have narrow pore size distributions and not well-shaped pores which render the structure more selective [21-22].

Slit-shaped model of ACFs demonstrated by transmission electron microscope is important to understand adsorption onto carbon in environmental applications. However, this model can not explain the nature of pores in ACFs which are connected in a complex manner. Seaton proposal seems more realistic. It is stated that graphitic planes contain heteroatoms that deviate structure from planar form [16]. Randomly distributed pores create structural non-uniformity (Figure 2.4). Another model recently supposed is reverse Monte Carlo method (RMC). This model takes carbon-carbon bonds obtained from XRD analysis. In this modeling, single-graphene layers in the size of 1-5 nm are taken according to Gaussian Distribution Function. As Monte Carlo simulation continue, Radial Distribution Function match with real experiment. Thomson and Gubbins' model uses perfect diffrerent sized graphene layers. By randomly distribution, adding, deleting graphene layers can approximate minimal configuration. This theoretical approximation of pores in ACFs is closely related with experimental data (Figure 2.5) [23].
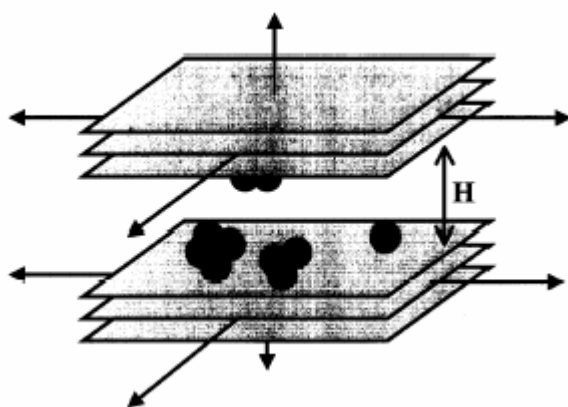
Figure 2.3. Theoretical model for slit-shaped structure of activated carbon fibers [23]
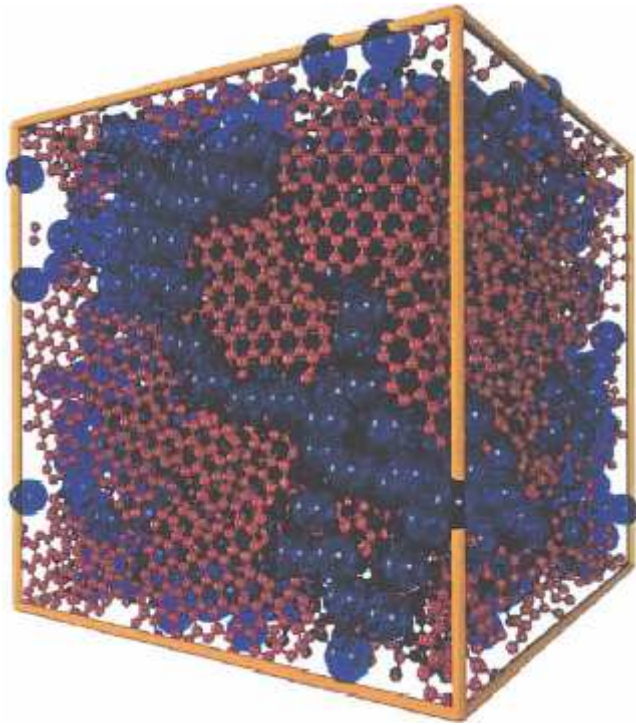
Figure 2.4. Reverse Monte Carlo theoretical approximation for ACFs. Structures in red designate graphitic layers [24].

Among carbonaceous materials activated carbon fibers have low pore distribution variation. This property gives an opportunity to use them widely in both practical and theoretical applications. They have faster adsorption-desorption and equilibrium rates and also their high liquid permeability enable them to be used in gas and liquid phase adsorption for fuel cell and supercapacitor applications. Microporosity in activated carbon fibers makes better physical sorption. Microporous structure inside ACFs creates selectivity for smaller organic molecules.

2.3. Activation Methods of Carbon Fibers

Chemical activation seems to be the best activation method since it requires lower activation temperatures and times relative to physical activation. It was demonstrated several times specific surface area of the fibers activated by chemical activation are higher than the ones done with physical activation methods. Yield in chemical activation is 47% while it is only 6% in CO_2 activation in order to obtain surface area about 2400 m^2/g [25]. Control of the sizes of the pores is much more easy. However, chemical activation wears away the surface that leads to reduction in strength of the material. Also washing is required to remove residues

[25]. Fu et al. [26] demostrated activated carbon fibers with steam contained micropores 0.5-2 nm in diameter as much as done with phosphoric acid. However, phosphoric acid activation has 30-40% wt. yield and large surface area ($\sim$950 m^2/g). But smaller pore diameters are observed in carbon fibers activated by phosphoric acid relative to steam. In the another study Fu et al. [26] showed steam activated sisal fibers have the highest surface area among phosphoric acid, potassium hydroxide and zinc chloride activation procedures. Interestingly they found surface area of activated carbon fibers at 350°C is bigger than this of five different activated carbon fibers. Air oxidation makes surface more porous and abundant in terms of oxygens which adsorbs polar molecules better [27]. At temperature above 750°C, fibers are aromatized and especially external surface loses heteroatoms and hydrogen occur. Activation with phosphoric acid makes material more aromatic. It is probably due to electron receiving nature of phosphorus atoms. Phosphorus makes afterwards rings more aromatic [28, 29]. Yoon et al. [30] presented a model for Carbon nanofiber activation by KOH activation (Figure 2.6). In this model they found (002) peak showed a decrease in the intensity that is arisen from destruction of graphene layers. This yielded a little change in the surface area. They also realized bundle of graphene layer arranged themselves in ladder-graphene structure as shown in middle picture of Figure 2.6. Further activation destroyed and caused graphene layer arrange themselves into amorphous structure [30].
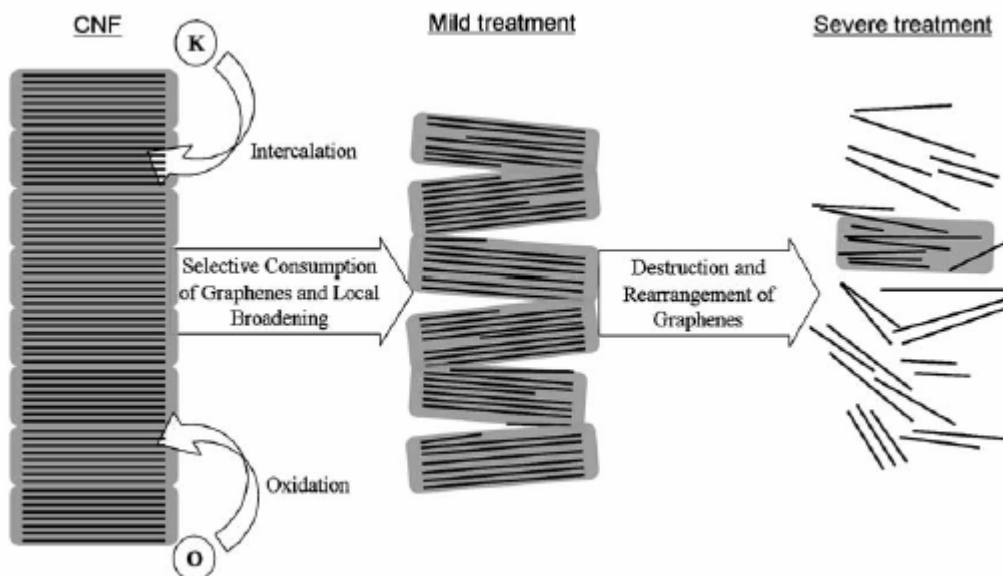
Figure 2.5. Chemical oxidation of Carbon NanoFibers with KOH proposed by Yoon et al. [30].

Degradation of cellulose which has four steps proceeding as desorption of physically adsorbed water; splitting off of structure water; chain scissions, or depolymerization, and breaking of C—O and C—C bonds within ring units, is accompanied by evolution of more water, CO, and CO_2, and aromatization, or formation of graphite-like layers. Sisal fibers activated at 250^oC have intense FT-IR peak at 1700 cm^{-1} arisen from carbonyl group conjugated with double bonds. However, this wavenumber shifts smaller values at higher temperature activations since material become more graphitic [31].

In XRD analysis, carbon fibers have two main broad peaks at 20-22° and 36-44° for 2θ. These values can be assigned to (002) and (10) (overlap of (100) and (101) planes). These peaks becomes sharper with increasing oxidation times which corresponds increasing crystallinity. However, single intense 2θ peak observed for graphite and oxidized graphite appears at 26-27° and 13-15°, respectively [32].

Mangun et al. [33] showed pore sizes of activated carbon fibers in acidic aqueous solutions are smaller than ones activated in air. Pore volume decreases with increasing oxidation. Oxidation begins firstly at graphitic-edges. At the surface functional groups such as quinones, carboxylic acids, phenolic hydroxides are observed (Figure 2.7). Amount of carboxylic acid groups continue increasing with increasing temperature. However, the opposite was observed for quinone and phenolic hydroxides structures in XPS analysis. During activation pore volume and surface area increases. Disordered graphitic layers become more crystalline since pores on the surface and voids inside of the fibers coalesces. This results in wider pores and finally greater surface area. On the other hand, increasing oxidation that refills voids and pores with functional groups tightens pore volumes and also decreases surface area. Wang's study confirms this assertion [33]. Wang observed that pore volumes increased to an extent while pore volumes decrease at longer activation times and feeds [33]. Functional groups are attached to disordered sites proven by lower sodium cation exchange in more activated carbon fibers [35].
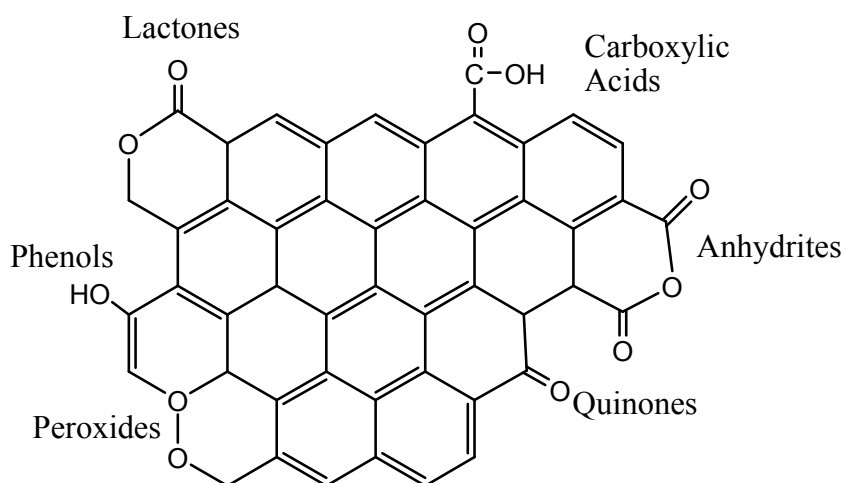
Figure 2.6. Possible functional groups in Activated Carbon Fibers [36]

Iiyama et al. proposed following procedure for the oxidation of carbon fibers [37]:
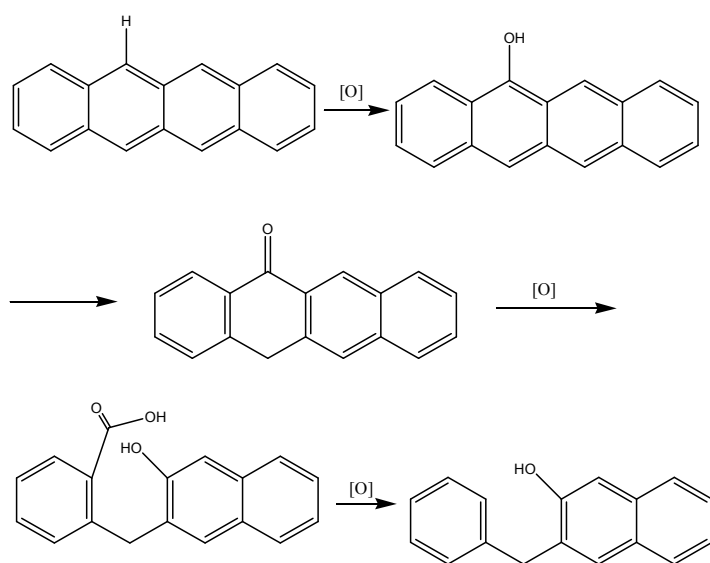
During chemical activation, oxidation-reduction reaction proceeds. For instance,

$$4NaOH + C \longrightarrow 4\,Na + CO_2 + 4H_2O \quad [37]$$
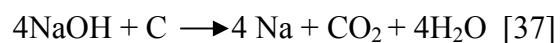
2.4. Applications of Carbon Fibers

ACFs have been used as catalyst support, high-water purification, and other environmental applications [38]. On the other hand, some theoretical studies show that SO_2, H_2O and CCl_4 mass up in the mesopores of carbon fibers [39-40].

Activated carbon fiber catalyst support has several advantages,

1) They have high surface area and abundant uniform micropores. (~1500 m^2/g)

2) They are inert especially in strong basic and acidic media. But the surface of the material can be modified to increase hydrophilic extent of the material. By means of this modification even ion-exchange materials can be prepared.

3) They have high melting point (~3000°C) relative to inorganic catalyst supports like alumina (~2050°C)

4) Their interaction with catalyst materials is relatively low. That is why more activation of the surface with oxygen sometimes is required to enable metal catalyst particles adhere to surface very well. Catalyst particles agglomerates on to the surface according to acidity of the surface. Surface can be evaluated as acidic, basic or neutral. If pH of the fiber is greater than isoelectronic point of solution fiber attracts anions and anions bind to surface. If opposite case is valid (pH< IEP of solution) then cations bind to acidic structures like carboxylic acids. These forces makes catalyst more dispersive. For example, carboxylic acids, lactones, quinines are acidic which attracts metal cations to agglomerate onto surface. This agglomeration generates more hydrophobic character on the surface, attracts more metal cations. This leads increase in the size of metal particles. The mechanism of this phenomena Simonov et al.[41-42] propose that Pd(II) ions are discharged by the localized electrons of carbon accompanied by adsorption of Cl- ions. C. is a positively charged "hole" which appears at the carbon surface when Pd(II) is reduced. The Cl- anions compensate the charge through the formation of an electric double layer on the carbon surface in their paper [43].

5) The pore size and structure can be tailored to obtain desirable properties for a specific reaction. Little work however, been done on modifying the pore size of ACFs (Kawabuchi *et al.*, 1996) as compared with that of activated carbons (Wang and Lu, 1997). It is meaningful to modify and study the microstructure of ACFs due to the many advanced features mentioned above, especially, for PAN-ACF, which have been reported to exhibit a high activity for chemical reaction due to their high nitrogen

content. Previous researchers have added compounds containing metals such as Ag, Co, Cu, Y and Al to polymeric and isotropic pitch precursors, formed these precursors into ACFs, and then measured their adsorption characteristics (Oya *et al.* 1996; Ikeuchi and Kojima 1997; El-Merraoui *et al.* 1998; Ryu *et al.* 1998; Ryu *et al.* 1999a; Ryu *et al.* 1999b; Yim *et al.* 2002). While these studies have shown that the metal additives can generate mesopores during activation, the attainment of a uniform distribution of these metals in the precursors has been a problem. Often the metals appear to coalesce during activation, leading to a wide variation in pore sizes.

6) Carbon fibers can be removed by burning to obtain especially precious catalysts.

7) Carbon catalyst supports but not fibers have lower cost than some other inorganic catalyst supports like alumina and silica [22].

8) Easy recovery of supported metals by burning off the catalyst.

9) As compared with standard granular or powder activated carbons (AC), ACFs have very fast adsorption/desorption rates and can easily avoid the attrition, channelling and bypass flows arising from the packing of the granular carbon system.

2.5. Adsorption Isotherms

Free and adsorbed gas molecules are in a dynamic equilibrium on solid materials. Fractional coverage, the ratio of occupied sites to all sites in material, depends on the amount of the adsorbed gas. The variation of the fractional coverage with pressure is called as adsorption isotherm.

2.5.1. The Langmuir Isotherm

This is the simplest isotherm form. In this model adsorption cannot proceed monolayer coverage. It is supposed surface has uniform structure. Adsorption ability of a molecule is independent from other adsorbed molecules. When adsorption-desorption is in a equilibrium, fractional coverage is defined as,

$$\Theta = KP/1+KP \qquad\qquad K=k_a/k_d$$

Θ: Fractional Coverage

P: Pressure

k_a: Rate constant for adsorption

k_d: Rate constant for desorption [43]

13

2.5.2. The BET (Brunauer-Emmett-Teller) Isotherm

These isotherms are used to determine microporosity of materials. These isotherms are used to calculate specific surface area of materials. The theory of calculation is established by Stephen Brunauer, Paul Emmett, Edward Teller standing for BET. This method is based on the calculation of adsorbed of liquid nitrogen onto surface of material at different P/P_o values. The total to determine the method used to determine surface area, showed that six of the respondents used a single point surface area of a catalyst can be measured by either a multipoint or single point technique. Results of a survey method, the remaining five respondents used a multipoint method. Most respondents used data points in the range of 0.05-.30 P/P_o, only one used a P/P_o below 0.05. In either the single point or multipoint method, the isotherm points are transformed with the BET equation :

$$\frac{1}{W[(P_0/P)-1]} = \frac{1}{W_m C} + \frac{(C-1)}{W_m C}\frac{P}{P_0}$$

where W is the weight of nitrogen adsorbed at a given P/P_o, and W_m the weight of gas to give monolayer coverage and C, a constant that is related to the heat of adsorption. A linear relationship between $1/W[(P_o/P)-1]$ and P/P_o is required to obtain the quantity of nitrogen adsorbed. This linear portion of the curve is restricted to a limited portion of the isotherm, generally between 0.05-0.30. The slope and intercept are used to determine the quantity of nitrogen adsorbed in the monolayer and used to calculate the surface area. For a single point method, the intercept is taken as zero or a small positive value, and the slope from the BET plot used to calculate the surface area. The surface area reported will depend upon the method used, as well as the partial pressures at which the data are collected. All data are collected on the same samples and instrument, the differences observed can only be attributed to method of calculation and relative pressure at which data are measured. All multipoint data are obtained at P/P_o values of 0.08, 0.11, 0.14, 0.17 and 0.20. The single point data are obtained at P/P_o value of 0.3. Directionally, the single point data are approximately 5% lower than the multipoint data [45].

2.5.3. Freundlich and Temkin Isotherms

Assumption of monolayer coverage and independence of gas molecules is not totally true. Also assumption on surface uniformity does not seem truly. In the adsorption, the most favorable sites are firstly occupied which causes negative enthalpy. In order to solve these scarcities Temkin offered an equation;

$$\Theta = c_1 \, In \, (c_2 p)$$

Θ: fractional coverage

c_1, c_2: constants changing with pressure

p: pressure

However, Freundlich supposed fractional coverage should depend on pressure logarithmically.

$$\Theta = c_1 \, p^{1/c2}$$

Θ: fractional coverage

c_1, c_2: constants changing with pressure

p: pressure

These isotherms are largely empirical which needs known parameters of reliable isotherms. Parameters are required especially coverage in heterogeneous catalysts. Isotherms are also valid only in some definite pressure ranges [46].

2.5.4. BJH(Barrett-Joyner-Halenda) Method

$$\Delta V_p = \Delta V_n R_n - C \Delta t_n R_n \sum \frac{2 \Delta V_{pi}}{r_i}$$

where

$$R_n = \left(\frac{r_n}{r_{kn} + \Delta t_n} \right)^2$$

$$C = \frac{r_n - t}{r_n}$$

ΔV_p = the volume of empty pores for n[th] desorption

ΔV_n = n-th stage of desorption as a change in adsorbtion value

Δt_n = change in thickness of layer adsorbed on the pore walls

r_n = average pore diameter

r_{kn} = average Kelvin's radius of the space between adsorbed layers [47]

2.6. Catalytic Dehydrogenation of Cyclic Organic Compounds

Combustion of conventional fuels cause increases of the CO_2 concentration of air. Currently, the majority seeks new ways to reduce formation of CO_2. Fortunately, hydrogen is the promising energy source for the future since products of hydrogen after usage is just water.

Dehydrogenation of cyclic organic compounds is now accepted as a potential hydrogen supply to some prospective applications like fuel cell. Dehydrogenation-hydrogenation is reversible. That is more useful method than metal hydrides. Also CO_2, CO are not formed. Since dehydrogenation is highly endothermic reaction, it requires catalyst. Transition metal catalysts are used to reduce activation energy of the reaction. Palladium is an effective metal for dehydrogenation. Studies show non-steady pulsed dehydrogenation, wet-dry multiphase conditions are more effective ways than conventional gas and liquid-phase treatments for dehydrogenations [48-50]. Dehydrogenation of cyclic hydrocarbons including vaporization of reactant and reaction heat absorbs 94–101 kJ mol^{-1} for 1 mol of hydrogen production. On the other hand, produced hydrogen, which is used for fuel cell systems or hydrogen combustion systems, desorbs 237 kJ mol^{-1} of heat [51].

16

Carbon fibers are proper materials to be used as catalytic supports because of their high surface area and variable porosity extent. Transition metal loaded carbon fiber catalysts have lower resistance to permeability of reactants. Narrow size distribution of ACFs enables faster adsorption-desorption. Easy separation of catalysts from solution without consuming time is another advantage [51]. However, poisoning of catalyst by dehydrogenated products, evolved hydrogen and reactants is main drawback. Reprocess yield also for these catalysts is almost vanished after twice usage [52].

The functionalities present on the carbon surface in the form of surface oxides (e.g. carboxylic groups, phenolic groups, lactonic groups, etheric groups) are responsible both for the acid/base and the redox properties of the activated carbon. These surface groups act as coalition parts for the generation of highly dispersed metallic crystallites. Depending on surface functional on the carbon surface, two mechanisms play a role: adsorption of ionic species at acidic and basic sites or deposition of metallic species by a redox reaction with the carbon. For the first mechanism, the point of zero charge of the activated carbon is of major importance. Mixtures of the two mechanisms are possible [53].

Many studies have been done to highlight reaction mechanism of production of hydrogen on catalyst surface. Mukhopadhyay *et al.* concluded that palladium forms palladium hydride while zinc donates 2 electrons to oxygen which cleavage simultaneously both O-H bonds (Figure 2.8). Reaction possibly progresses between the interfaces of palladium and zinc [54]. Reaction of the temperature is main important criteria. This is determined according to boiling point of substance in conventional reactors. However, temperature can be increased to desired values in setups like batch reactors. Kariya *et al.* bimetallic Pt-Rh catalyst showed higher activities than monometallic Pt in the dehydrogenation of cyclohexane. This is probably arising interactive effect of high C–H bond cleavage ability of Rh and high hydrogen recombination ability of Pt [55]. Second metal also attenuates the formation of coke.
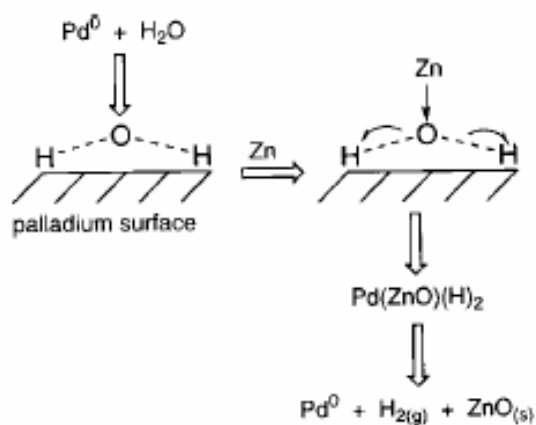
Figure 2.7. Hydrogen gas production via palladium. Zinc behaves as oxygen acceptor [54].

Grant et al. proposed dehydrogenation occurs at much lower temperatures over Pt/ZnO catalyst. On the platinum surfaces reactions were observed via Li ion Scattering (LEIS),

$$c\text{-}C_6H_6(a) \longrightarrow 3C_2H(a) + 3H(a) \text{ at } 540 \text{ K}$$

$$3C_2H(a) \longrightarrow 6C(a) + 3H(a) \qquad \text{between } 570\text{-}800 \text{ K}$$

$$c\text{-}C_6H_{12}(a) \longrightarrow c\text{-}C_6H_9(a) + 3H(a) \qquad \text{between } 230\text{-}300 \text{ K}$$

$$\longrightarrow c\text{-}C_6H_6(a) + 6 H(a) \qquad \text{at } 290\text{-}340 \text{ K}$$
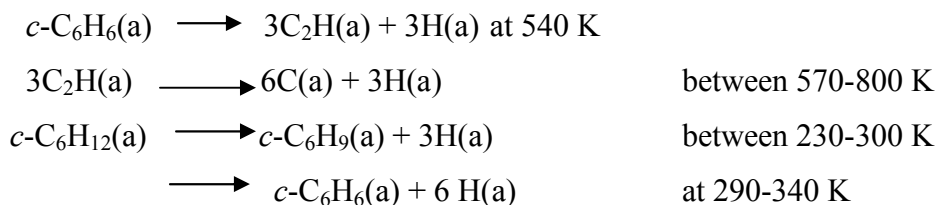
This reaction was observed on Pt(111). However, cyclohexadiene, cyclohexadialkylidene, cyclohexene were detected on other Pt surfaces. Finally, H_2 desorbs from surface.

$$2H(a) \longrightarrow H_2(g) \qquad \text{at } 350 \text{ K } [56]$$

18

CHAPTER 3. EXPERIMENTAL

3.1. Materials

Wet-spun poly (acrylo nitrile) fibers were kindly provided by Aksa Akrilik Kimya Sanayi A.Ş. (Yalova). They were 12μm in diameter. The fibers were used without doing any further purification treatment.
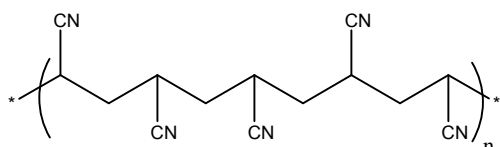
Figure 3.1. Wet-spun Poly (acrylo nitrile)

Cyclohexane was a product of LaChema.

$PdCl_2$ of Fluka in 99% purity was used as palladium source.

3.2. Equipment

Oxidation of PAN fibers was done in Thermolyne 62700 Furnace. Thermolyne 2110 tube furnace was used for carbonization at higher temperatures at inert N_2 media. The flow rate of gas was

Bruker Equinox 55 FTIR spectrometer with Attenuated Total Reflectance (ATR) attachment was used for Fourier Transform Infrared analysis of fibers and precursors.

Information about surface topology of precursors and carbon fibers was examined by using LEO Supra VP35 FE scanning electron microscope, after coating of all surfaces with carbon in Emitech K950X sputter coater.

Surface area of carbon fibers and activated carbon fibers was analyzed in Quantachrome NOVA 2200e Surface Analyzer. The determination is based on the measurements of the adsorption isotherms of nitrogen at 77 K. Surface area of the samples were determined by using BET equation in the relative pressure range of between 0.05 to 0.3, seven adsorption points.

Netzsch DSC 204 Phoenix Differential Scanning Calorimetry was used to find degradation and dehydrogenation temperatures of cyclohexane.

DSC Mettler stainless steel micro-reactors of 270 µL volume with gold caps were used for the dehydrogenation experiments.

Shimadzu GC-MS Q4228 was used to analyze products obtained after treatment of cyclohexane. Column, injection and detector temperatures were 45, 250 and 300°C.

3.3. Experimental

PAN fibers were stabilized at 200°C for 1, 2, 3, 4, 5h and also at 300°C for 0.5, 1, 2h after applying tension to wet-spun fibers to prevent shrinkage and obtain better fiber precursors. These steps were followed by carbonization of precursors at 500, 600, 700, 800, 900, 1000°C. FT-IR spectrums of all carbon fibers and carbon precursors were taken. Surface topology of the carbon fibers and carbon precursors was investigated with SEM.

After carbon fiber synthesis, according to surface area of samples activation step was done. Activation was done by carbon dioxide. CO_2 is more effective at 800°C as an activating agent. Lower temperatures were not feasible for activation. However, all precursor was burned in the carbonization at 1000°C. Stabilized precursors at 300°C for 1 h were activated in N_2 atmosphere at 800°C for 0.5 and 1 hour, 900C for 1 hour.

PAN is mixed with $AlCl_3$ in 1:5 ratio in 25 ml diethyl ether for 4 hours at room temperature. PAN fibers were stabilized at 300°C for 1 hour after filtering and washing with diethyl ether. Stabilized precursor was carbonized at 800°C for 1 hour in N_2 atmosphere. Finally carbon fibers were washed with HCl/water solution in 1:4 ratio.

Carbon fibers, carbonized at 800°C that were stabilized previously at 300°C for 1h, were selected as catalyst support material since it has one of the largest surface area. Also this temperature was compared with surface area of carbon fibers after activation.

0.5 g carbon fiber was put to the beaker containing 20 ml of water at room temperature. 0.0417 g $PdCl_2$ was added an stirred with carbon fiber. Suddenly $NaBH_4$ was added to the solution as reducing agent for Pd^{2+}. Final solution was stirred for 10 minutes at room temperature.

0.0060 gram 5% Pd-loaded carbon fiber was added into a Mettler micro-reactor of 270 µl volume. Micro-reactor was tightly closed after adding 100 µL cyclohexane (Lachema). In DSC analysis, this micro-reactor was placed to sample side. One more of the same micro-reactor was put into other side as reference crucible. Micro-reactor was heated to 350°C in the rate of 20K/min at nitrogen atmosphere and hold at this temperature for 15, 30 and 60 minutes. In addition to these samples two more samples were taken. First one is cyclohexane and products obtained after the first degradation peak of cyclohexane in DSC. Other is

cyclohexane and products obtained till the first degradation peak of cyclohexane. These samples were analyzed with GC-MS system as described.

CHAPTER 4. RESULTS AND DISCUSSION

4.1. SEM Images and FT-IR Spectra of Fibers and Precursors

Wet-spun PAN fibers have fibril structure, irregular rod-like helix model, in central due to CN- repulsion during spinning process. Laterally ordering of distorted-helix PAN-chains increases towards external surface. Increase in the fibril structure also increases the extend of graphitization. Gupta and Harrison found that intramolecular reactions within the rod-like helix dominate at lower temperatures (below 290°C) whereas intermolecular reactions between adjacent helices occur between 300 and 380°C [51]. PAN-based carbon fibers have higher orientation and larger crystallites on the surface or cover region than that in the internal of the fiber. This difference is arising from the radial structure of fiber. Outer cover is subjected to higher extent of stabilization than inner part. Higher degree of carbonization refers to higher elimination of nitrogen. Nitrogen content is higher than interior part [52].

The absorption bands in the 1640–1500 cm^{-1} region suggests the overlapping of aromatic ring bands and double band (C=C) vibrations with the bands of C=O moieties in the FT-IR spectra. The oxidation of the ACFs enhances also the absorption in the range 1250–1000 cm^{-1} that suggests the increase of each ether (symmetric stretching vibrations), hydroxylic, and phenolic structure (vibrations at 1180 cm^{-1}) [1]. According to Deki et al. sp^2 bonds occurs during stabilization of PAN even at 300°C [53]. PAN fibers have amorphous or ordered rods and crystalline phases or ordered rods forming of 30%. Cyclization starts at amorphous phases in oxidative stabilization processes. At higher temperatures like 300°C intermolecular cross-linking begins at crystalline phase. But intramolecular cross-linking of –CN bonds begins at 175°C and 215°C in amorphous and crystalline phases [52].
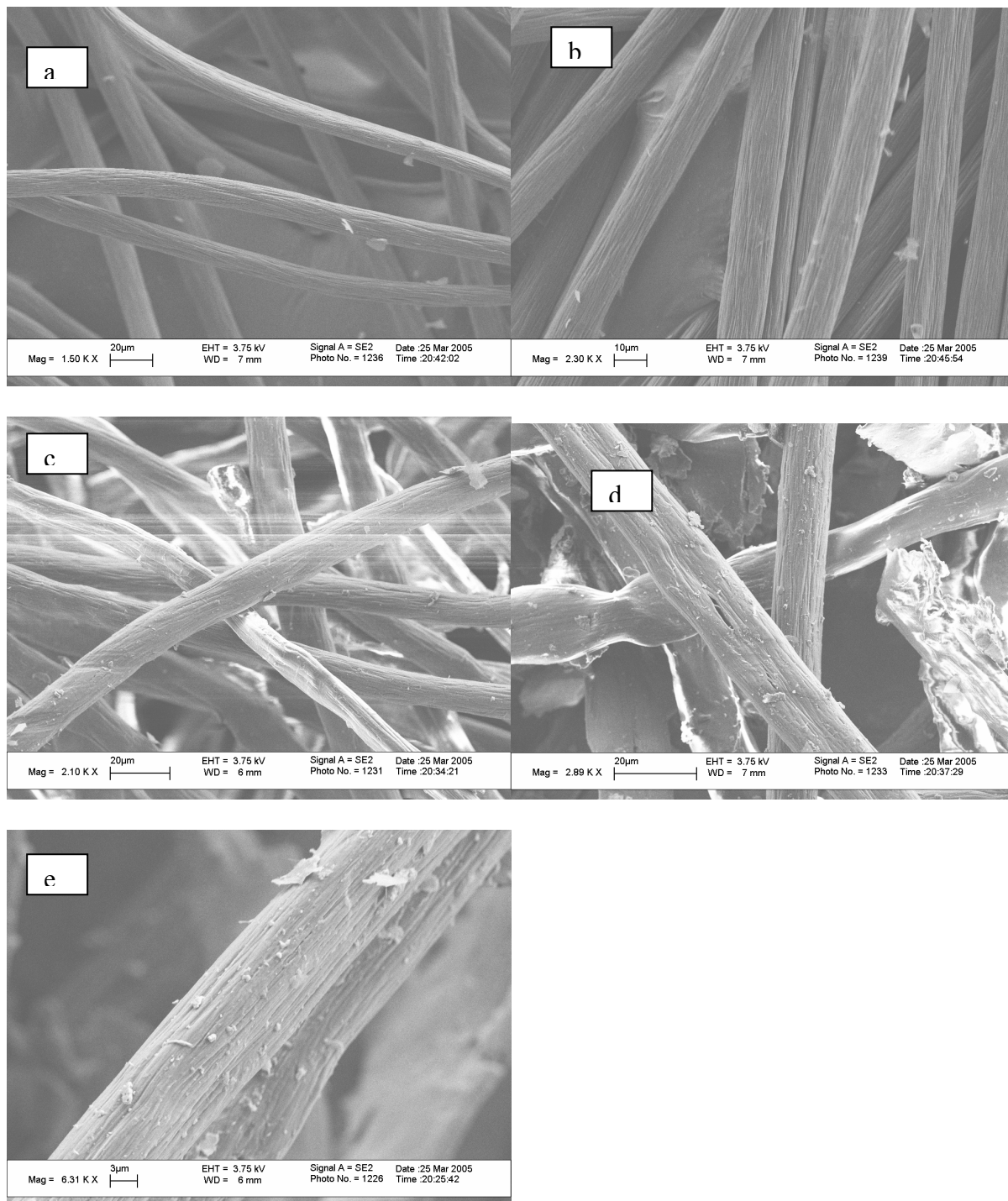
Figure 4.1.1. Wet-spun PAN fibers stabilized at 200°C for a) 1 hour b) 2 hours c) 3 hours d) 4 hours e) 5 hours
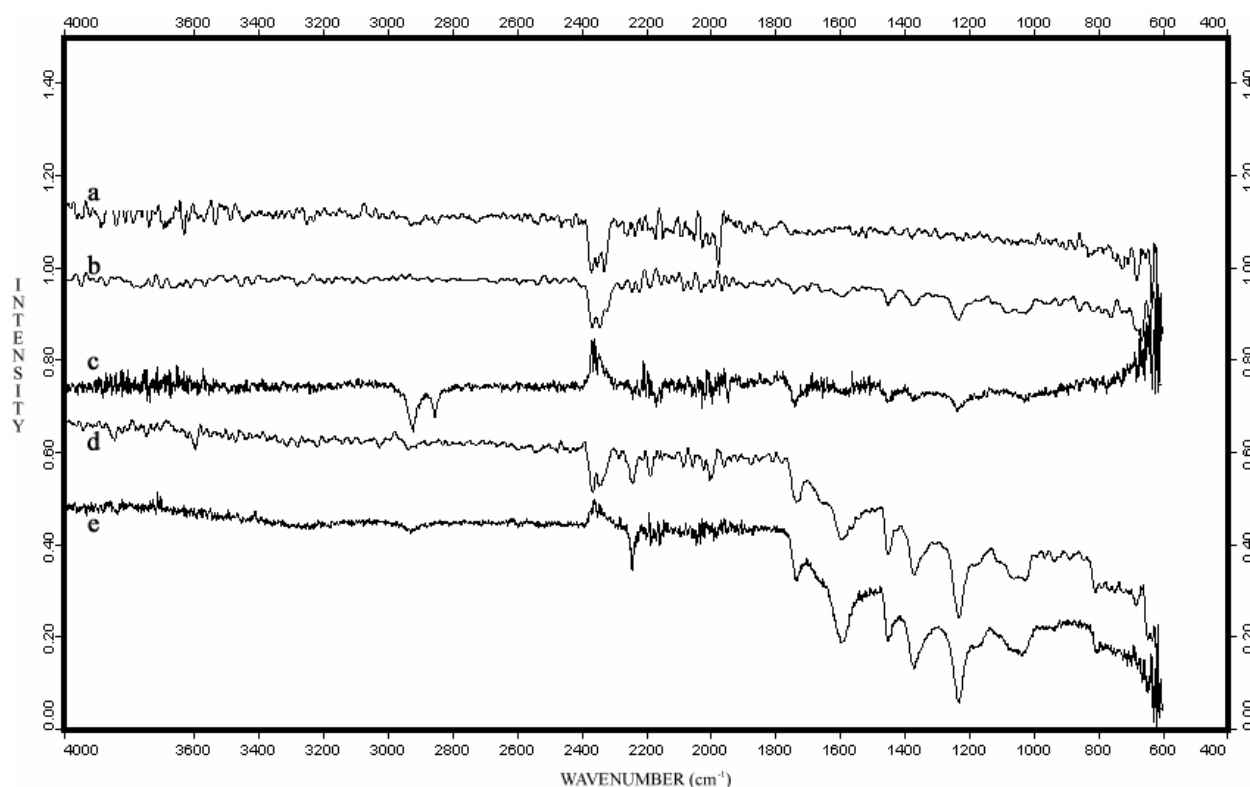
Figure 4.1.2. FT-IR spectra of precursors stabilized at 200°C for a) 1 hour b) 2 hours
c) 3 hours d) 4 hours e) 5 hours

FT-IR spectra showed there were two main peaks at 1190 and 1580 cm^{-1} (Figure 4.1.2-31). These peaks belong to –C-H and -C=C- or –C=N-, respectively [52, 53]. As pore diameters increase surface area reduces. When FT-IR spectra of precursors were examined 200°C stabilization has no peak at 1600cm^{-1}. 1600cm^{-1} belongs to carbonyl functional group. Intensity of peak at 1250 cm^{-1} indicating C-O stretching vibration in aromatic structure increased with increasing heating steps. Same trend also observed in peak at 1400 cm^{-1} O-H vibration of oxime (-C=N-OH) (Figure 4.1.2). Growing peak at 1750 cm^{-1} probably belonged to C=C stretching vibration. In the same spectra a weak peak at 2000 cm^{-1} interestingly might belong to quaternary ammonium. In figure 4.1.20, aromatic quarternary ammonium was observed at 2900 cm^{-1}.
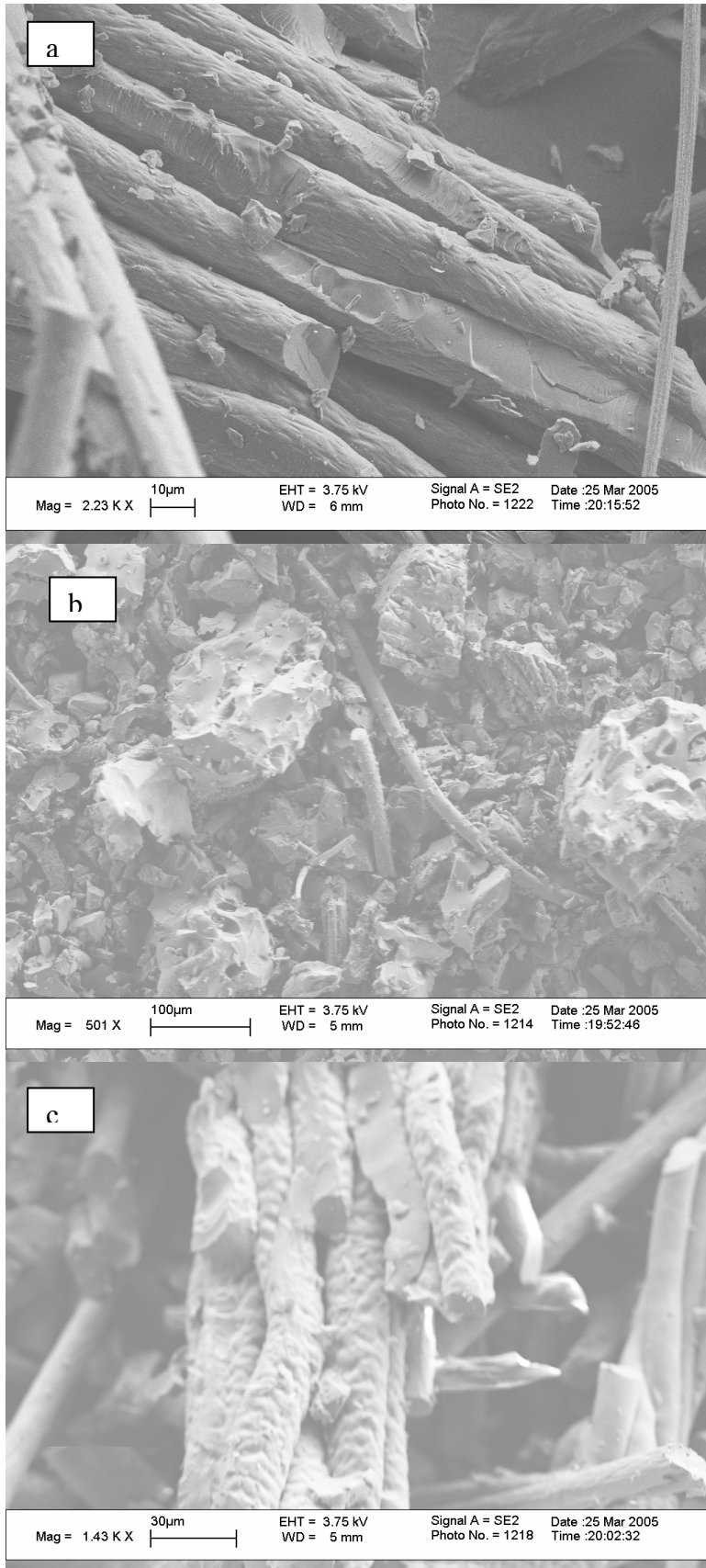
24

Figure 4.1.3. Wet-spun PAN fibers stabilized at 300°C for a) 0.5 hour b) 1 hours c) 2 hours
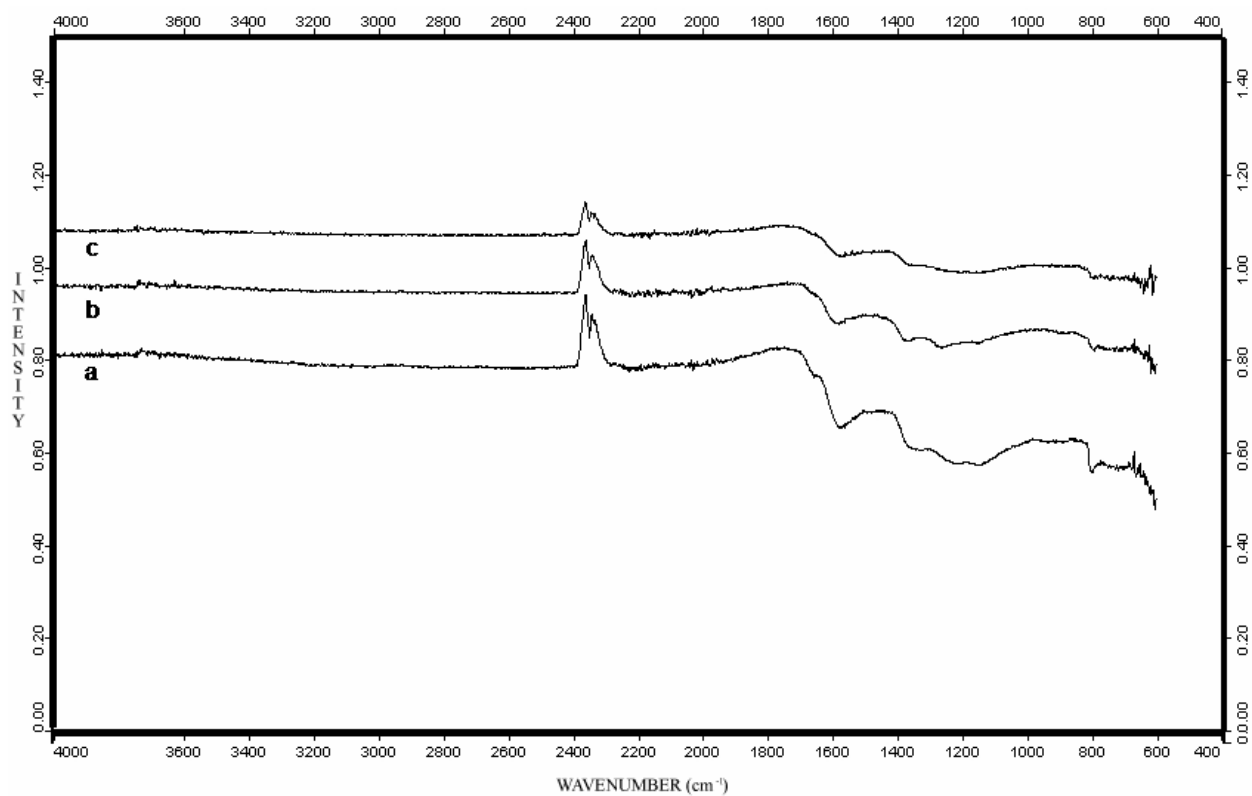
Figure 4.1.4. FT-IR spectra of precursors stabilized at 300°C for a) 0.5 hour b) 1 hours c) 2 hours

This caused fibers stabilized at 300°C for 1 hour have higher surface area values (Figure 4.1.4). Precursors stabilized at 300°C for 0.5 and 2 hours does not have such characteristic morphology (Figure 4.1.4). Weak peak at 1360 cm^{-1} probably was due to symmetric -N=C=O stretching vibration. Intensified peak 800 cm^{-1} with increasing stabilization time signified C-H vibrations bonded to cyclic =C=N-C.

26

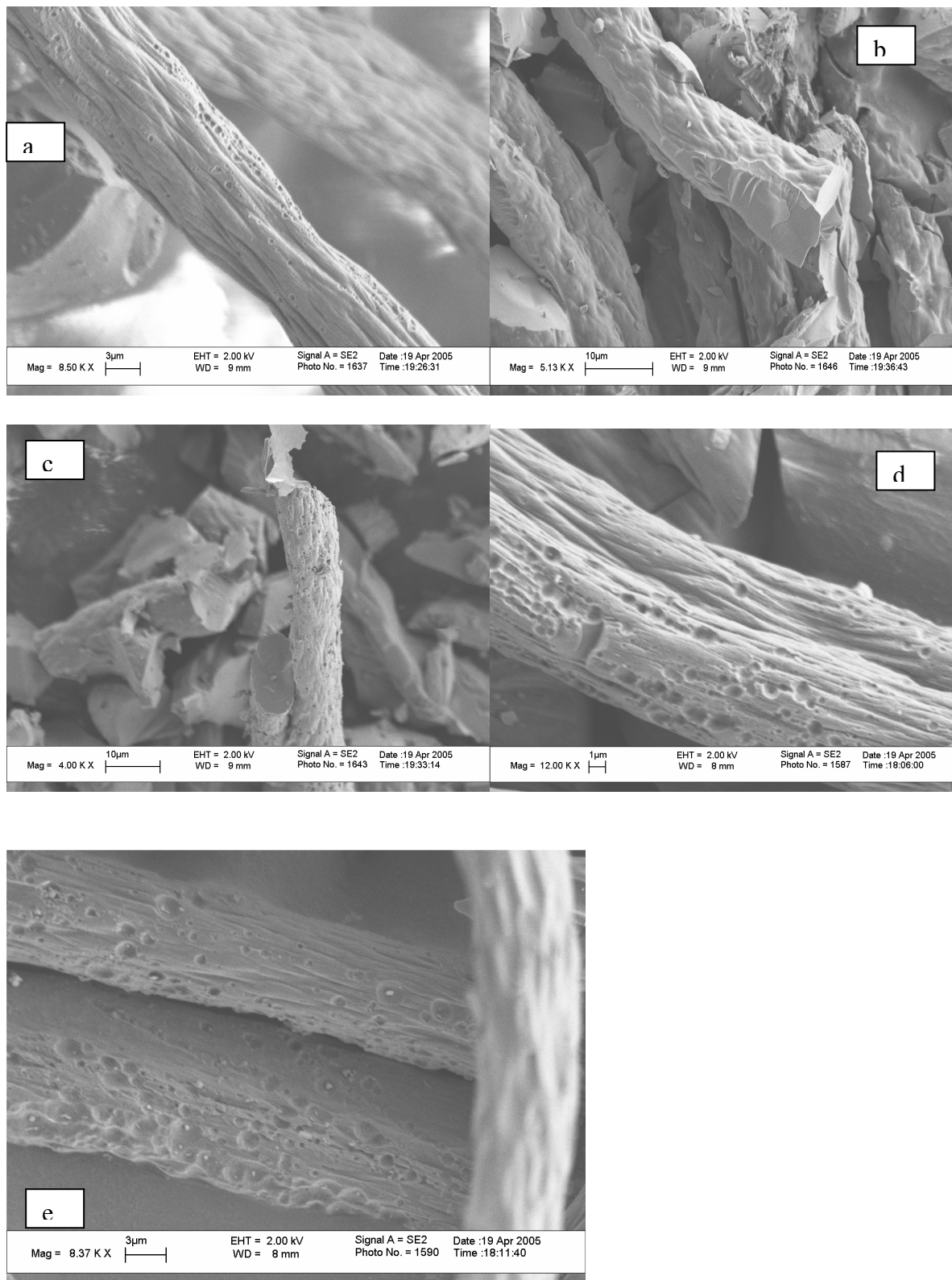Figure 4.1.5. Carbon Fibers before carbonization at 500°C stabilized at 200°C in air media for a) 1 hours b) 2 hours c) 3 hours d) 4 hours e) 5 hours.

Figure 4.1.6. FT-IR spectra of carbon fibers carbonized at 500°C stabilized at 200°C for
   a) 1 hour b) 2 hours c) 3 hours d) 4 hours e) 5 hours

Carbon fibers stabilized at 200°C had CO_2 peaks even after carbonization (Figure 4.1.6-Figure 4.1.26). Stabilization at 200°C resulted in relatively smaller areas to ones stabilized at 300°C (Table 4.3.1). This property might be attributed to shorter fibers interact with heat and carbonized better than other fibers. The composition and morphology of the precursors also play a very important role in the processes of preoxidation, precarbonization and carbonization [52]. Stabilization at 200°C showed when stronger peaks at 1600 cm^{-1} of –C=C- were observed, surface area of fibers were higher (Figure 4.1.6-26). Probably shrinkage of fibers during stabilization and graphitization created pores on the surface. However, at carbonization at 1000°C led to nearly same surface areas (Table 4.2.1). Because high temperature converted open pores to closed ones on the surface [54]. Removal of carbon on the surface made CO_2 peaks of fibers stabilized at 200°C and carbonized at 1000°C by FT-IR (Figure 4.1.26). On the surface of the CF carbonized at 500 and stabilized at 200°C for 1 hour and 300°C for 2 hours 500 nm pores in diameter were observed (Figure 4.1.3- Figure 4.1.9).

28

Figure 4.1.7. Carbon Fibers before carbonization at 600°C stabilized at 200°C in air media for a) 1 hours b) 2 hours c) 3 hours d) 4 hours e) 5 hours.
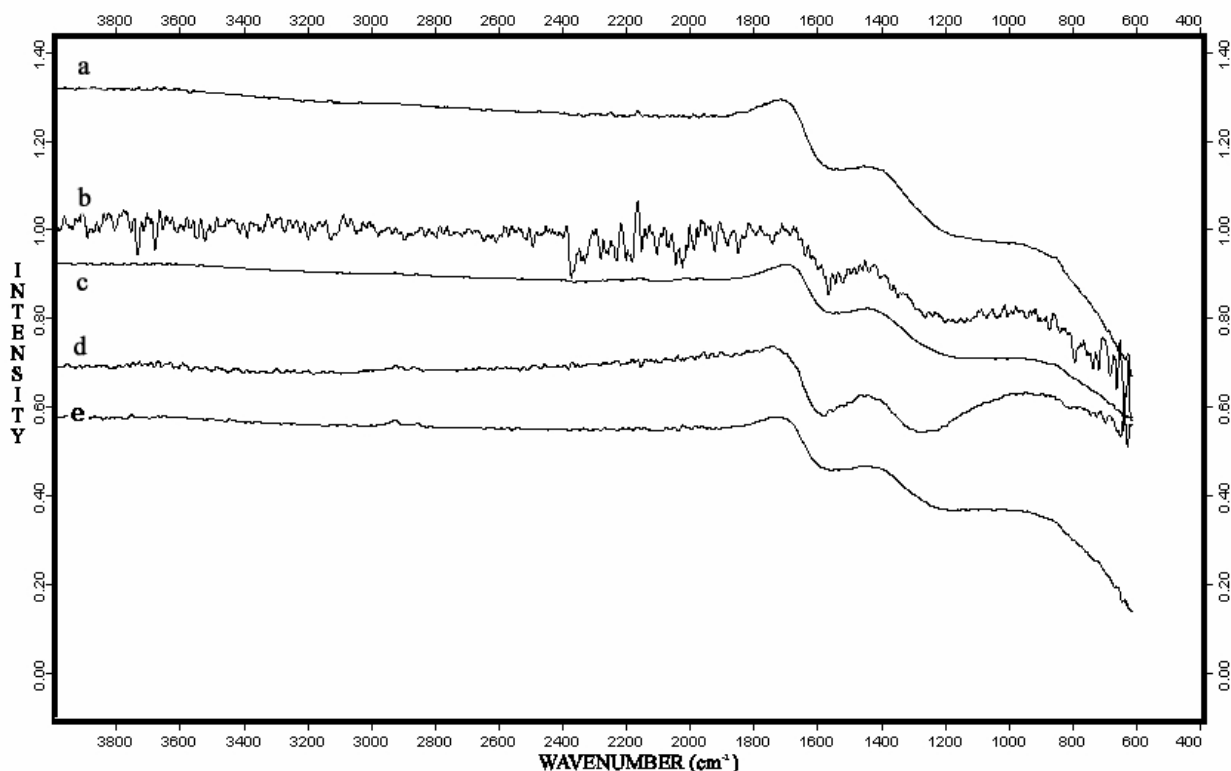
Figure 4.1.8. FT-IR spectra of carbon fibers carbonized at 600°C stabilized at 200°C for
a) 1 hour b) 2 hours c) 3 hours d) 4 hours e) 5 hours

Weak peak around 800 cm^{-1} that became intensive with increasing time indicated C-H bending vibration of cyclic structures. Peak at 2000 cm^{-1} revealed benzene derivative cyclic structures. –CH$_2$ asymmetric stretching was observed at 2900 cm^{-1} interestingly at same intensity (Figure 4.1.8). These bonds probably were taken place at the backbone of PAN.
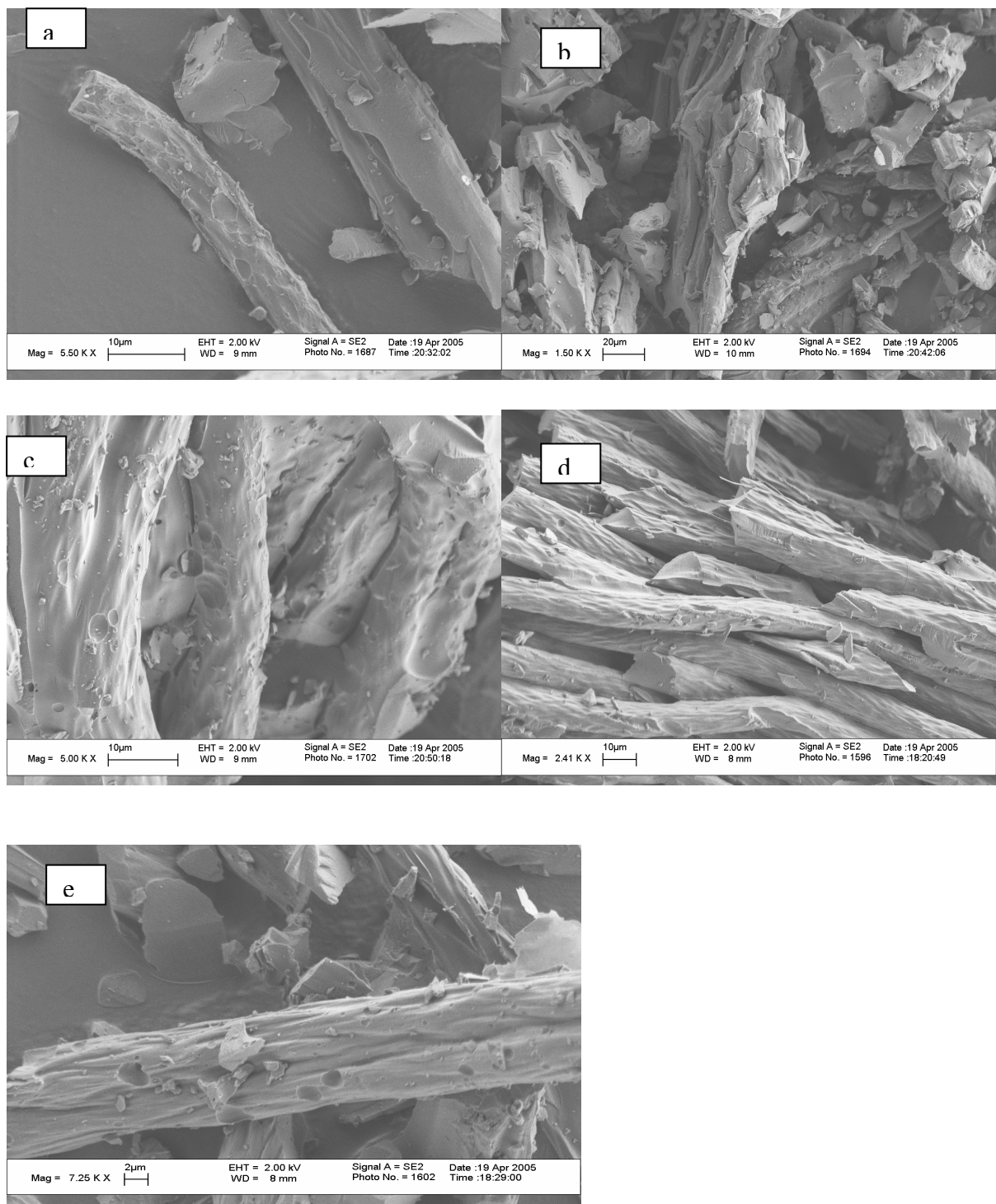
Figure 4.1.9. Carbon Fibers before carbonization at 700°C stabilized at 200°C in air media for a) 1 hours b) 2 hours c) 3 hours d) 4 hours e) 5 hours.
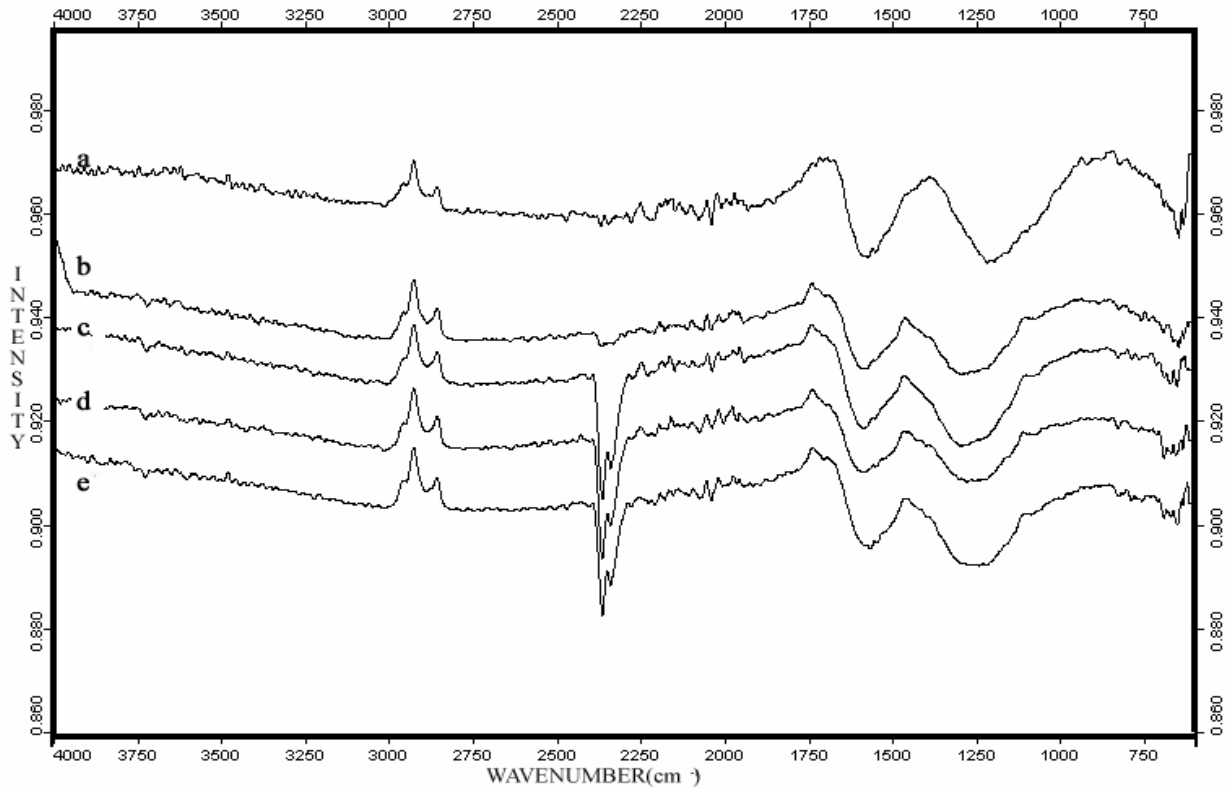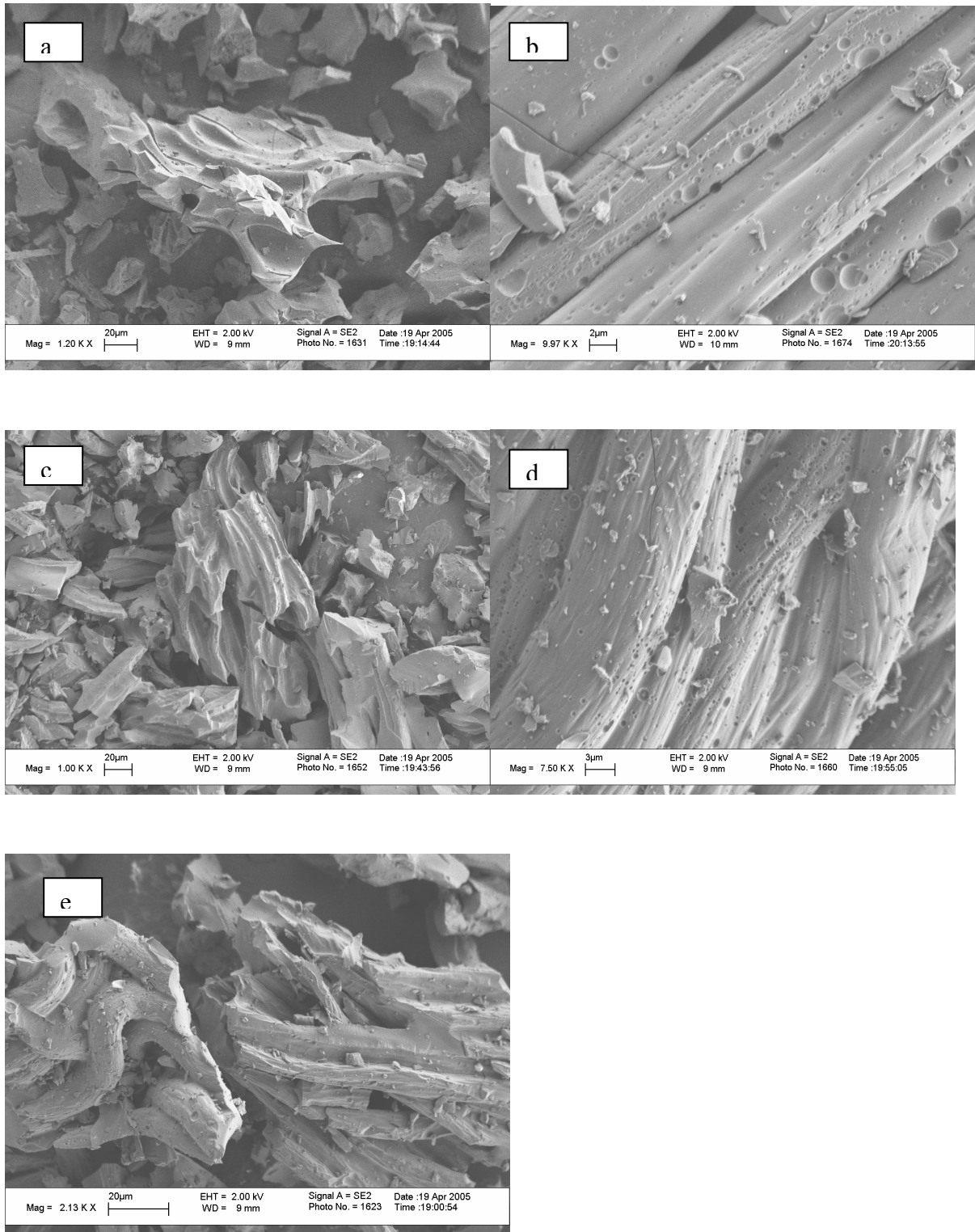
Figure 4.1.10. FT-IR spectra of carbon fibers carbonized at 700°C stabilized at 200°C for a) 1 hour b) 2 hours c) 3 hours d) 4 hours e) 5 hours

Aromatic =C-H in-plane vibrations at 1240 cm^{-1} were obtained (Figure 4.1.10). SEM images showed stabilization times almost had no effect on pore sizes and surface morphology (Figure 4.1.9). Conjugated C=C bonds at 2000 cm^{-1} appeared after 3 hours activation (Figure 4.1.10).

Figure 4.1.11. Carbon Fibers before carbonization at 800°C stabilized at 200°C in air media for a) 1 hours b) 2 hours c) 3 hours d) 4 hours e) 5 hours.
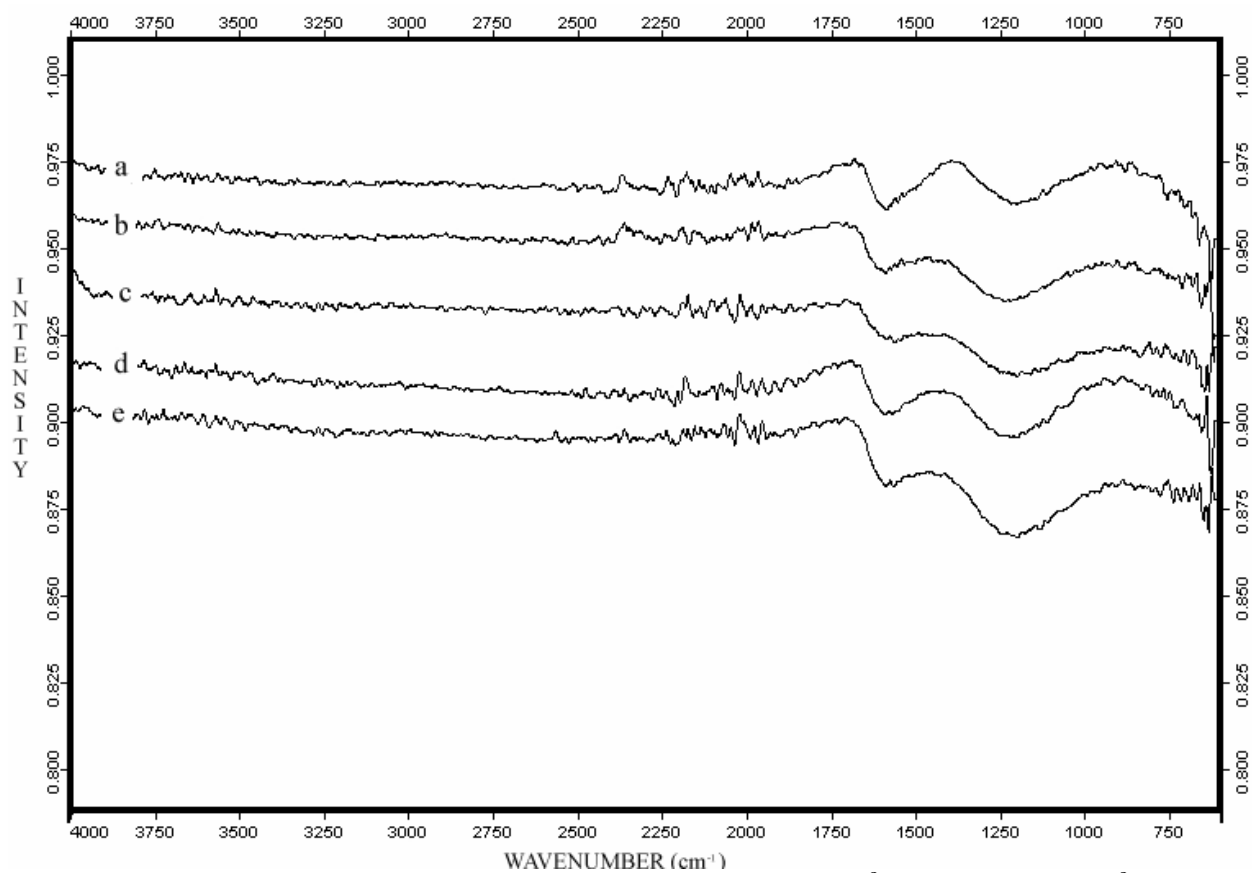
Figure 4.1.12. FT-IR spectra of carbon fibers carbonized at 800°C stabilized at 200°C for
  a) 1 hour b) 2 hours c) 3 hours d) 4 hours e) 5 hours

Interestingly, carbonized fibers at 800, 900 and 1000°C stabilized at 200°C have CO_2 peak near 2350 cm^{-1} (Figure 4.1.12-26) [62]. This might be due to CO_2 in air or burned and adsorbed to samples [50]. Around 3700 cm^{-1} aromatic alcohol O-H stretching was observed in small intensity. This peak gradually increased with increasing stabilization time.
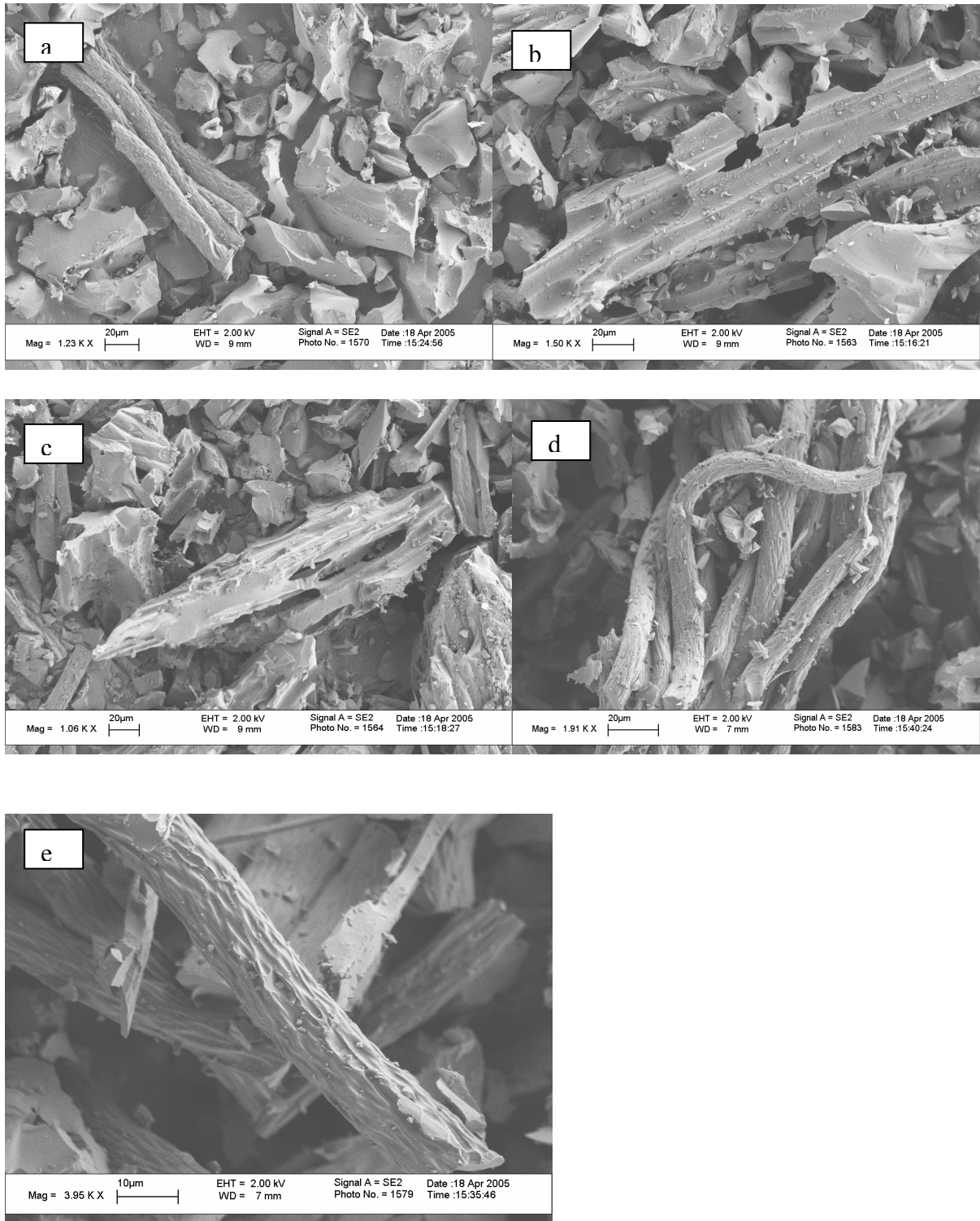
Figure 4.1.13. Carbon Fibers before carbonization at 900°C stabilized at 200°C in air media for a) 1 hours b) 2 hours c) 3 hours d) 4 hours e) 5 hours.

Figure 4.1.14. FT-IR spectra of carbon fibers carbonized at 900°C stabilized at 200°C for
a) 1 hour b) 2 hours c) 3 hours d) 4 hours e) 5 hours

Carbon Fibers carbonized at 900°C stabilized at 200°C in air media were transformed to granular activated carbon structures (Figure 4.1.13).
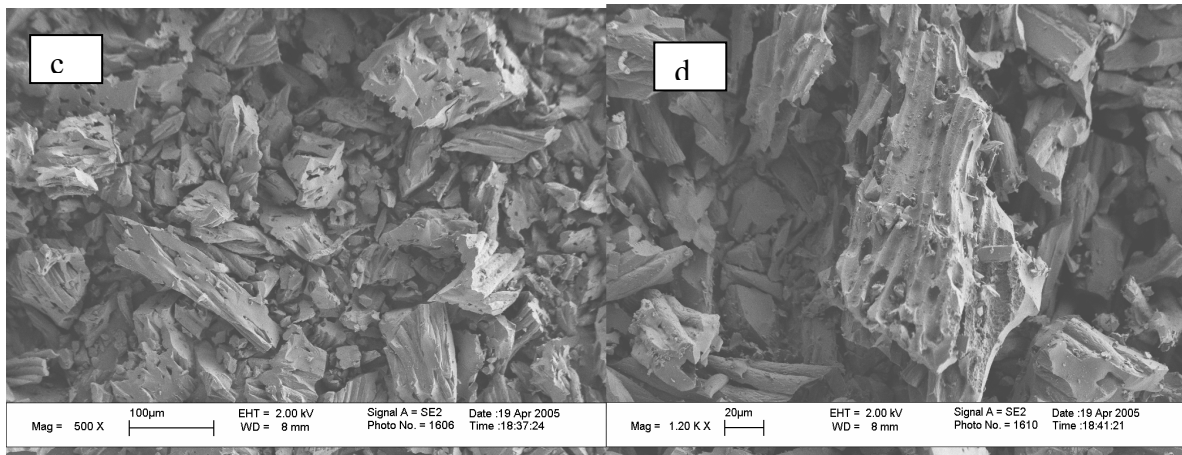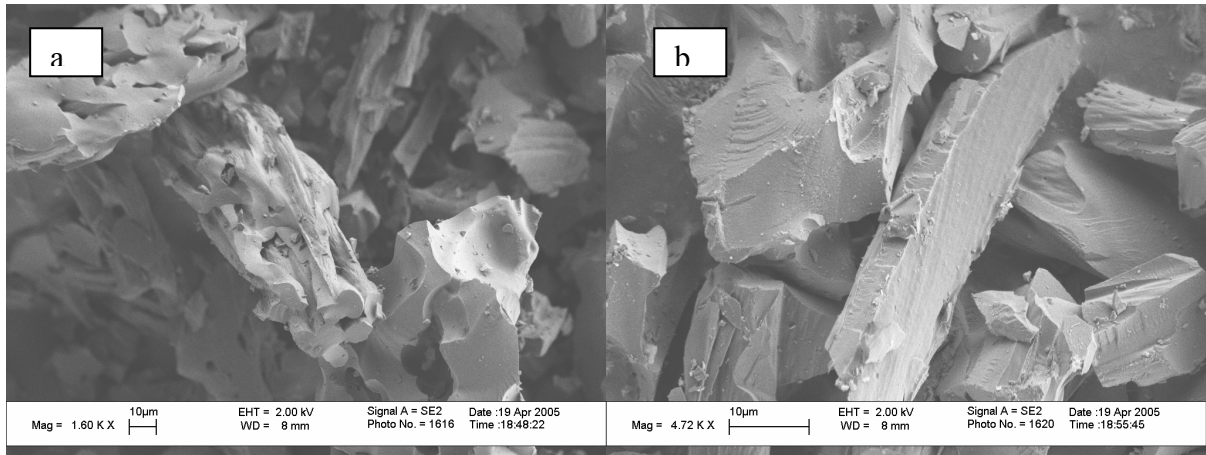
Figure 4.1.15. Carbon Fibers before carbonization at 1000°C stabilized at 200°C in air media for a) 1 hours b) 2 hours c) 3 hours d) 4 hours e) 5 hours.
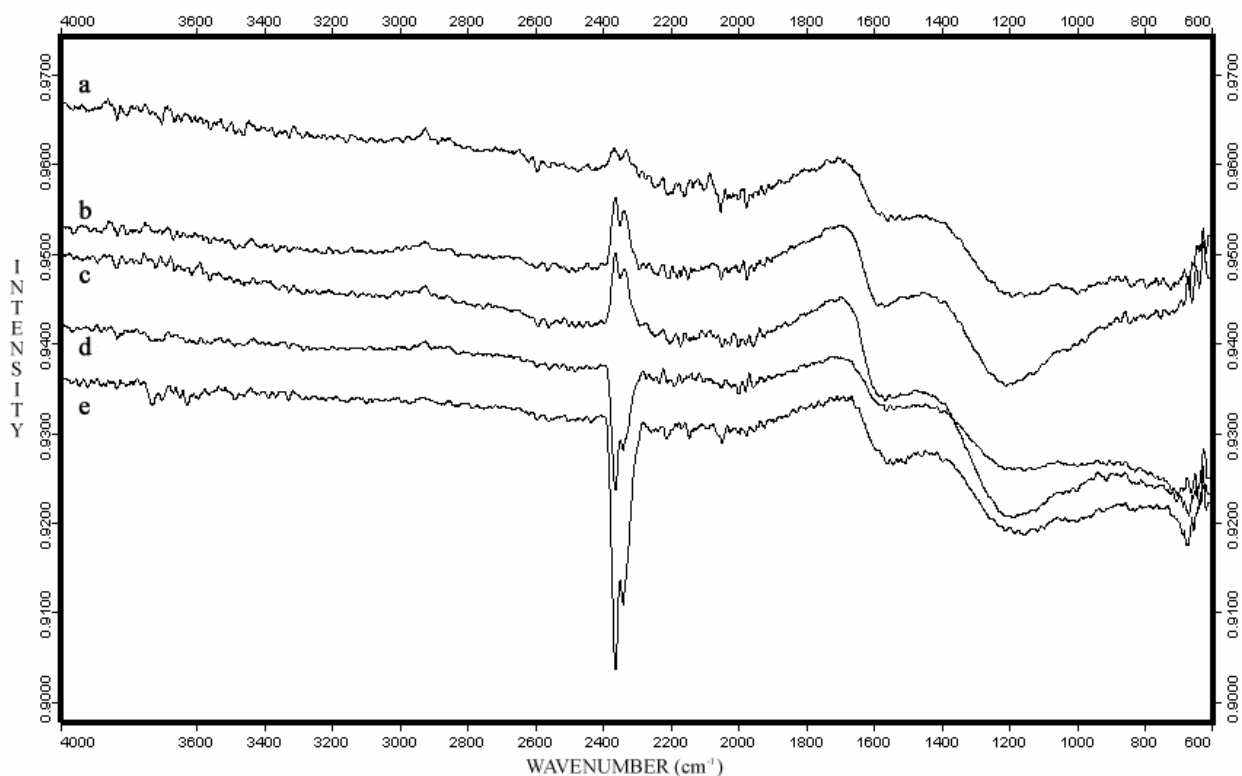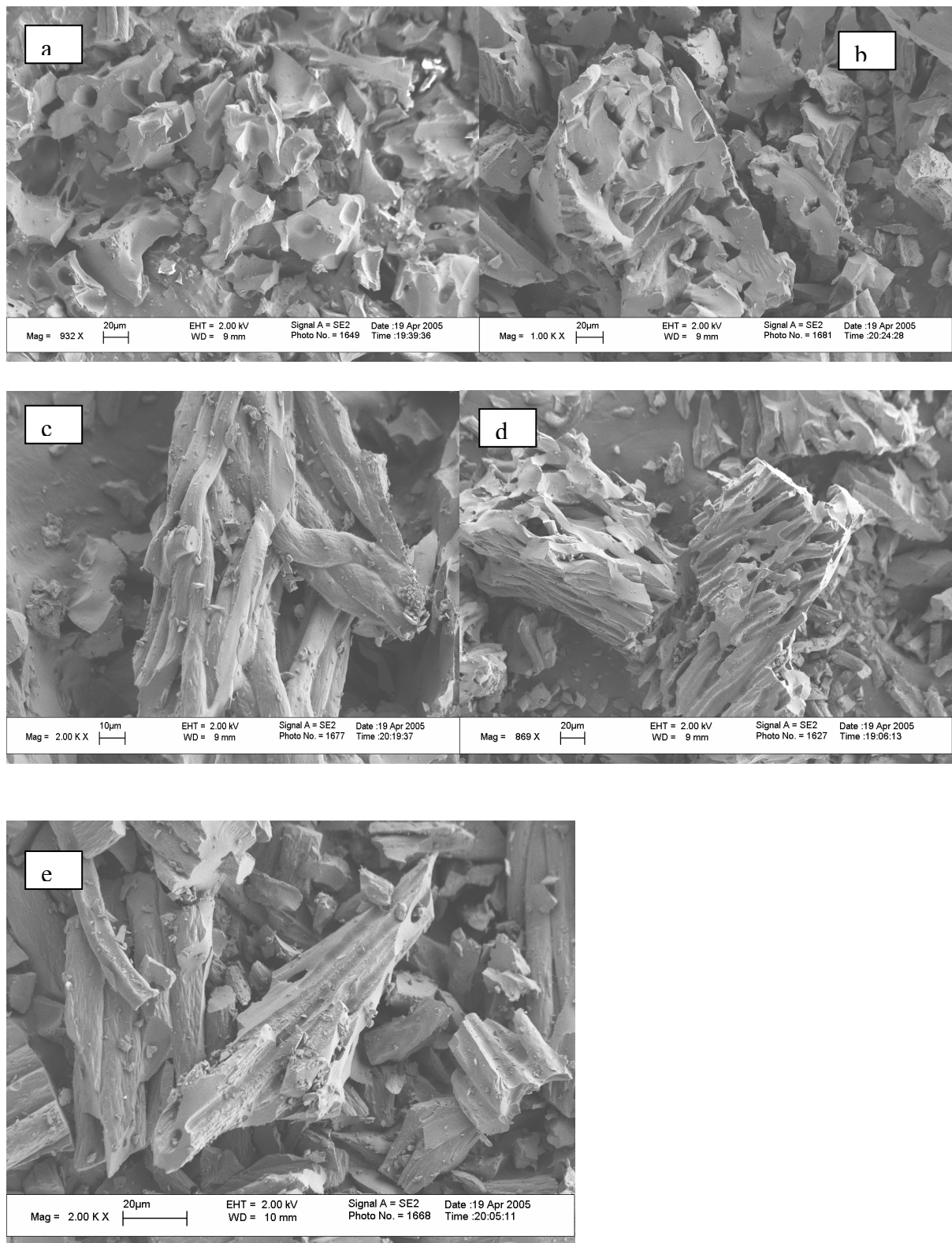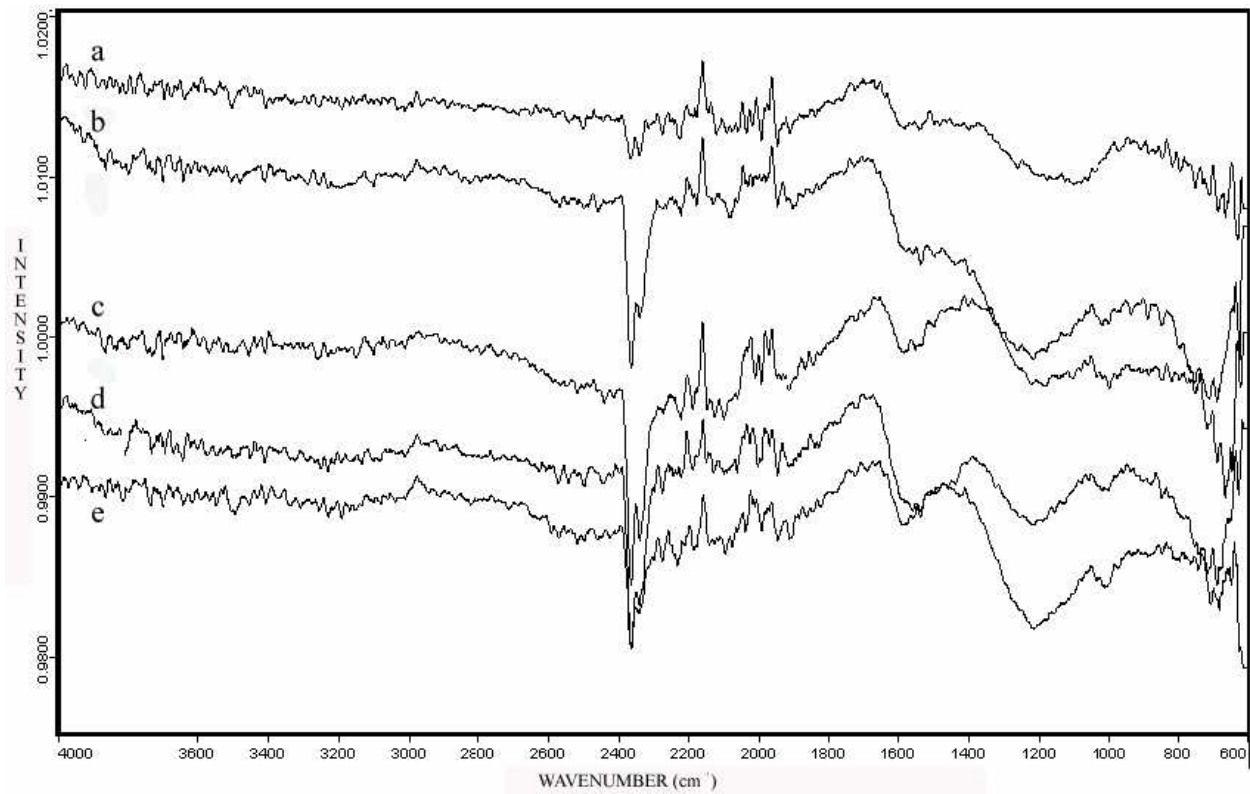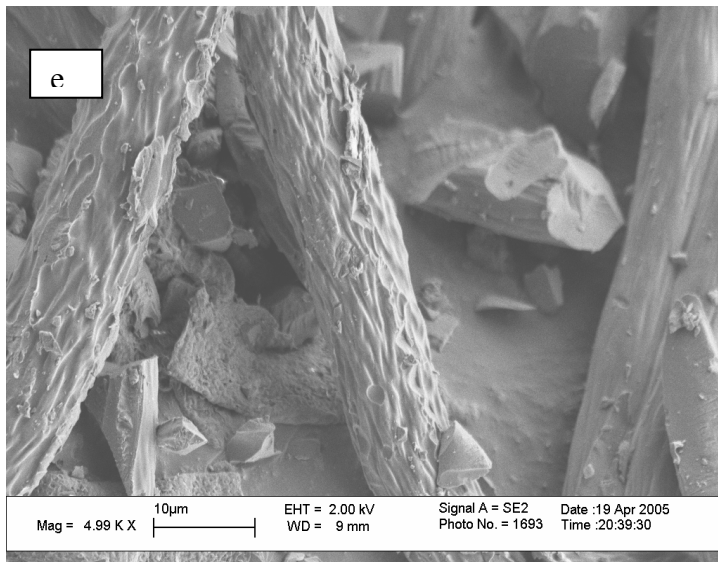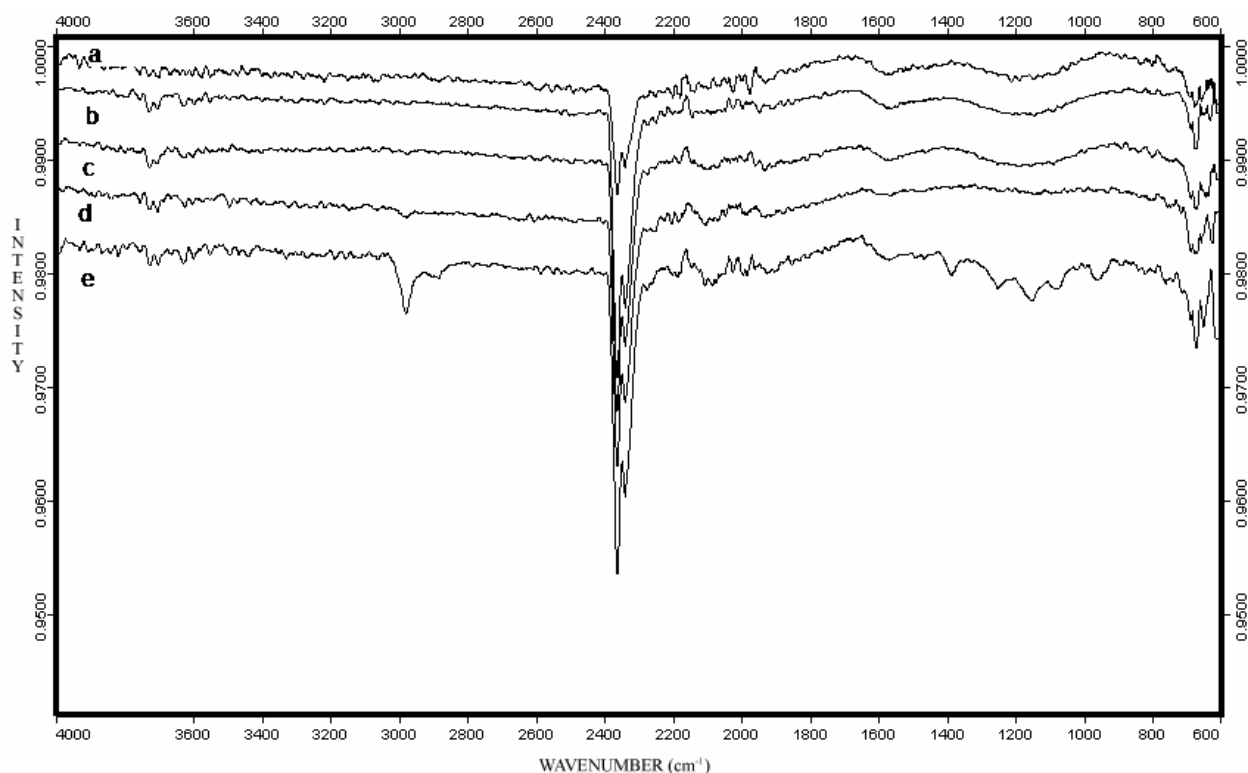
Figure 4.1.16. FT-IR spectra of carbon fibers carbonized at 1000°C stabilized at 200°C for a) 1 hour b) 2 hours c) 3 hours d) 4 hours e) 5 hours

Intermolecular cyclization occurred at 300°C more than at 200°C. That's why –CN or –C=N- peaks were still obtained even after carbonization of stabilized PAN fiber at 200°C in more amounts (Figure 4.1.23-24) [54]. FT-IR spectra of stabilized fibers at 200°C had CO_2 peak. However, this much weaker at 300°C stabilized fibers (Figure 4.1.25-Figure 4.1.28). SEM images showed especially surface was etched to an extent. This might be due to amorphous phase of PAN fiber was taken place on external surface. It was removed through high temperature (Figure 4.1.15). Carbon fiber stabilized at 200°C for 5 hours has peak at 3000 cm^{-1} of =C-H (Figure 4.1.16 and 4.1.28). Same –C-H- peak was observed at carbon fibers stabilized at 200°C.

	10µm	EHT = 2.00 kV	Signal A = SE2	Date :18 Apr 2005
Mag = 5.06 K X		WD = 9 mm	Photo No. = 1555	Time :15:03:19

	20µm	EHT = 2.00 kV	Signal A = SE2	Date :18 Apr 2005
Mag = 1.97 K X		WD = 9 mm	Photo No. = 1521	Time :14:07:43

	3µm	EHT = 2.00 kV	Signal A = SE2	Date :19 Apr 2005
Mag = 6.58 K X		WD = 9 mm	Photo No. = 1655	Time :19:47:37

Figure 4.1.17. Carbon Fibers before carbonization at 500°C stabilized at 300°C in air media for a) 0.5 hours b) 1 hours c) 2 hours.
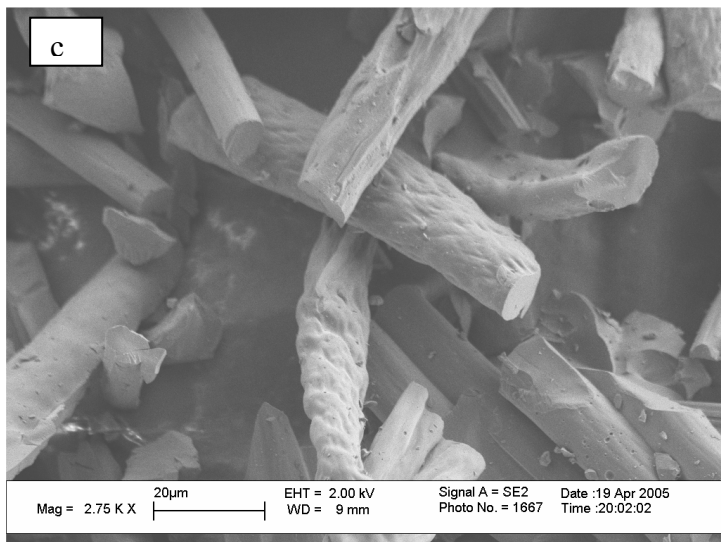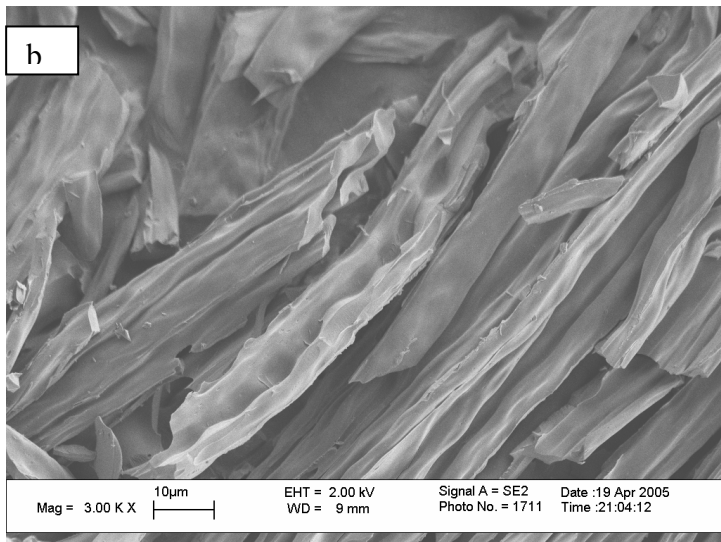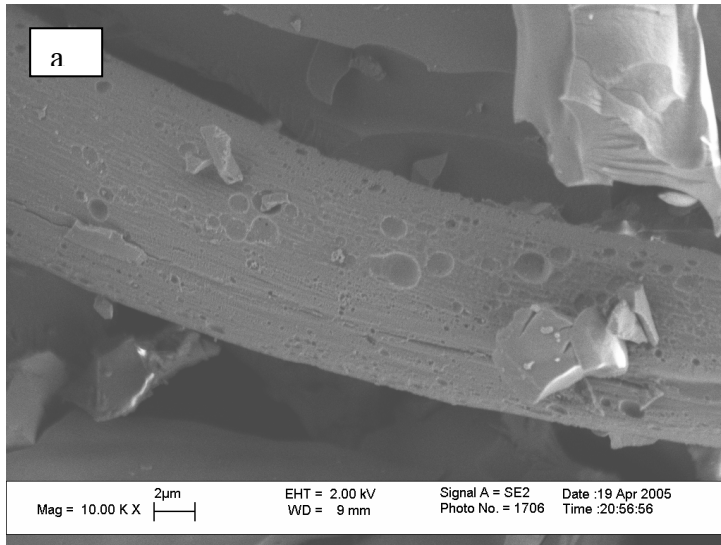
Figure 4.1.18. Carbon Fibers before carbonization at 600°C stabilized at 300°C in air media for a) 0.5 hours b) 1 hours c) 2 hours.
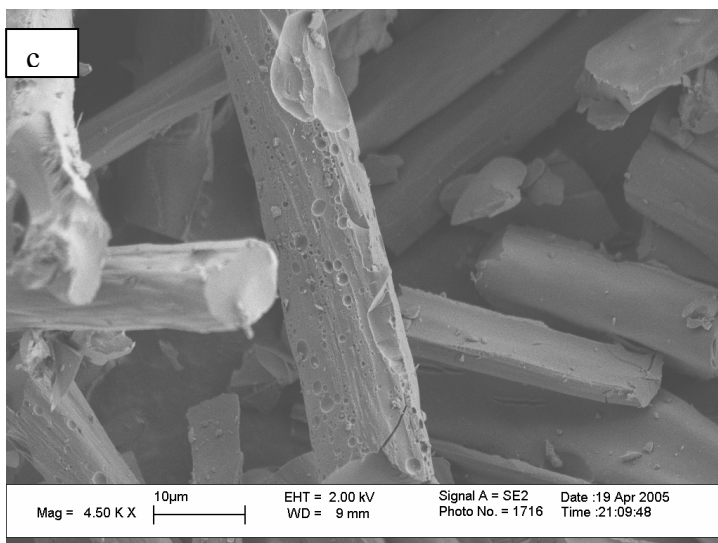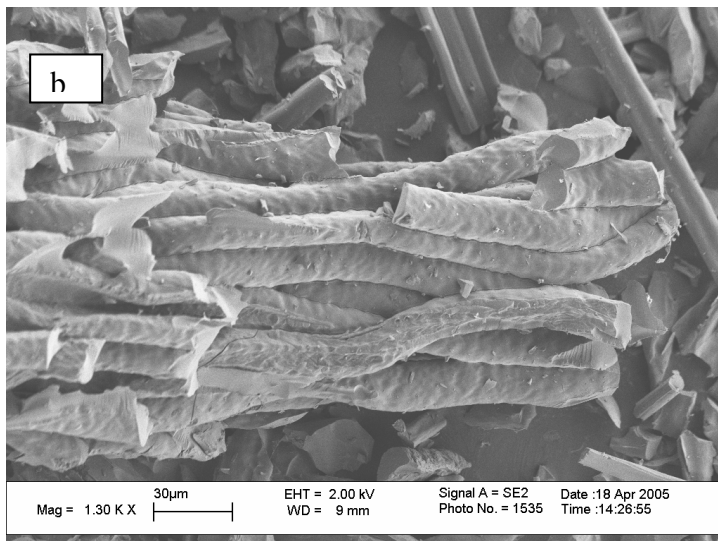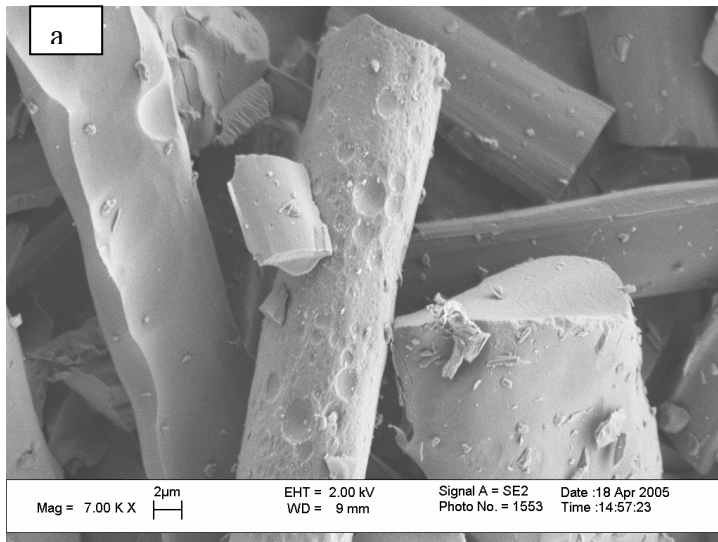
Figure 4.1.19. Carbon Fibers before carbonization at 700°C stabilized at 300°C in air media for a) 0.5 hours b) 1 hours c) 2 hours.
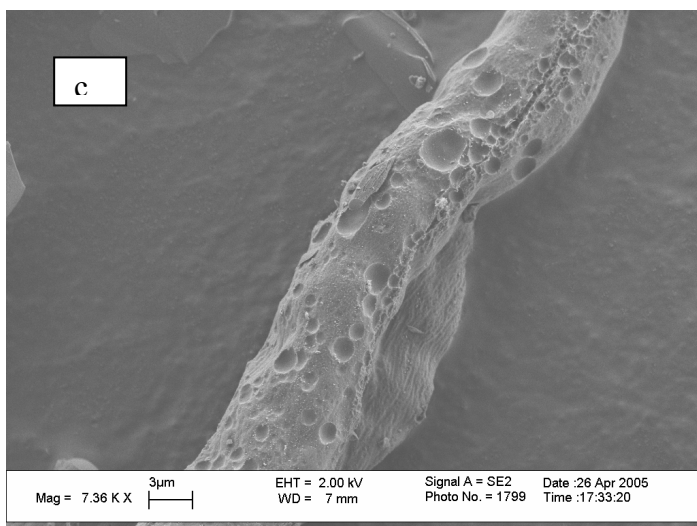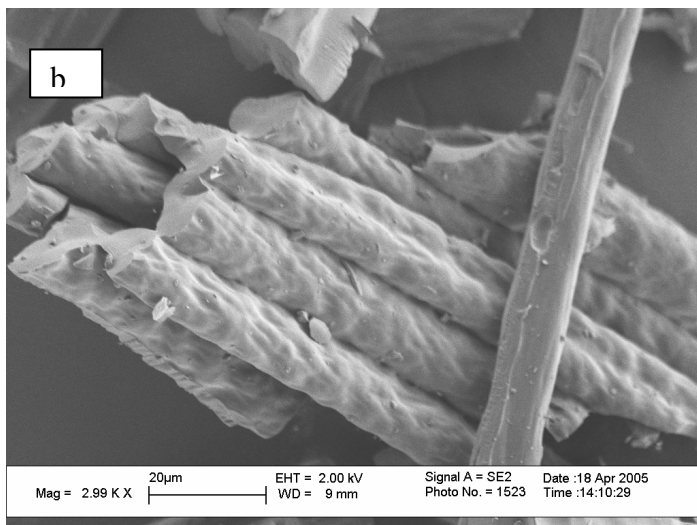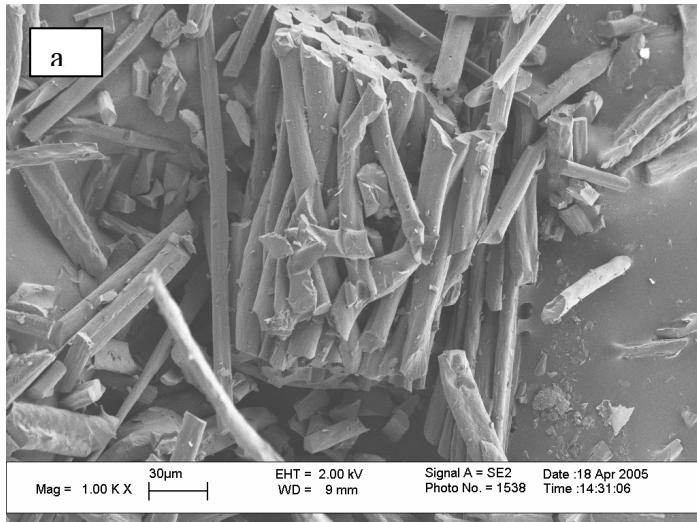
Figure 4.1.20. Carbon Fibers before carbonization at 800°C stabilized at 300°C in air media for a) 0.5 hours b) 1 hours c) 2 hours.
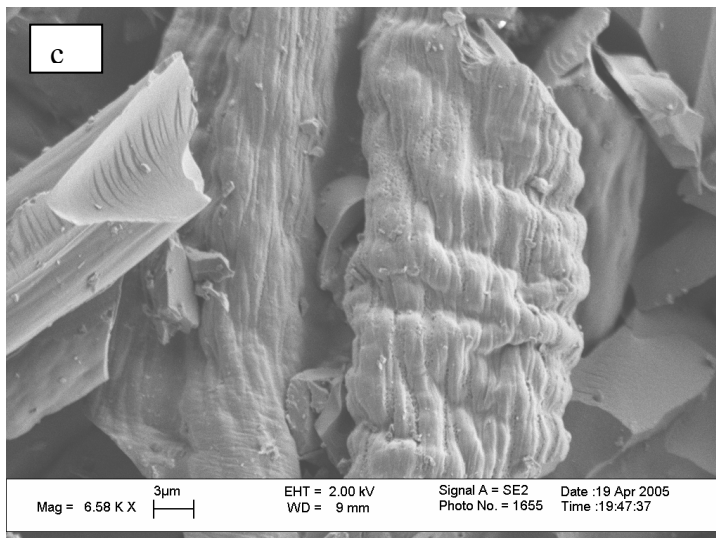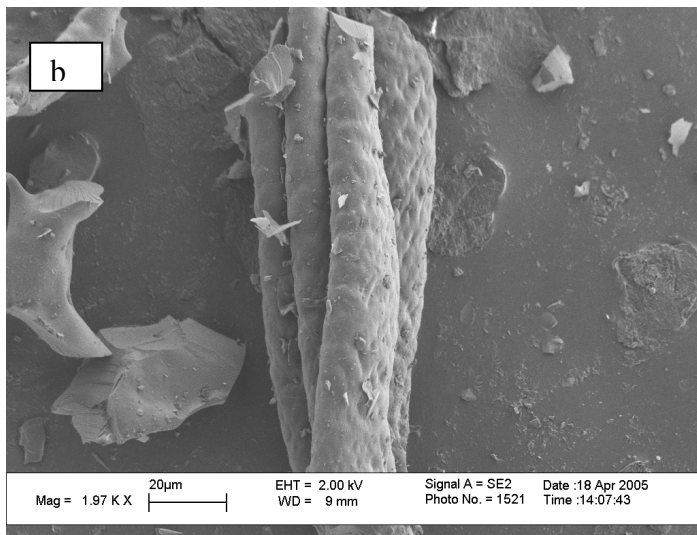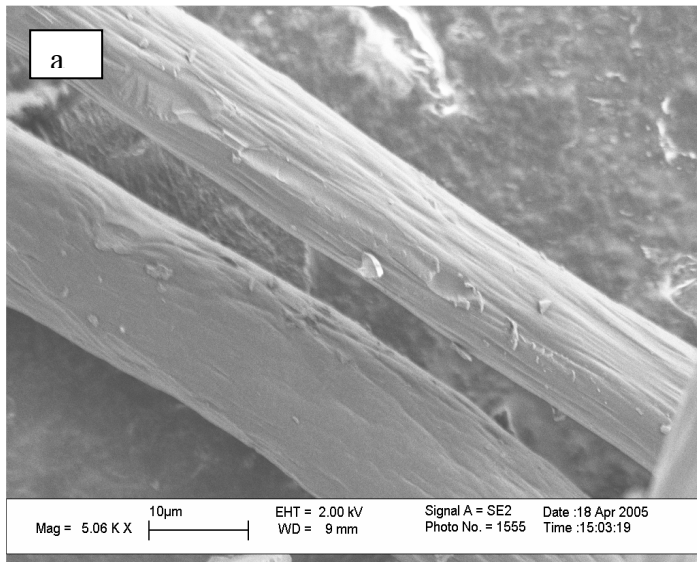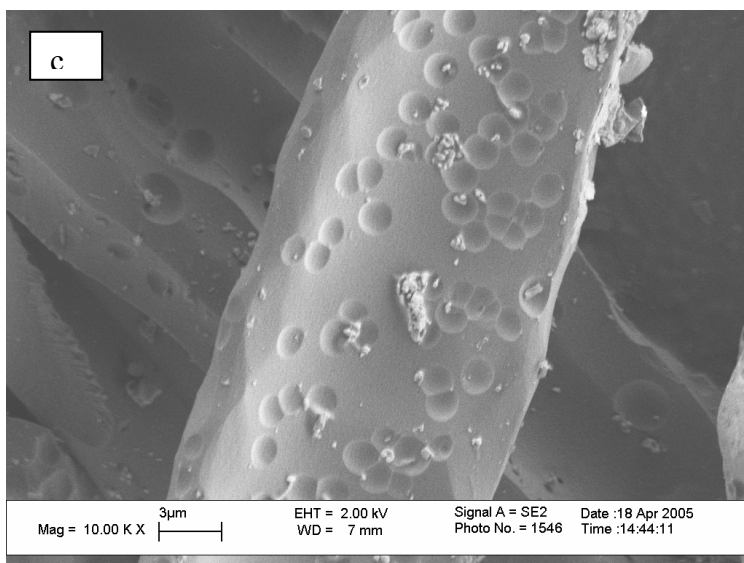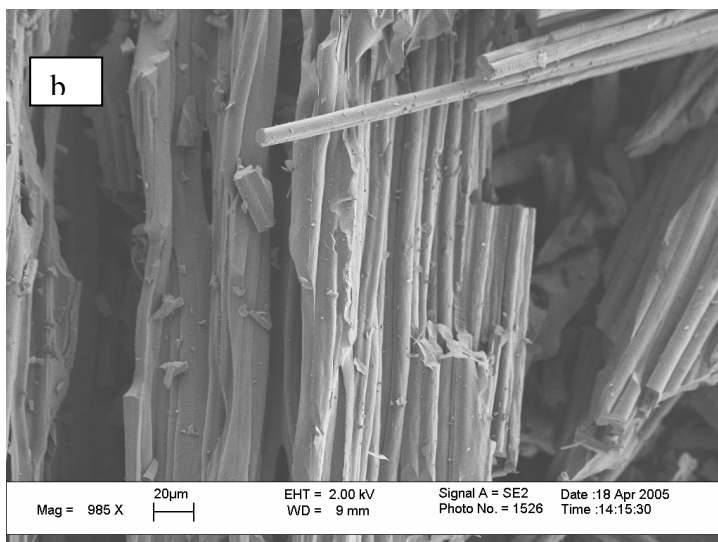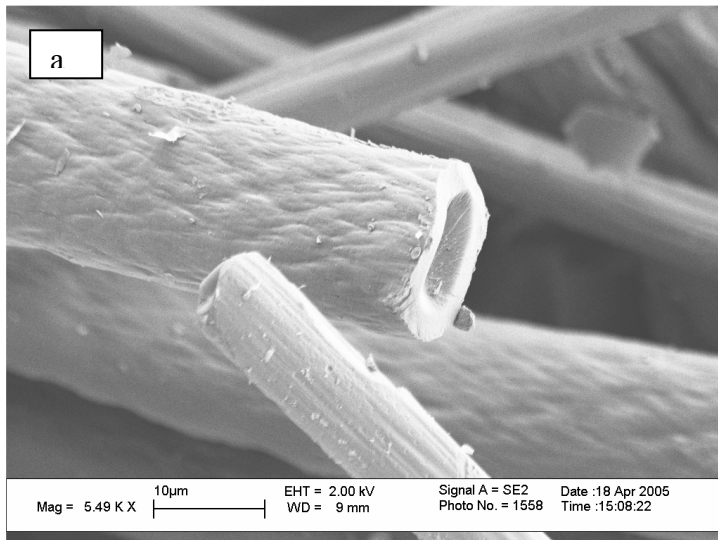
Figure 4.1.21. Carbon Fibers before carbonization at 900°C stabilized at 300°C in air media for a) 0.5 hours b) 1 hours c) 2 hours.
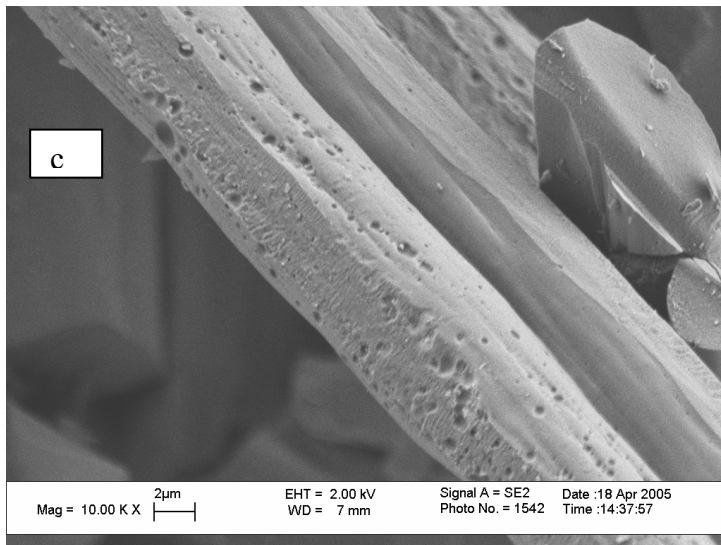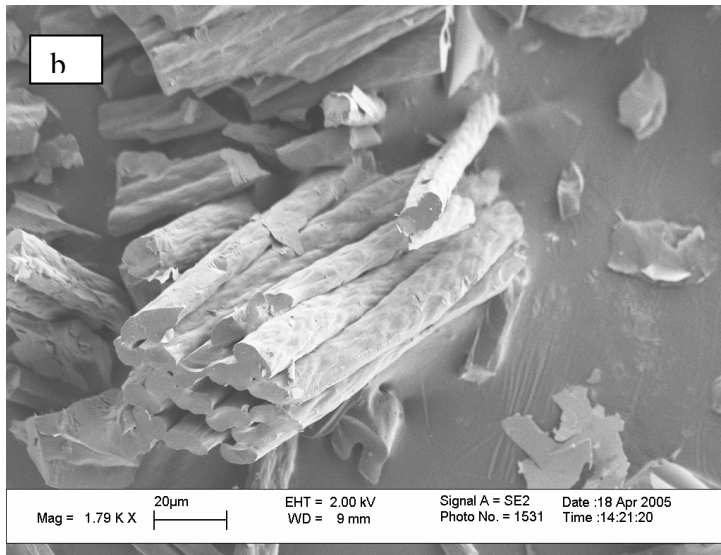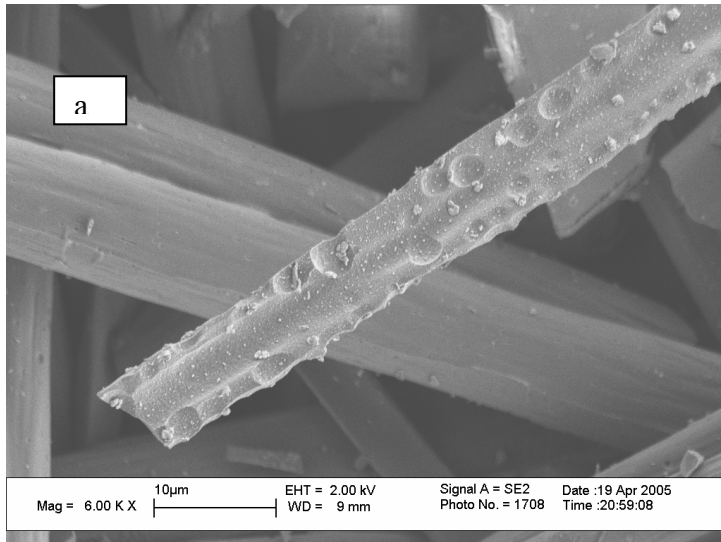
Figure 4.1.22. Carbon Fibers before carbonization at 1000°C stabilized at 300°C in air media for a) 0.5 hours b) 1 hours c) 2 hours.
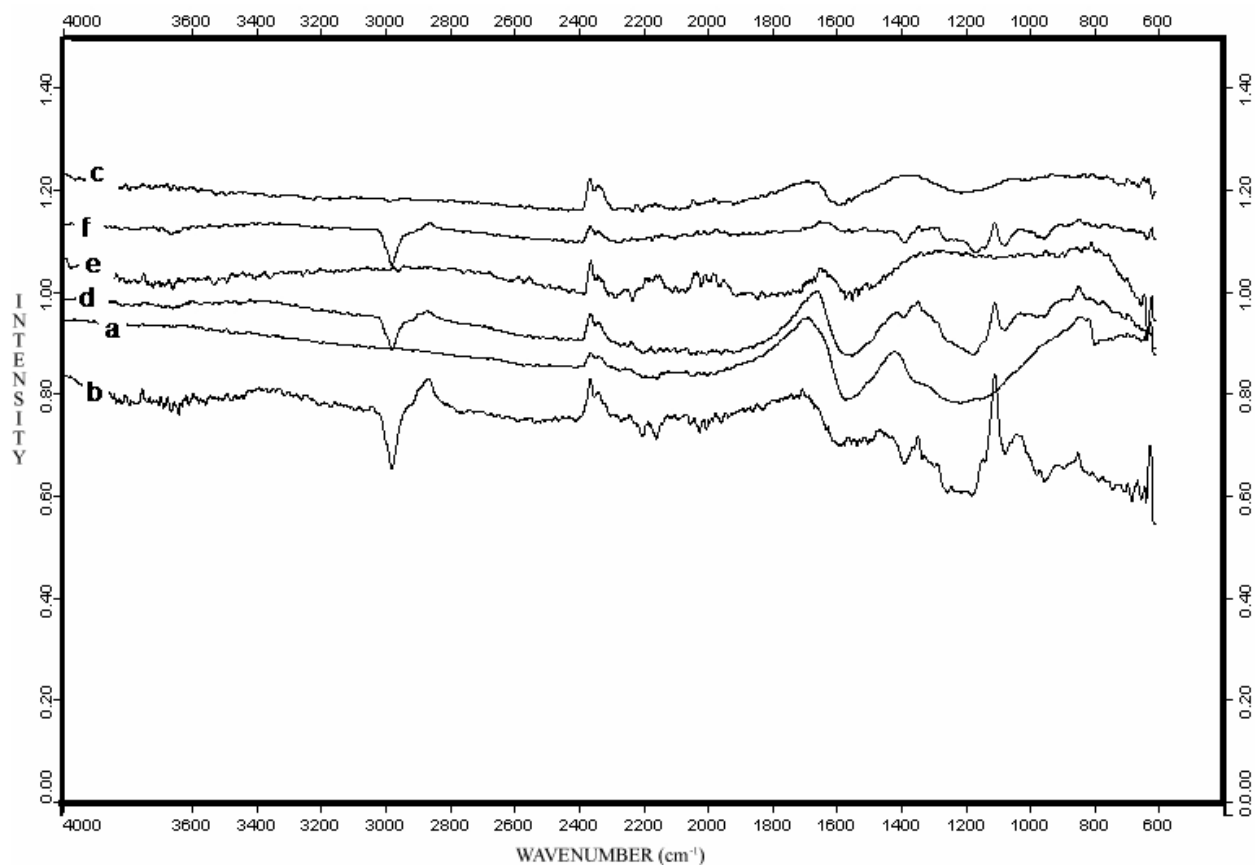
Figure 4.1.23. FT-IR spectra of carbon fibers stabilized at 300^oC for 0.5 hour a) 500^oC b) 600^oC c) 700^oC d) 800^oC e) 900^oC f) 1000^oC
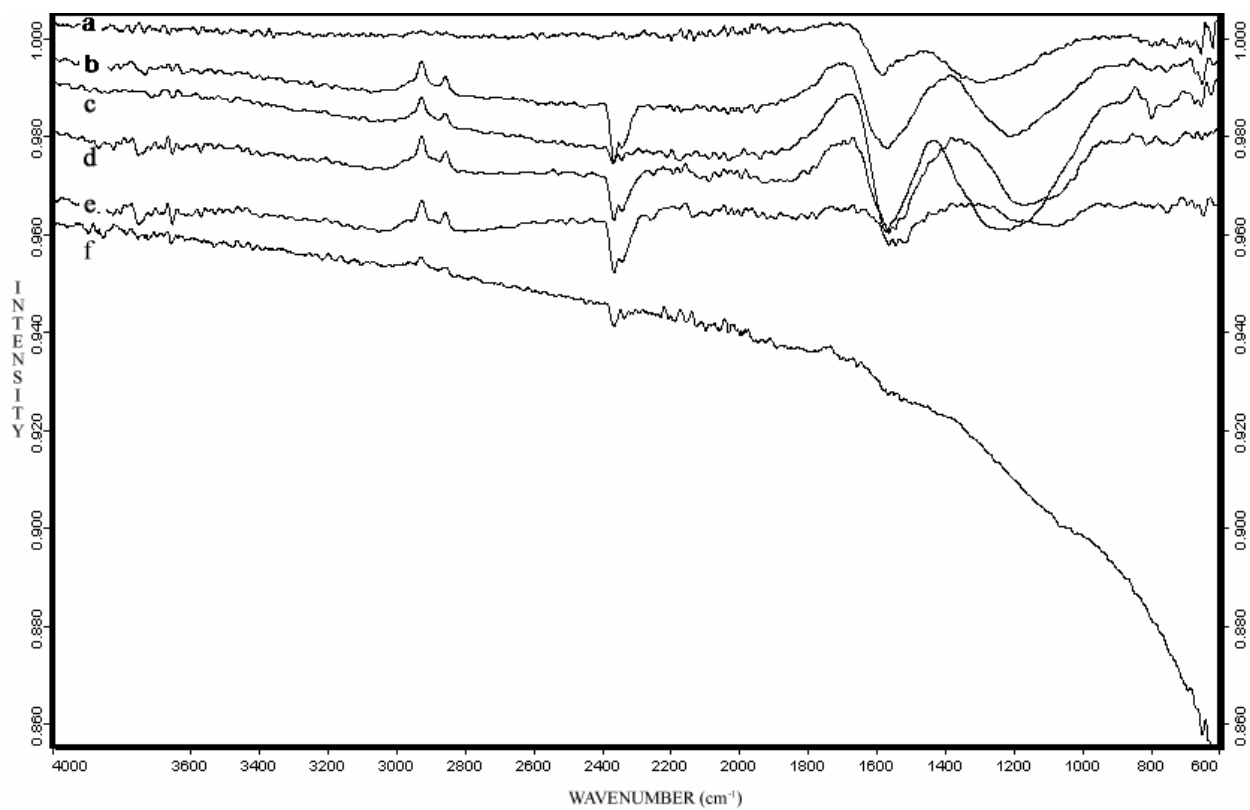
Figure 4.1.24. FT-IR spectra of carbon fibers stabilized at 300^oC for 1hour a) 500^oC b) 600^oC c) 700^oC d) 800^oC e) 900^oC f) 1000^oC

Oxidative stabilization at 300°C for 2 hours made fibers fractured to shorter fibers (Figure 4.1.17-22). Fibers probably were exposed to higher oxidation time that sheared chains. Peaks around 1450-1600 cm^{-1} might belong to enaminonitrile (=C-N-) formed due to partial cyclization or degradation [53-54]. SEM micrographs showed higher stabilization caused the diameter of fibers shrunk from 13 to 9μm (Figure 4.1.22). When the four fibers with the highest surface areas were examined, peaks at 2250 cm^{-1}, CO_2, were observed even after carbonization [62]. Pores seem to be smaller than the other carbon fibers stabilized at different times [51]. SEM images of stabilized precursors at 300°C for 1 hour showed these precursors were damaged more in oxidative media. This is also clear that fibers were exposed to higher scission due to presence of oxygen. Also FT-IR results show stabilized fibers at 300°C for 1 hour have more intense and shifted to lower frequency values for peak of –C=C- around 1580 cm^{-1} than precursors stabilized at 300°C for 0.5 and 2 hours (Figure 4.1.23-25). On the other hand 1 μm pores in diameter were observed in 5 h stabilization (Figure 4.1.15). When having a glance through carbon fibers stabilized at 300°C for 2 hours they have CO_2 peaks too (Figure 4.1.23-25). Gupta et al. [54] stated 300°C is not sufficient for stabilization. CO_2 groups still remained intact in carbon fiber samples after 300°C oxidative stabilization except 500°C. Nevertheless, stabilization at 300°C of PAN fibers showed that increase in stabilization times shifts peak at 1600 cm^{-1} to the lower frequency. This means formation of more conjugated –C=C- bonds (Figure 4.1.24). -O-H stretching vibration of C=N-OH was observed at 3650 cm^{-1} (Figure 4.1.29). Other characteristic vibration in oxime N-O stretching but this was concealed by peak of C=C-H.
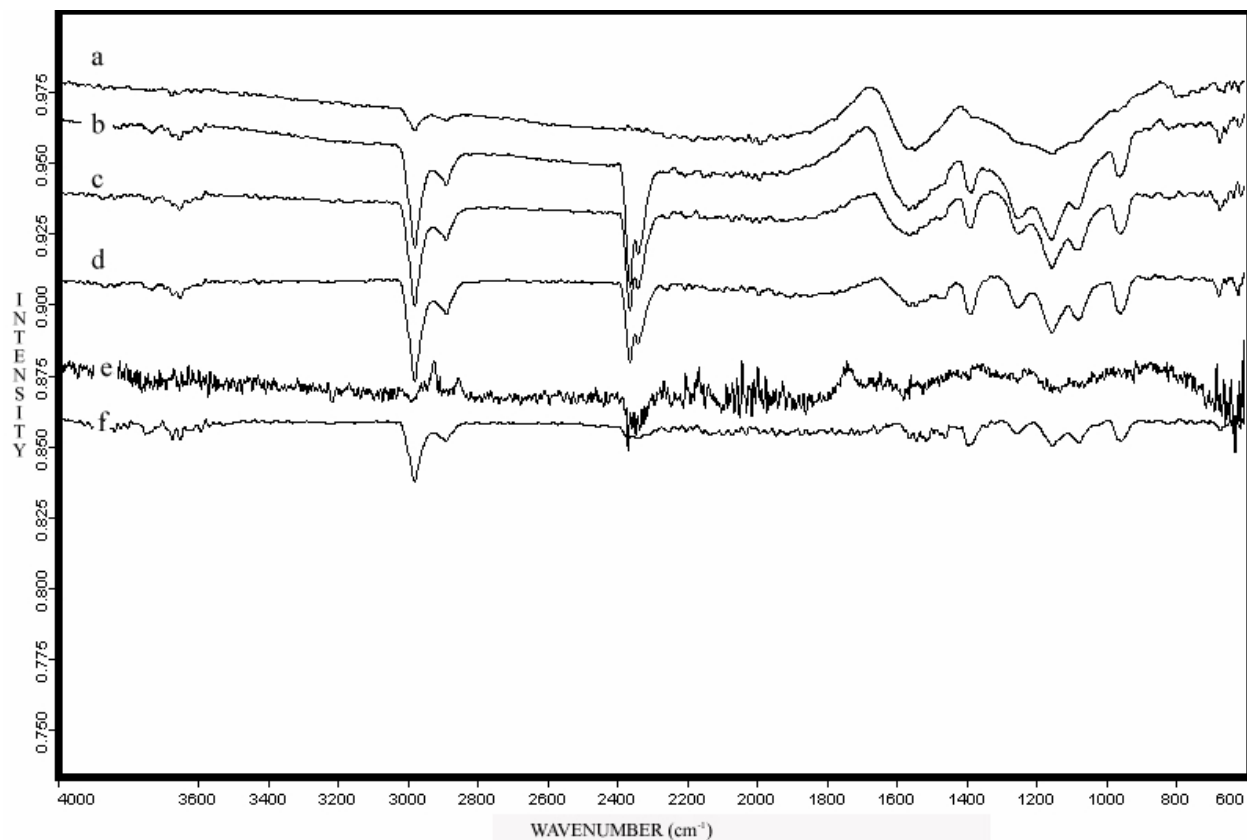
Figure 4.1.25. FT-IR spectra of carbon fibers stabilized at 300°C for 2hour a) 500°C b) 600°C c) 700°C d) 800°C e) 900°C f) 1000°C
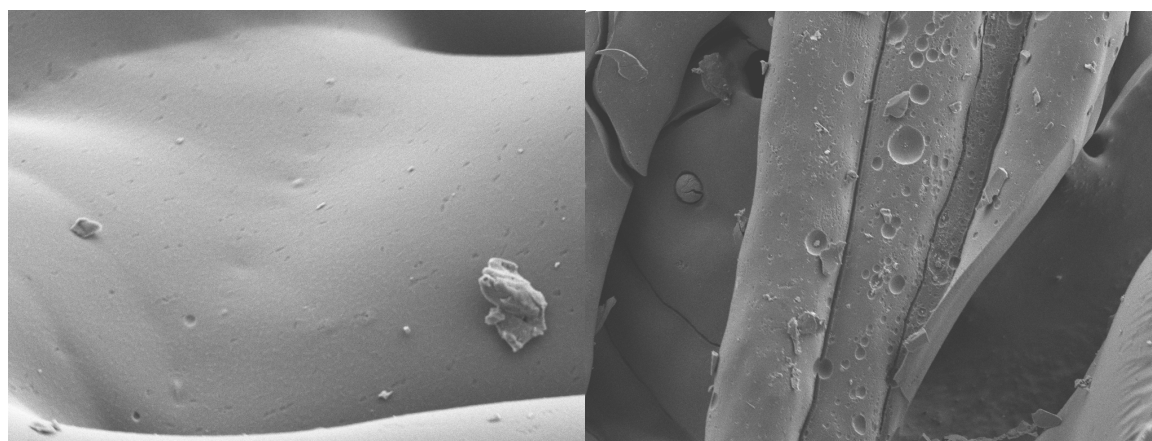
Figure 4.1.26. SEM Micrographs of Carbon Fibers activated at 800°C for 0.5 hour at CO_2 media
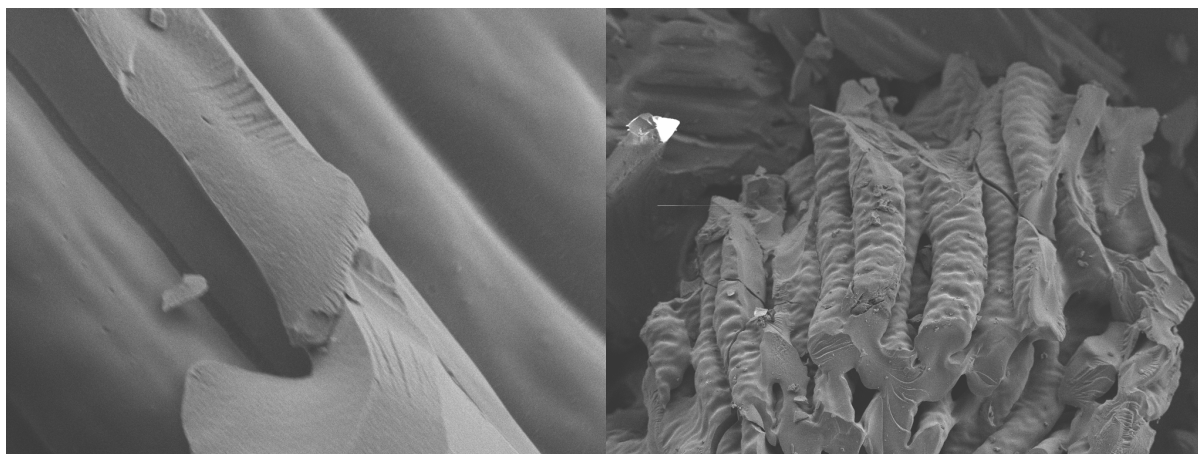
Figure 4.1.27. SEM Micrographs of Carbon Fibers activated at 800$^{\text{o}}$C for 1 hour at CO$_2$ media
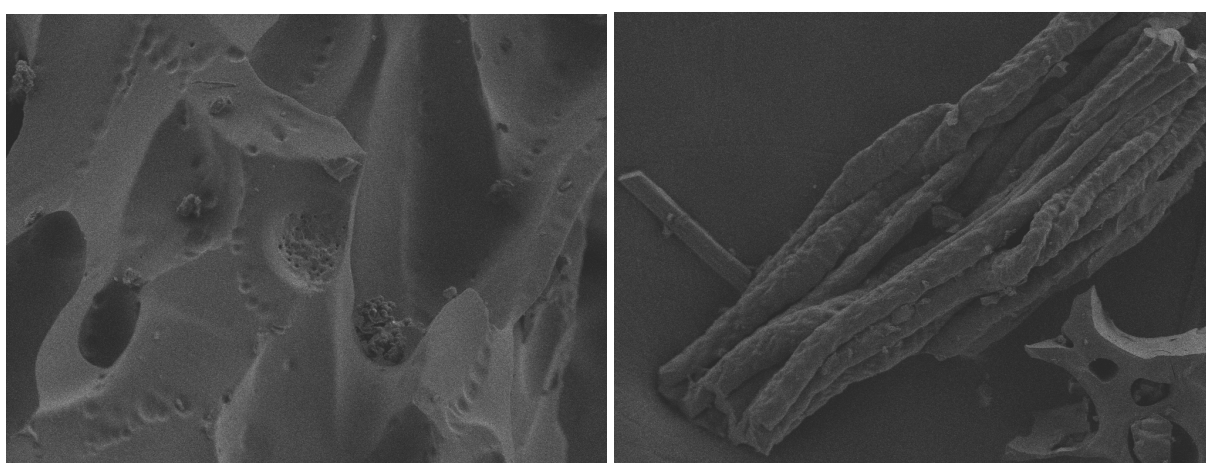
Figure 4.1.28. SEM Micrographs of Carbon Fibers activated at 900$^{\text{o}}$C for 1 hour at CO$_2$ media
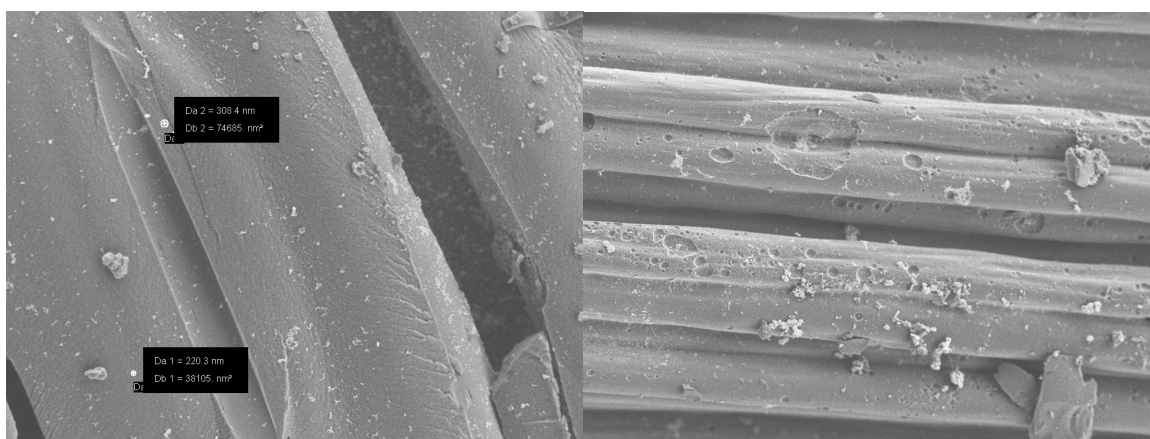
Figure 4.1.29. SEM Micrographs of %5 Pd-loaded Carbon Fibers activated at 800$^{\text{o}}$C for 1 hour at CO$_2$ media
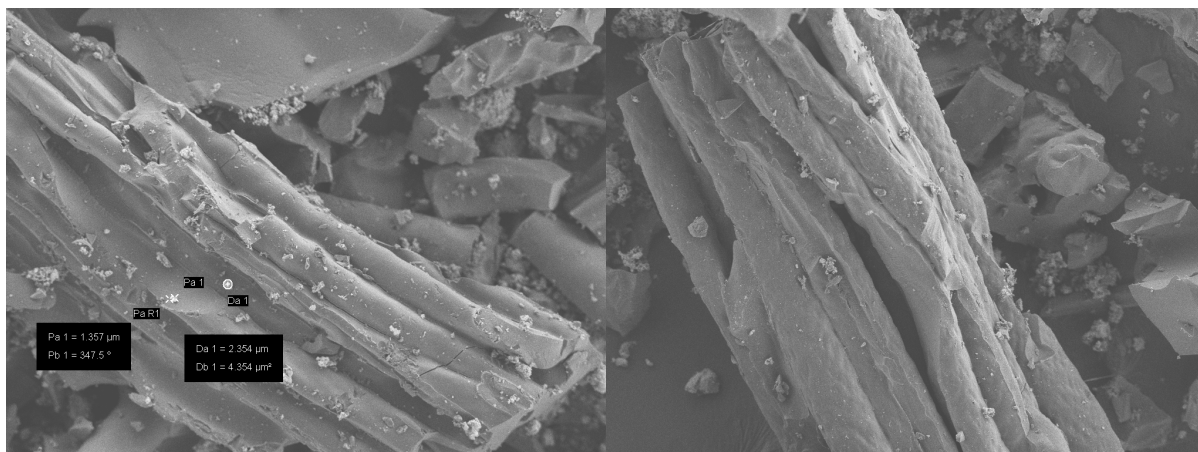
Figure 4.1.30. SEM Micrographs of %5 Pd-loaded Carbon Fibers carbonized at 800°C for 1 hour at N$_2$ media

SEM images showed us that stabilization step is really important steps in the carbonization. Oxidation of wet-spun PAN fibers made etched surface during carbonization step. Pores on the surface were determined by stabilization step. More oxidation of the surface created pores in variable sizes in 2-500nm. Pd particles were then examined with SEM. Their particle sizes are from 200 nm to 2.5 μm in diameter. It can be said Pd particles were dispersed well. However, clusters of particles were also observed. Carbon fibers carbonized activated at 800°C for 1 hour at CO$_2$ media had macropores (Figure 4.1.29). This might cause the loss of selectivity of catalyst systems. Since reactants in solution diffuse in and out from the pores easily. This means increase in catalytic activity. However, selectivity probably will decrease.
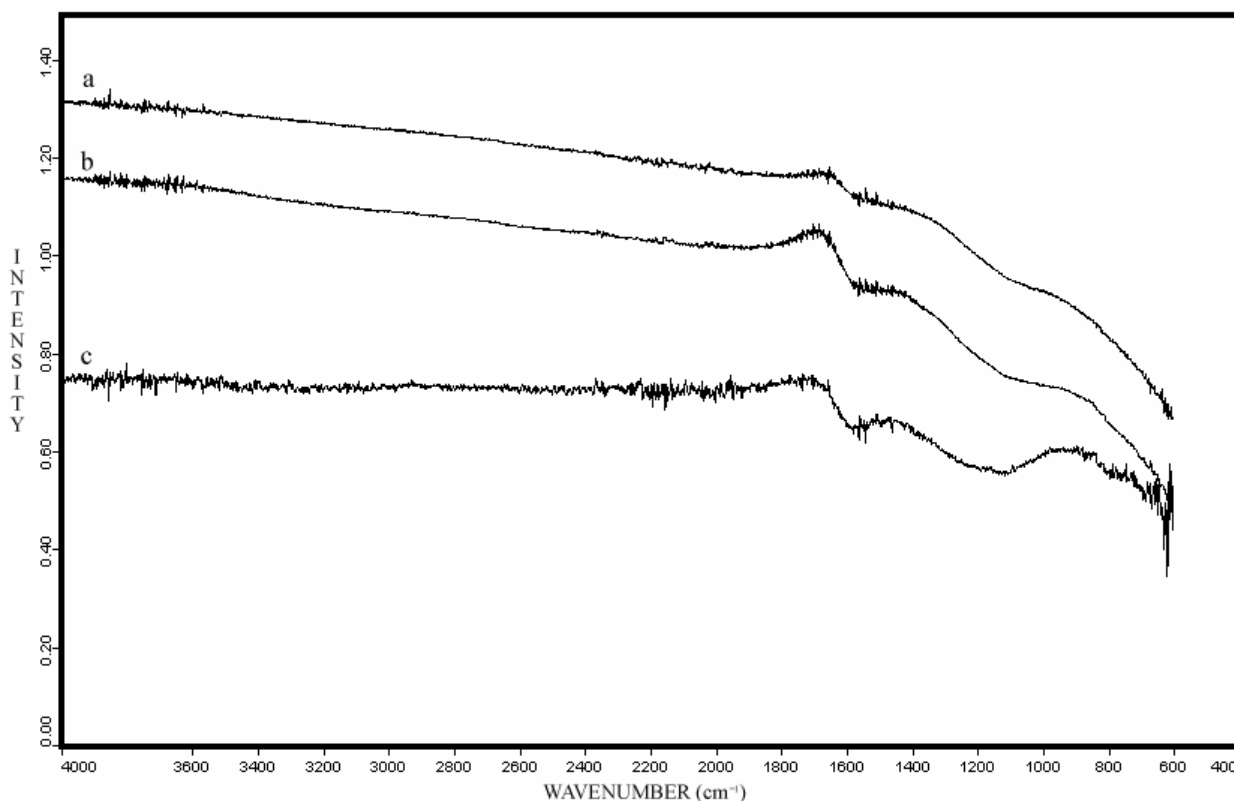
Figure 4.1.31. FT-IR spectra of carbon dioxide-activated carbon fibers a) Carbon Fiber activated at 800C for 0.5h b) Carbon Fiber activated at 800C for 1h c) Carbon Fiber activated at 900C for 1h (All PAN fibers were previously stabilized at 300C for 1 h in air media)

Activating agents attack to edges and non-regular parts of basal planes containing nitrogen [54]. Enough stretch applied to PAN induces fiber orientation more [54]. Wang et al. proposed activating agent preferentially interacts with heteroatoms. This removes nitrogens from the structure and increases the C/N ratio. Our observations were in accordance with those of Wang's. In the activation of carbon fibers by CO_2 we did not observe any –CN peak in the FTIR spectra (Figure 4.1.31). However, there might be still – C=N- under the 1600 cm^{-1} band. Peaks at 1200 and 1600 cm^{-1} were more visible in the carbonized fibers produced at 900°C than ones carbonized at 800°C for 0.5 and 1 hour. Higher extent of activation under an atmosphere of CO_2 made more ordered graphitic layers proved by FT-IR. The higher temperature was also enough to suppress entropy of carbon fibers to make closed pores [27]. Carbon fiber activated at 900°C for 1 hour in media of CO_2 had smaller surface area. On the other hand, 800°C was more practicable to generate ACFs have higher surface areas (Table 4.2.1).

50

4.2. Surface area and Pore distributions of Activated and Non-Activated Carbon Fibers

Adsorption processes can be divided into three to four stages with relative pressures of 10^{-6}–10^{-4}, 10^{-4}–10^{-2}, 10^{-2}-10^{-1}, 0.9-1.0. These can be ascribed to the multistage pore filling process (i) the filling of narrow micropores such as ultramicropores, (ii) the formation of a monolayer on the surfaces of wider micropores such as supermicropores and small mesopores, (iii) the filling of mesopores by capillary condensation, and (iv) the filling of macropores by capillary condensation, which takes place at a relative pressure close to unity [63].

When pore distributions of CFs and ACFs were compared it was observed that the carbon fibers carbonized at 600°C and stabilized at 300°C for 1 hour had mainly 3nm pores in diameter (Figure 4.2.2). There were smaller amounts of 4.7 and 10 nm pores in diameter. CF carbonized at 700°C and stabilized at 300°C for 1 hour had also pore in 3nm and 70nm in smaller amounts (Figure 4.3.4). CF carbonized at 800°C and stabilized at 300°C for 1 hour had more complicated pore distribution. It had 1.5, 2.1, 3, 5   and 70nm pore in decreasing amounts. It was similar to CF carbonized at 800°C and stabilized at 300°C for 1 hour. But latter one also had 2.5 and 70nm pores (Figure 4.2.6).

Carbon fibers activated by carbon dioxide at 800°C for 0.5 hour and stabilized at 300°C for 1 hour contained pores with diameter of 110 nm (Figure 4.2.10). However, CF activated by carbon dioxide at 800°C for 1 hour and stabilized at 300°C had pores with 82 nm diameter (Figure 4.2.12). CF activated by carbon dioxide at 900°C for 1 hour and stabilized at 300°C had variable pores changing in diameter from 1.5nm to 18 nm in a decreasing trend in terms of number of pores that was similar to that of carbon fiber activated by $AlCl_3$-Et_2O at 800°C for 1 hour and stabilized at 300°C (Figure 4.2.14- Figure 4.2.16). These results showed activation made smaller pores converted to the bigger pores from 3nm to approximately 100nm. This was arising from CO_2. This was reflected less to the surface area. Surface area increased approximately 30%. However, the surface area of fiber decreased after the activation done by $AlCl_3$. Smaller pores were formed by activation with $AlCl_3$. However, decrease of surface area was due to increase in graphitization of fiber by aid of evolving ethoxy groups from diethyl ether. When the fibers activated for 0.5 and 1 hour by CO_2 were compared, it was observed that longer activation times made pores smaller. This was due to CO_2 damaged surface and created smaller pores in larger amounts. Also FT-IR images showed longer activation times made intense peak of -C=C- at 1600cm^{-1} (Figure 4.1.31). This was probably due to the ordering of graphitic sheets on the surface. However, CF activated by carbon dioxide at 900°C

for 1 hour and stabilized at 300°C had pores in different distributions. BJH pore distribution trend of carbon fibers carbonized at 600, 700, 800, 900°C was such that number of pores in 1.5 nm were taken place at carbon fibers carbonized at 800, 900°C ten times bigger than carbon fiber carbonized at 600 and 700°C (Figure 4.3.1- Figure 4.3.16). However, carbon fiber carbonized at 800°C had pores approximately 1.5 nm twice more than carbon fiber carbonized at 900°C (Figure 4.3.6, Figure 4.3.8). This microporous character gave carbon fiber carbonized at 800°C had the largest surface area. But after activation this microporous character vanished in the presence of CO_2 (Figure 4.3.6, Figure 4.3.10). Interestingly, activated carbon fiber by $AlCl_3$-Et_2O had ten times more 2nm pores than carbon fibers carbonized at 800°C (Figure 4.2.6, Figure 4.2.16). Although they were treated in nitrogen atmosphere and same temperature, activated carbon fiber by $AlCl_3$ had smaller area than CF carbonized at 800°C.

Carbon Fiber activated by carbon dioxide at 900°C for 1hour and stabilized at 300°C for 1 hour carbon fiber activated by $AlCl_3$-Et_2O at 800°C for 1 hour and stabilized at 300°C for 1 hour had a mesoporous structure (Figure 4.2.13-Figure 4.2.15). However, carbon fibers carbonized at 800°C for 1hour and stabilized at 300 ^{o}C for 1 hour and at 900°C for 1hour and stabilized at 300°C for 1 hour indicated a steep curve at near P/P_o equals to 1. This was probably the beginning of capillary condensation in mesopores and macropores due to high relative pressure (Figure 4.2.5- Figure 4.2.7). The initial part of the isotherm was observed as micropores. The plateau in the isotherm belonged to adsorption of nitrogen to meso- and macropores on the surface (Figure 4.2.1). In some isotherms there was a decrease in the volume of adsorbed nitrogen. This was probably because of formation of layers on the surface (Figure 4.2.3). Capillary condensation occurs at the last part of the isotherm. These isotherms showed that main pore diameters of the fibers decreased with increasing temperature. Surface area of fibers did not show the same trend. Carbon fiber carbonized at 600°C and 800°C had nearly the same surface area. These fibers were filled even at P/P_o was below 0.1 that indicated fibers were microporus. But if higher relative pressures could be obtained, adsorption onto fiber capillar condensation might begin. These type isotherms probably indicated continual interconnection of pores even inside of the fiber. Most of nitrogen uptake occurred at relative pressure lower than 0.1 (Figure 4.2.7). Nitrogen uptake of carbon fiber activated by carbon dioxide at 900°C for 1hour and stabilized at 300°C for 1 hour (Figure 4.2.13) was much lower than other samples. It had rather a curve that increase with increasing relative pressure. This was indicative of mesoporous structure. Micropores was rather widened by CO_2 etching. All isotherms showed a wide hysterisis loop. This emphasized all fibers had variable pore distribution.
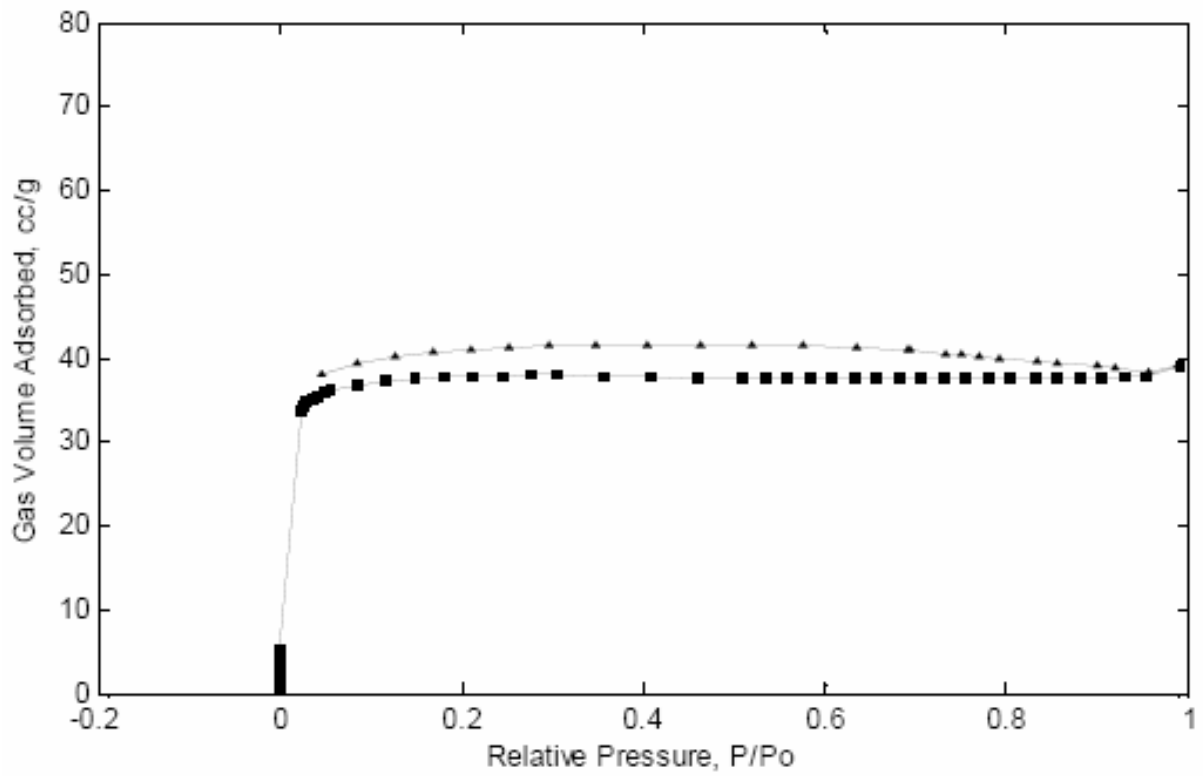
Figure 4.2.1. BET graph of Carbon Fiber carbonized at 600°C for 1hour and stabilized at 300 ^{o}C for 1 hour.
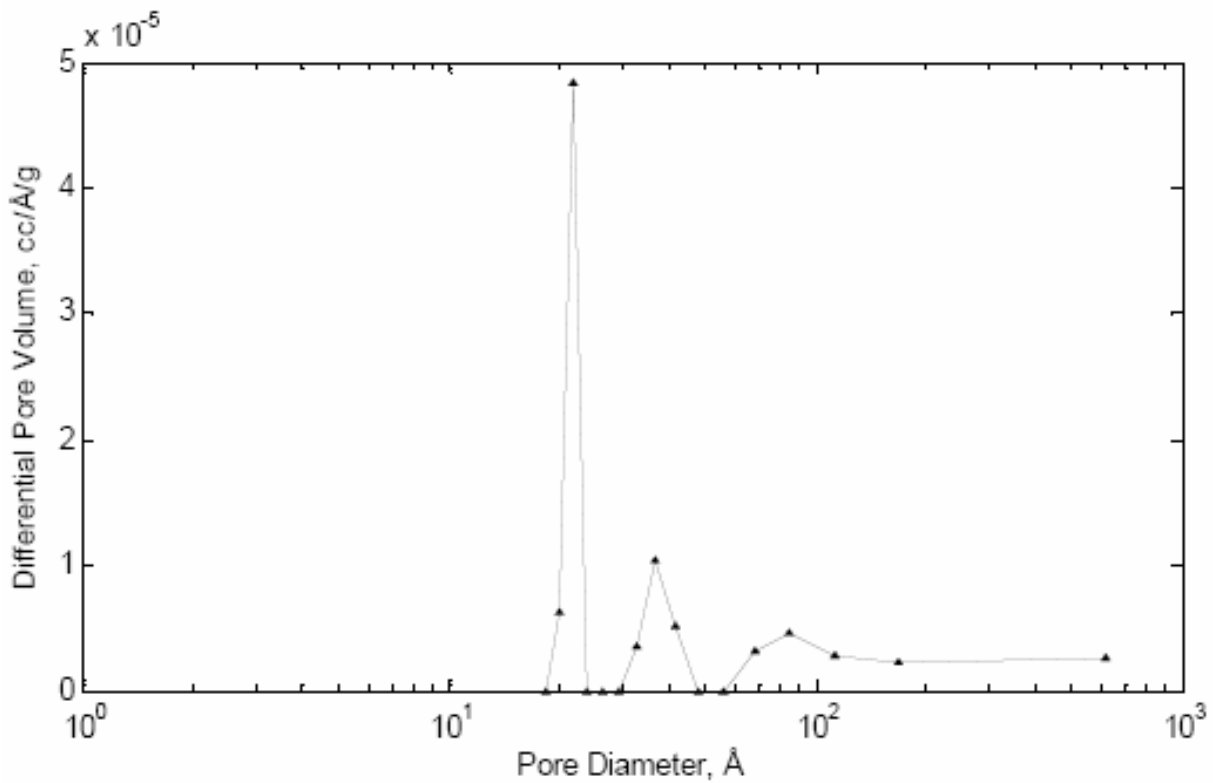
Figure 4.2.2. BJH pore distribution graph of Carbon Fiber carbonized at 600°C for 1 hour and stabilized at 300 ^{o}C for 1 hour.
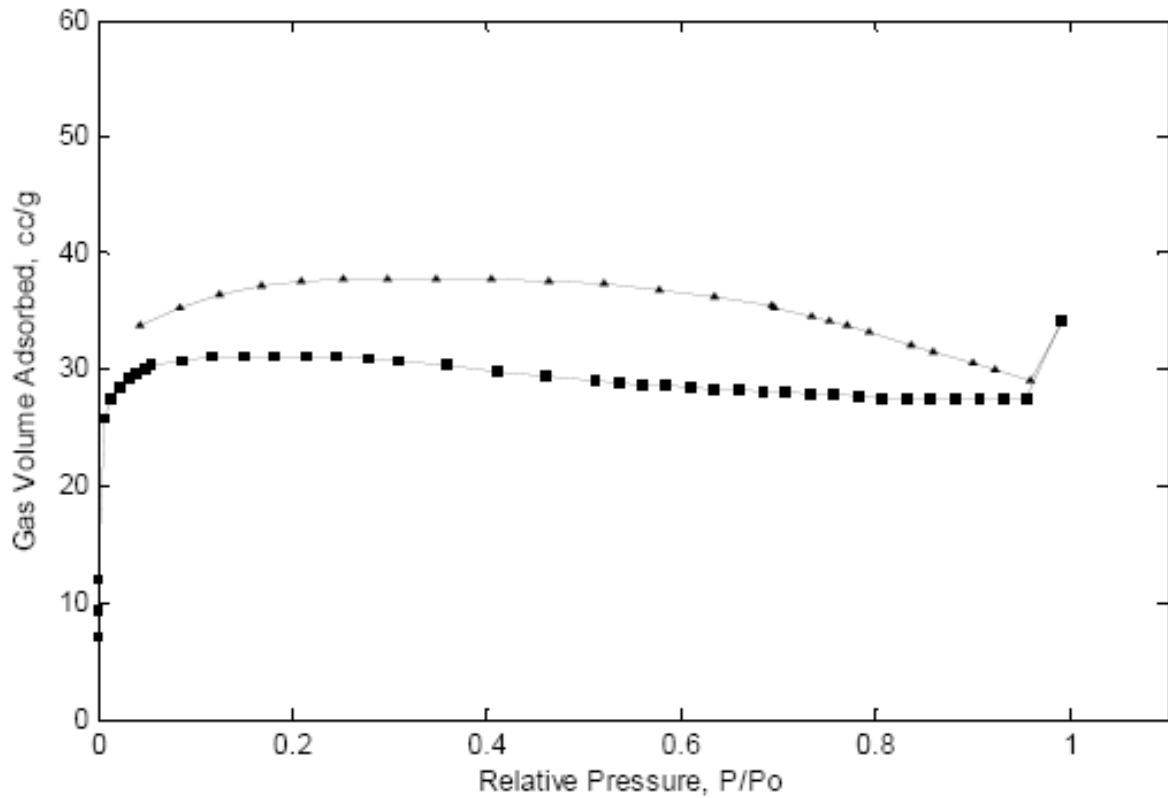
Figure 4.2.3. BET graph of Carbon Fiber carbonized at 700°C for 1hour and stabilized at 300 °C for 1 hour.
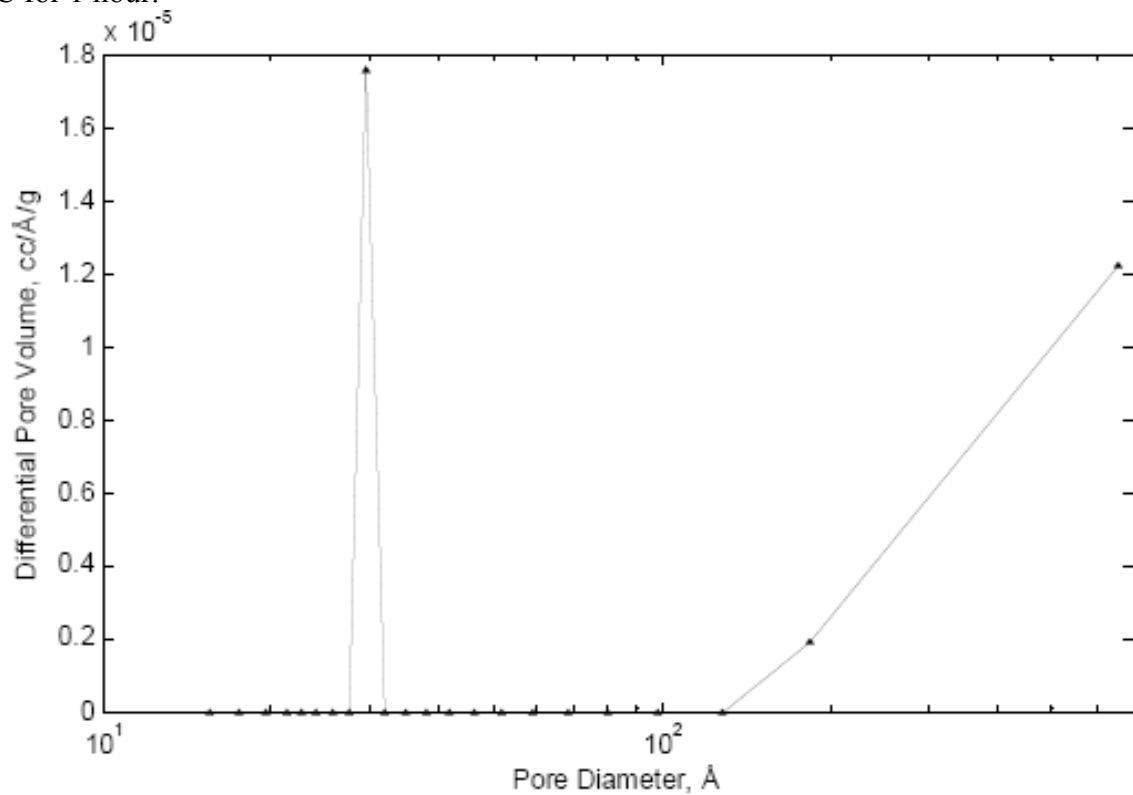
Figure 4.2.4. BJH pore distribution graph of Carbon Fiber carbonized at 700°C for 1 hour and stabilized at 300°C for 1 hour
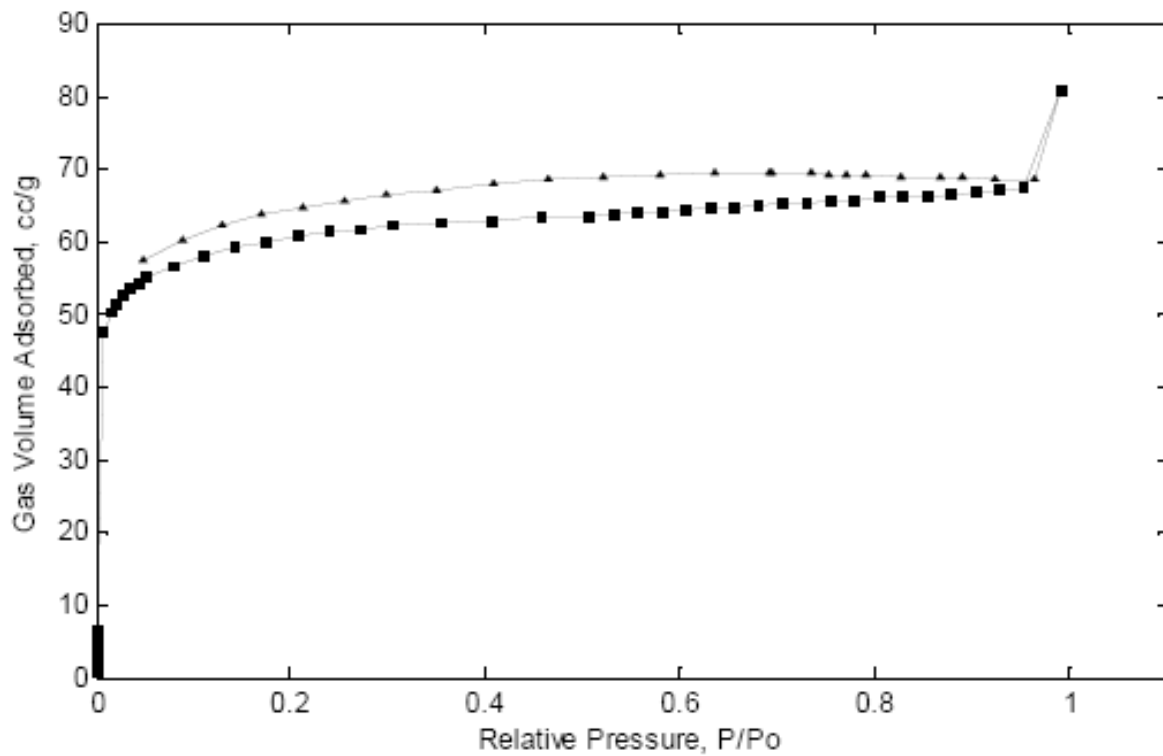
Figure 4.2.5. BET graph of Carbon Fiber carbonized at 800°C for 1hour and stabilized at 300°C for 1 hour
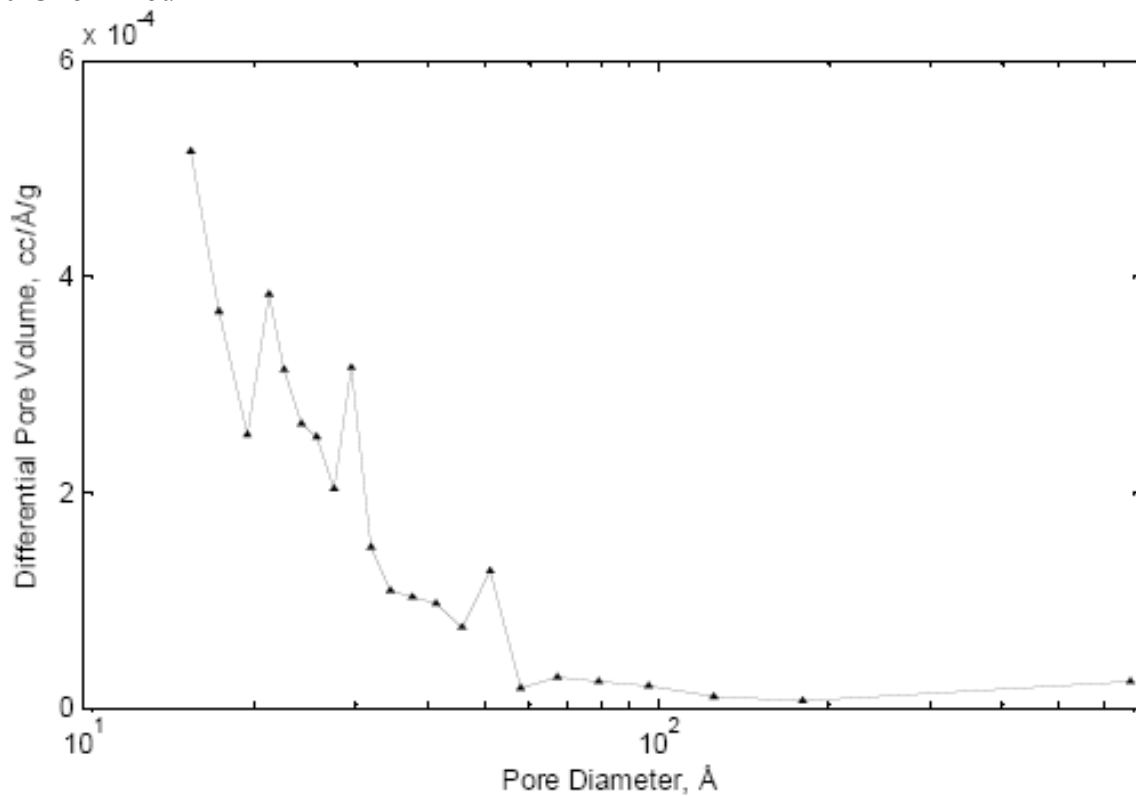
Figure 4.2.6. BJH pore distribution graph of Carbon Fiber carbonized at 800°C for 1 hour and stabilized at 300°C for 1 hour
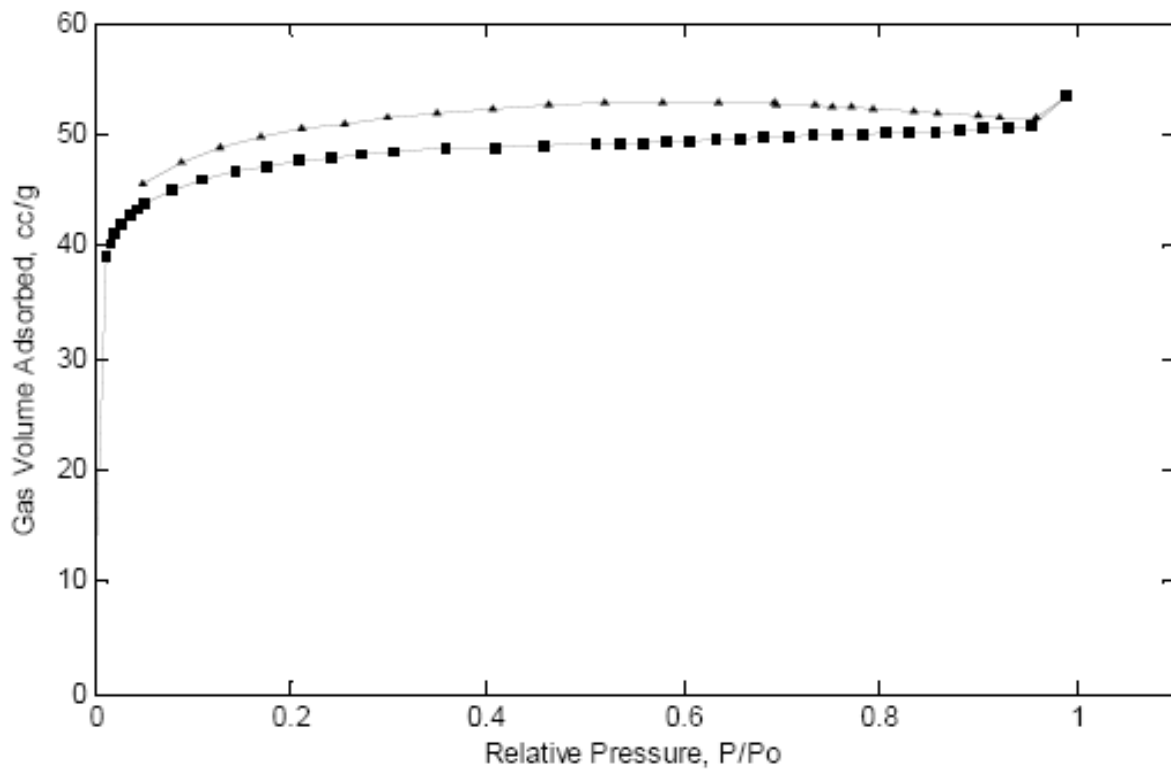
Figure 4.2.7. BET graph of Carbon Fiber carbonized at 900°C for 1hour and stabilized at 300°C for 1 hour
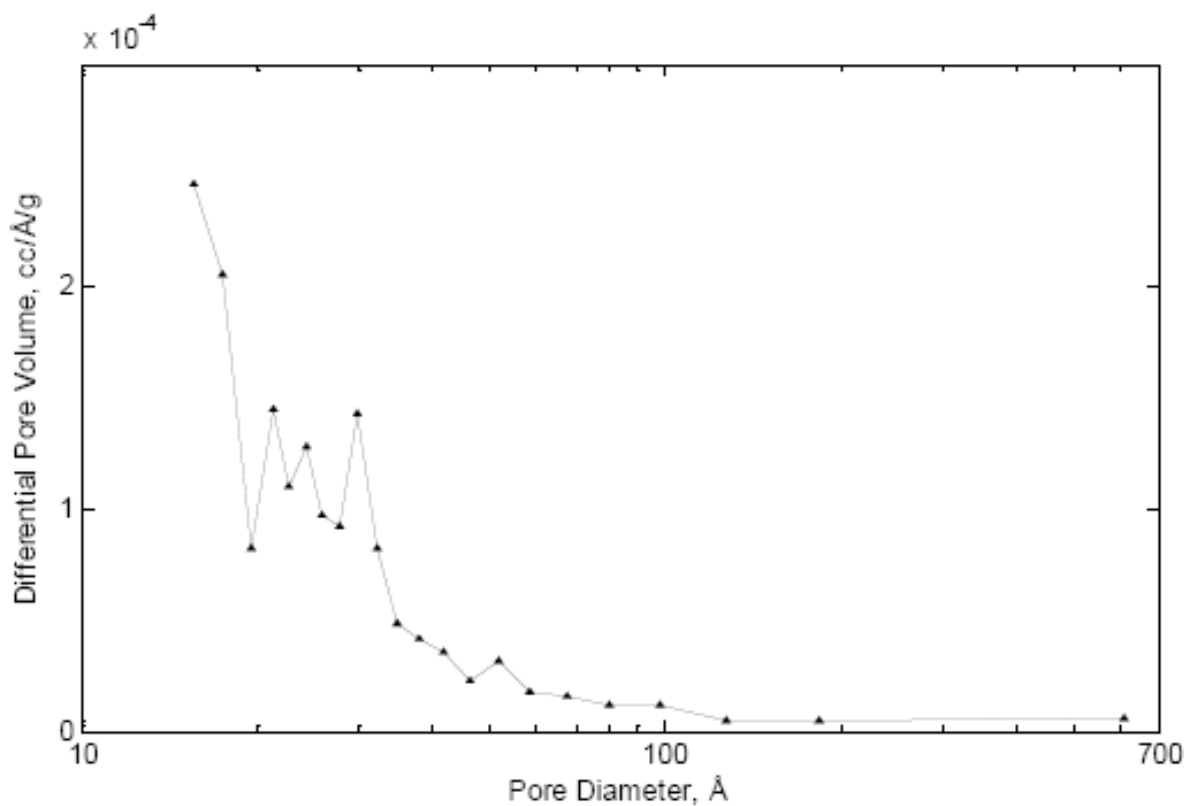
Figure 4.2.8. BJH pore distribution graph of Carbon Fiber carbonized at 900°C for 1 hour and stabilized at 300°C for 1 hour
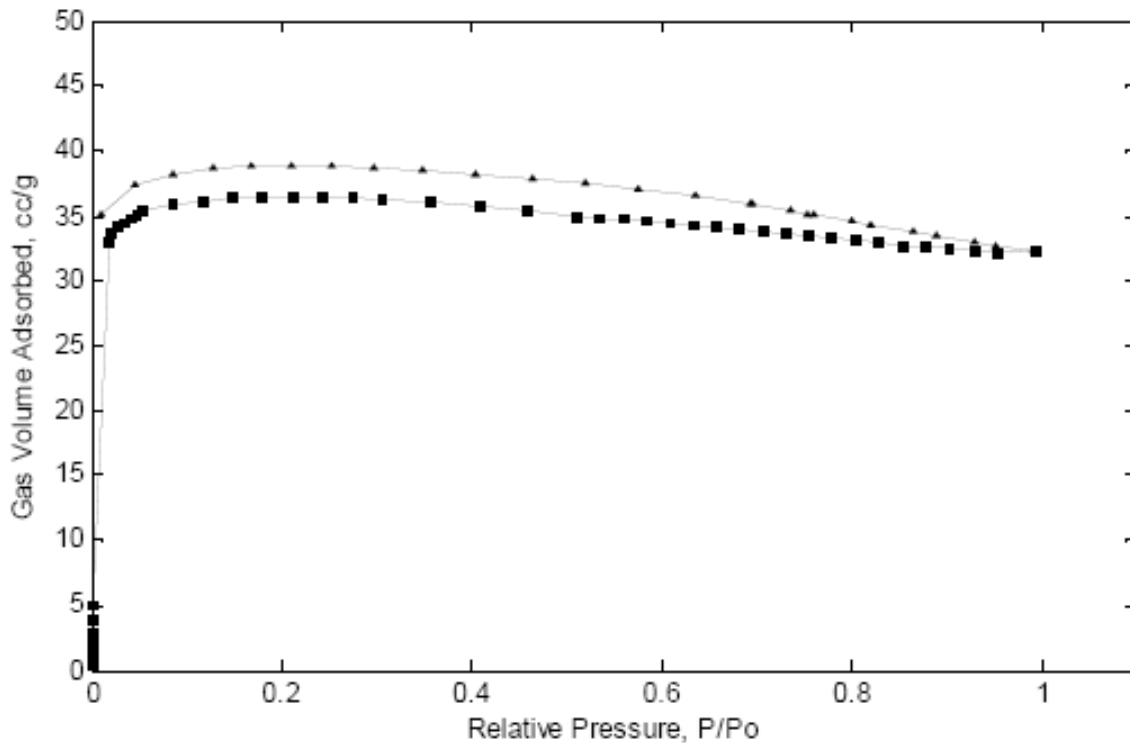
Figure 4.2.9. BET graph of Carbon Fiber activated by carbon dioxide at 800°C for 0.5 hour and stabilized at 300°C for 1 hour.
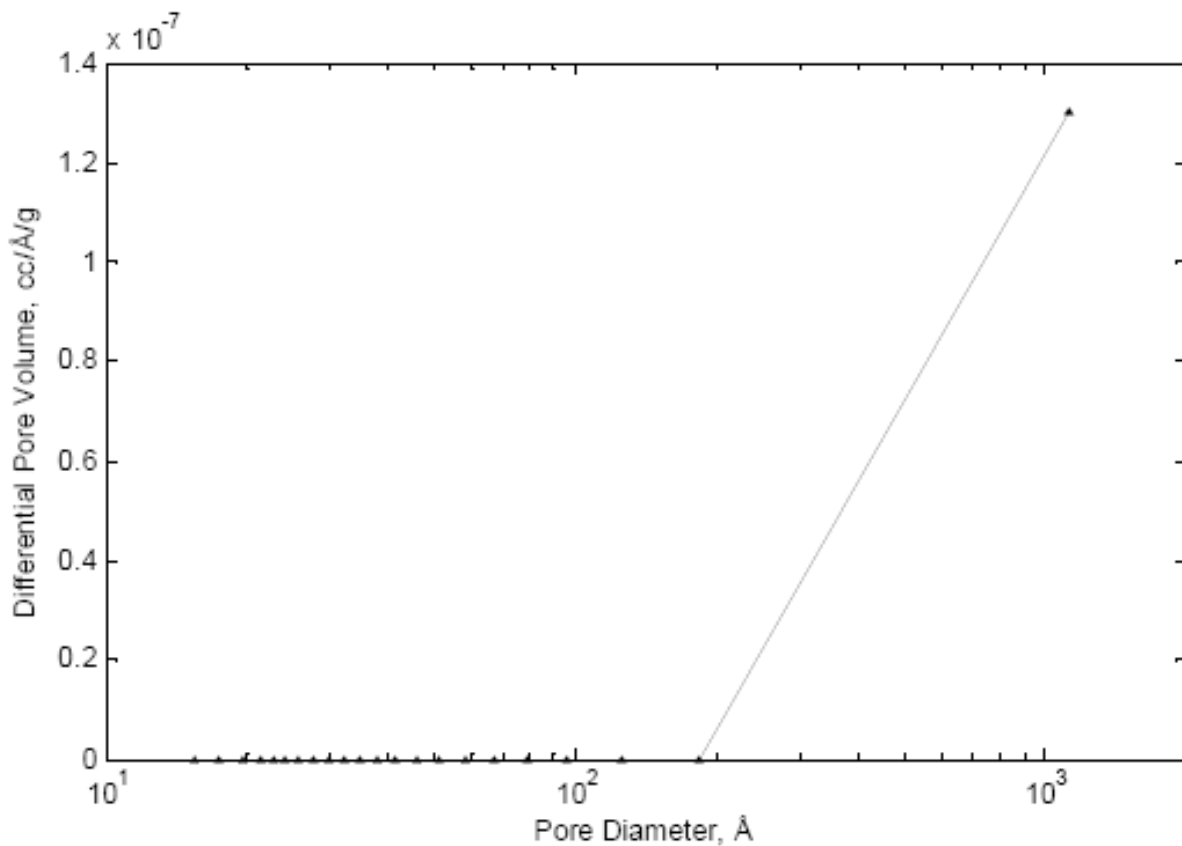
Figure 4.2.10. BJH pore distribution graph of Carbon Fiber activated by carbon dioxide at 800°C for 0.5 hour and stabilized at 300°C for 1 hour.
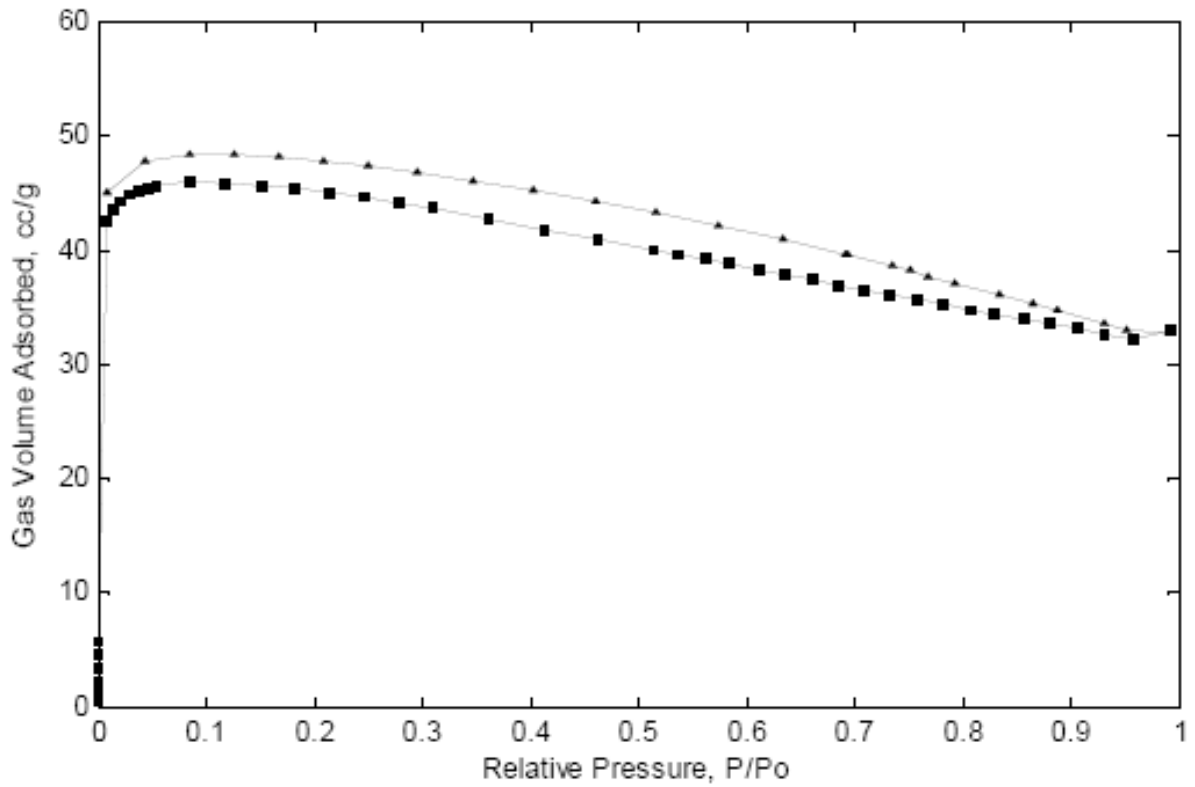
Figure 4.2.11. BET graph of Carbon Fiber activated by carbon dioxide at 800°C for 1hour and stabilized at 300°C for 1 hour.
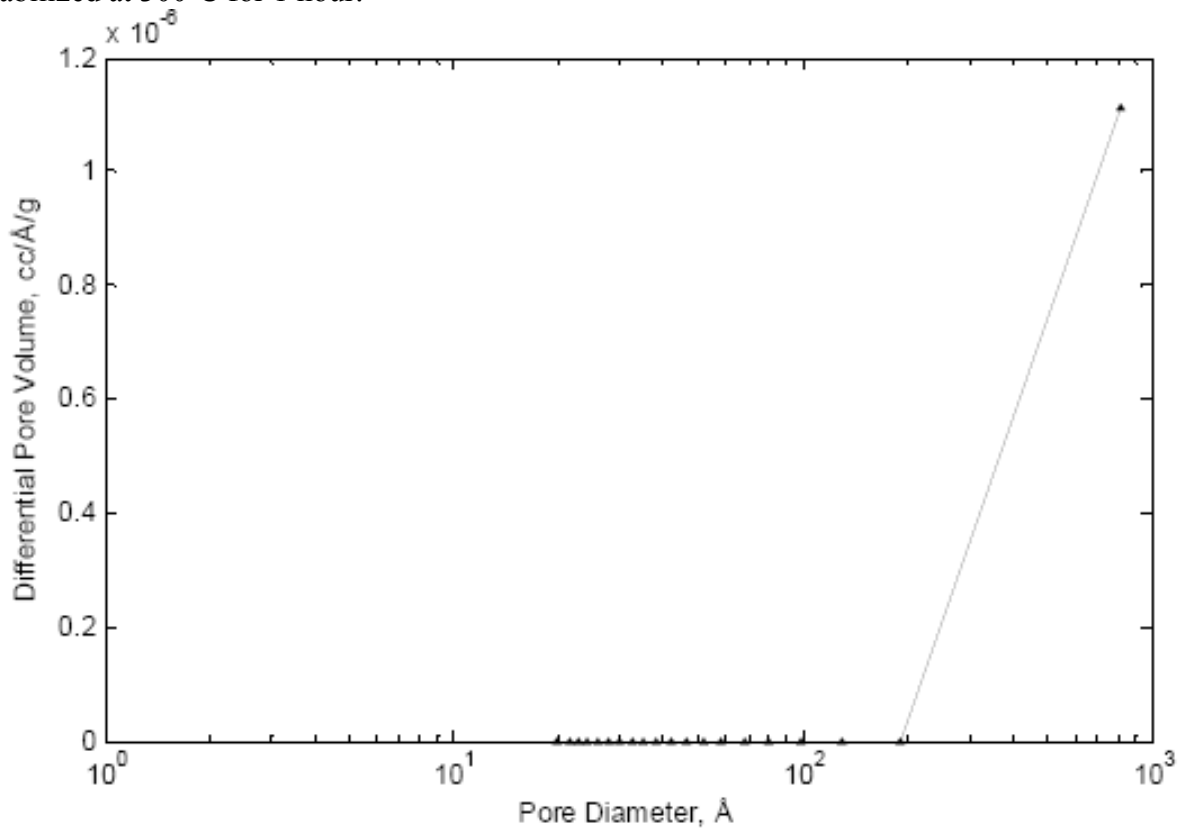
Figure 4.2.12. BJH pore distribution graph of Carbon Fiber activated by carbon dioxide at 800°C for 1 hour and stabilized at 300°C for 1 hour.
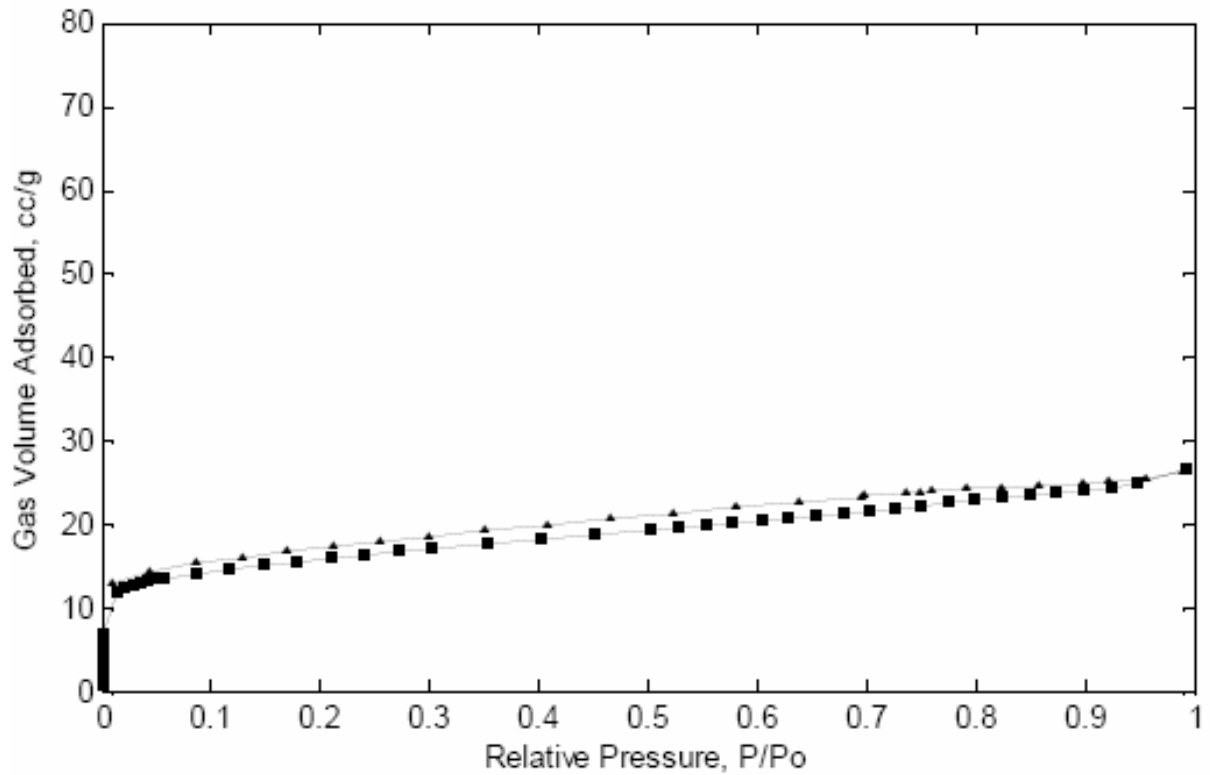
Figure 4.2.13. BET graph of Carbon Fiber activated by carbon dioxide at 900°C for 1hour and stabilized at 300°C for 1 hour.
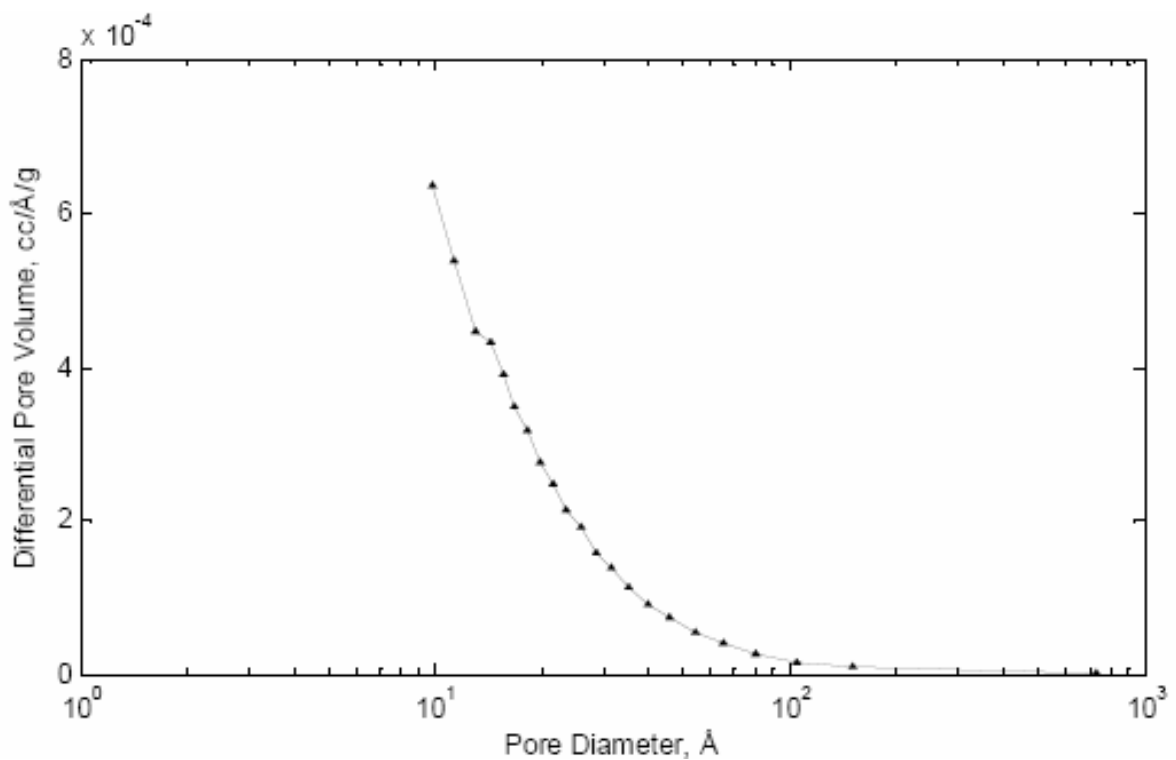
Figure 4.2.14. BJH pore distribution graph of Carbon Fiber activated by carbon dioxide at 900°C for 1 hour and stabilized at 300°C for 1 hour.
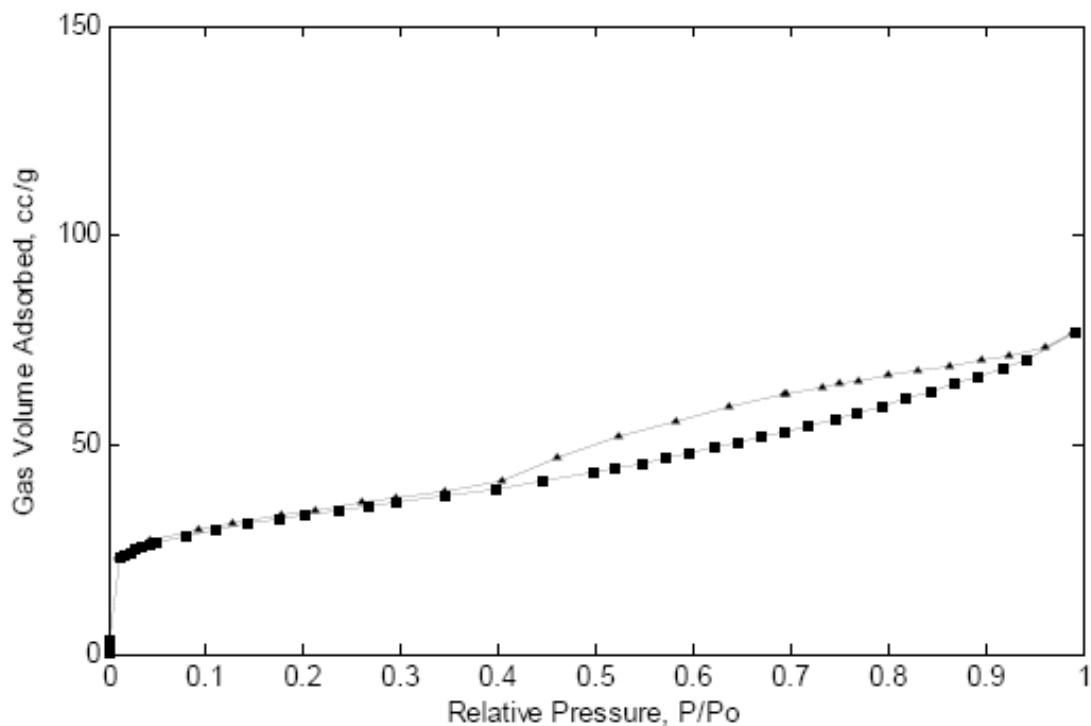
Figure 4.2.15. BET graph of Carbon Fiber activated by $AlCl_3$-Et_2O at 800^oC for 1 hour and stabilized at 300^oC for 1 hour.
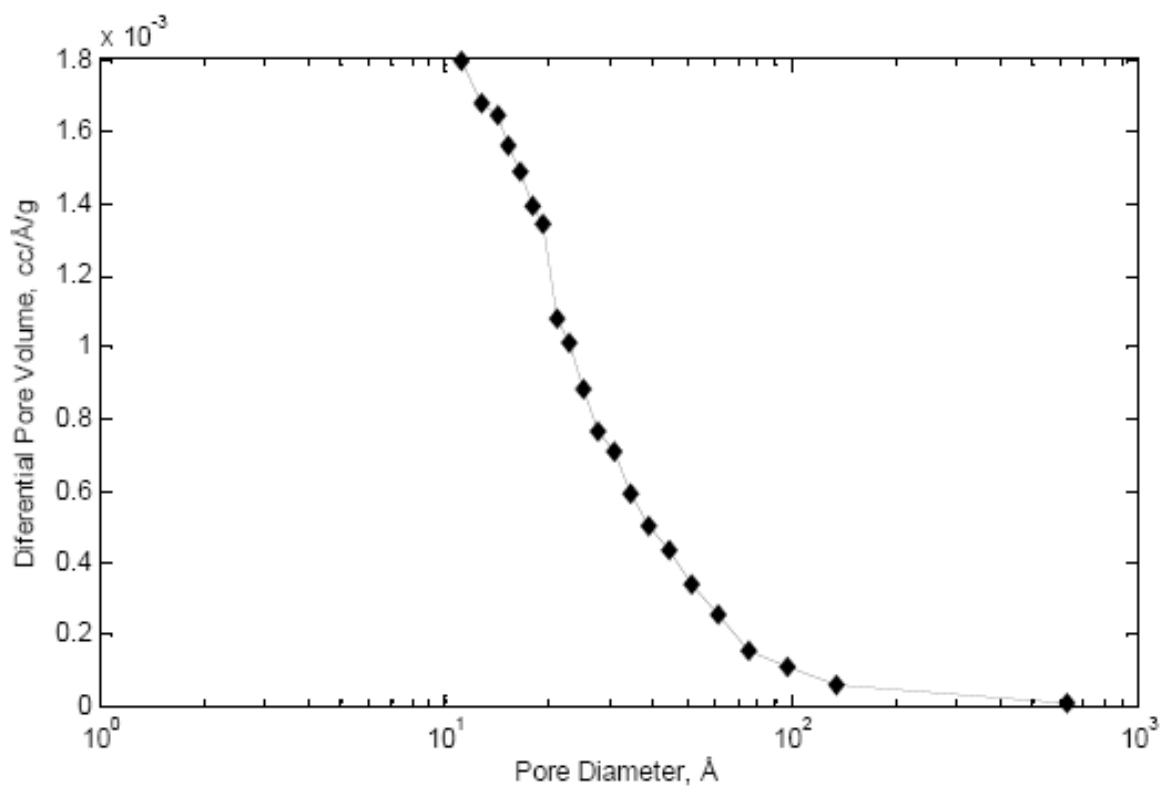
Figure 4.2.16. BJH pore distribution graph of Carbon Fiber activated by AlCl3-Et2O at 800^oC for 1 hour and stabilized at 300^oC for 1 hour.

Table 4.2.1. Surface Areas of Carbon Fibers before chemical activation

BET Surface Area of Carbon Fibers (m^2/g)							
200°C Stabilization					300°C Stabilization		
	1h	2h	3h	4h	5h	0.5h	1h	2h
500	53	13	6	27	38	10	45	90
600	39	51	28	25	58	60	144	55
700	36	73	30	108	20	93	117	139
800	21	24	22	56	92	21	136	68
900	11	16	61	22	111	113	122	79
1000	20	9	18	22	22	30	54	46

Since oxidation on the PAN fibers during stabilization step causes growth of graphitic layer through cyclic-PAN precursors. This results in coupling of PAN precursors at carbonization temperature. This phenomena causes decrease in surface area of carbon fibers. However, fibers carbonized at 500°C at both stabilization temperatures and all times have nearly the smallest areas among all fibers (Table 4.2.1). This tells higher surface area at carbonized at 500 and stabilized at 200°C for 1 hour was an expected result (Table 4.2.1). Since removal of nitrogen on the surface makes surface more graphitized relative to inner part [53].

Table 4.2.2. Surface Areas of Carbon Fibers after activation

Carbonization and Activation Temperatures of CFs (^{o}C)	Surface Area of Fibers before Activation of Carbon Fibers (m^2/g)	Surface Area of Fibers after Activation of Carbon Fibers (m^2/g)
800(0.5h)	129	150
800(1h)	136	190
900(1h)	122	55
1000(1h)	54	burned
800(1h)*	136	117

*This carbon fiber was activated with AlCl$_3$ given as in the experimental part.

4.3. Catalytic dehydrogenation of cyclohexane by Pd doped activated carbon fibers

Cyclohexane conversion was 89.1% after treatment at 350°C for 60 minutes over 5%Pd/CF catalyst. Higher temperatures might also degrade cyclohexane but in lower yields as given in the reactions above.

Other DSC graphs for 30 and 60 minutes treatments at 350°C showed similar behavior. All reactions over Pd/CF realized in the first 20 minutes. This proved reactions over Pd/C was independent of time after 20 minutes at applied heat treatment. Although micro-autoclaves that had same properties were used, concave up curve in the first 10 minutes was arising from mass differences of micro-autoclaves. After treatments in micro-autoclaves compounds whose retention times at 13, 20, 21.5 and 27.5 minutes notably increased their intensity (Figure 4.3.6-11).

In the dehydrogenation of cyclohexane held at 350°C for 15 minutes in the microreactor there were two endothermic reactions near 300°C and 350°C (Figures 4.3.1-4.3.3). In order to identify the compounds dehydrogenation experiments were stopped after each endothermal peak was observed in the thermograms (Figures 4.3.4 and 4.3.5) and the content of the microautoclave was analyzed with GC-MS. The total ion chromatograms of the products obtained after dehydrogenation experiments are presented in Figures 4.3.6-4.3.11.
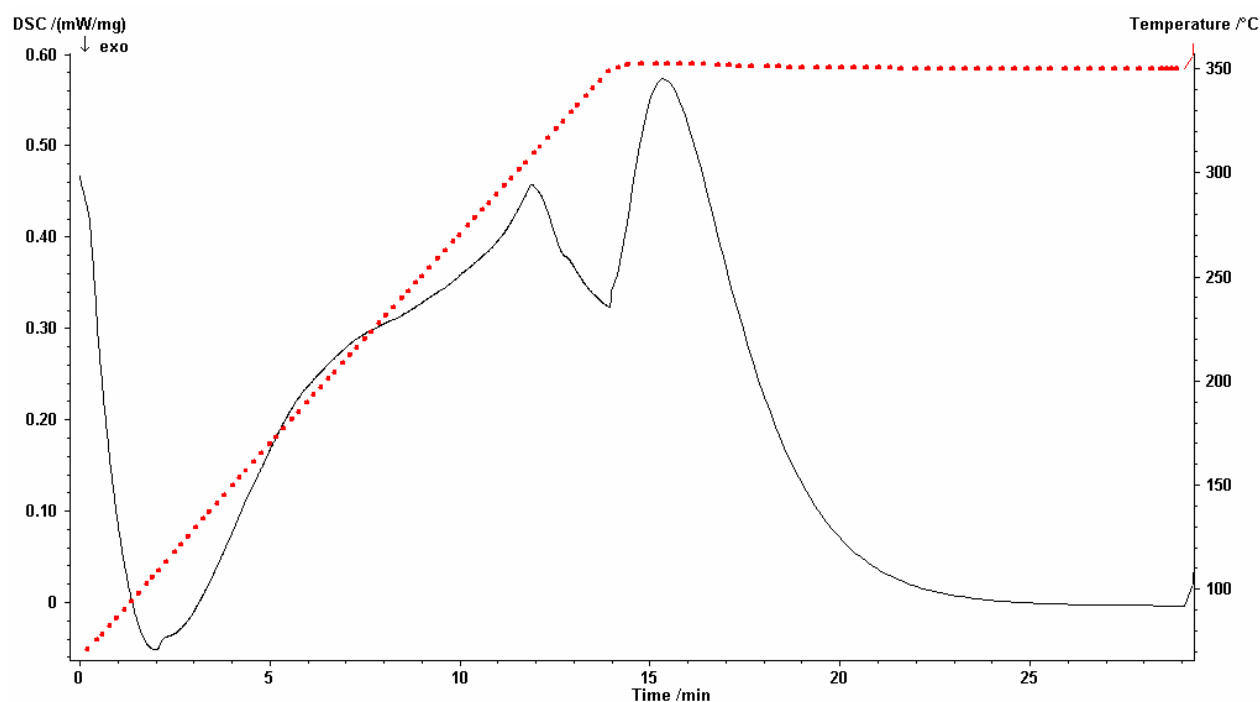
Figure 4.3.1. Differential Scanning Calorimetry graph of Cyclohexane held at 350°C for 15 minutes in the microreactor containing %5 Pd loaded-Carbon fiber
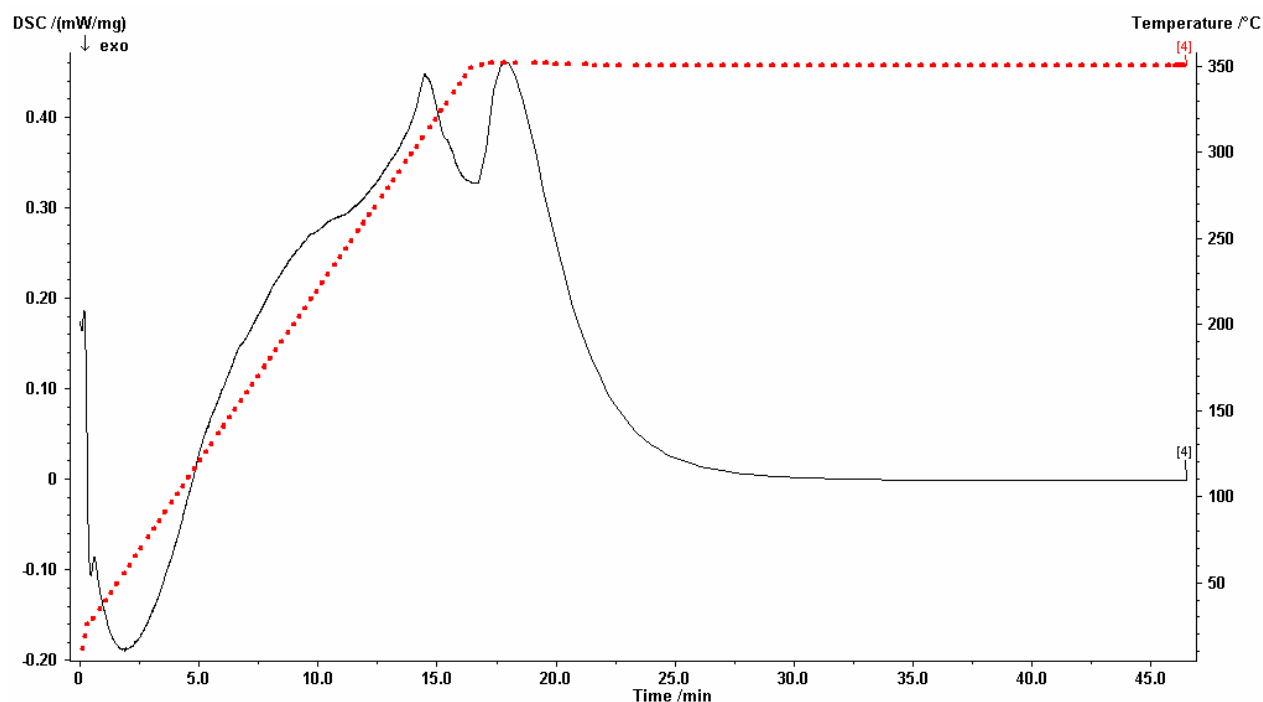
Figure 4.3.2. Differential Scanning Calorimetry graph of Cyclohexane held at 350°C for 30 minutes in the microreactor containing %5 Pd loaded-Carbon fiber
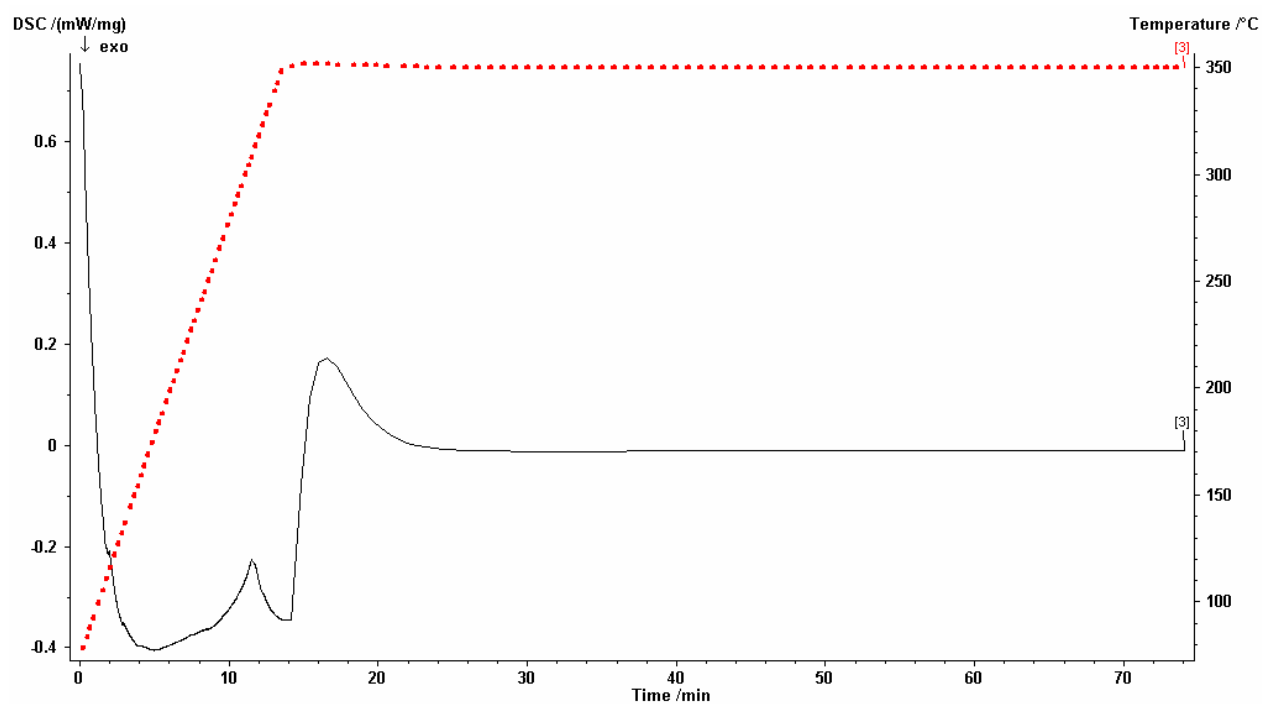
Figure 4.3.3. Differential Scanning Calorimetry graph of Cyclohexane held at 350°C for 60 minutes in the microreactor containing %5 Pd loaded-Carbon fiber
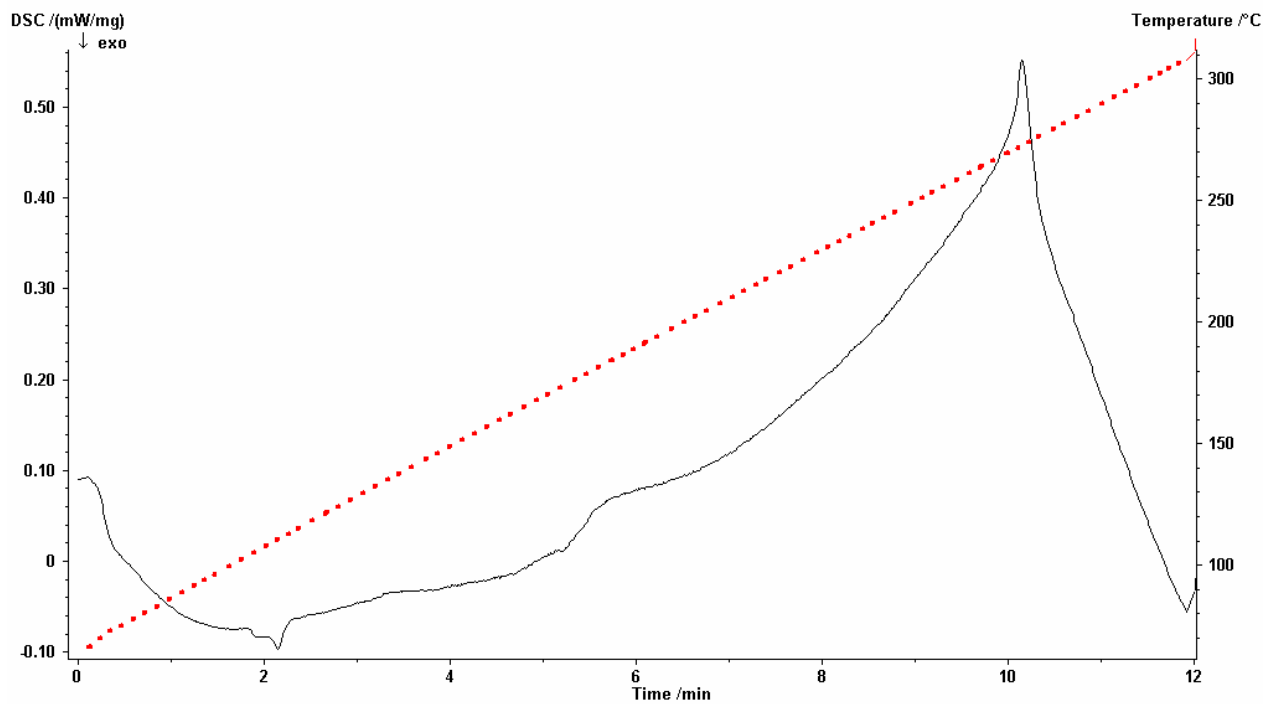
Figure 4.3.4. Differential Scanning Calorimetry graph of Cyclohexane held at $350^{o}C$ for 16 minutes which was stopped after first degradation of cyclohexane
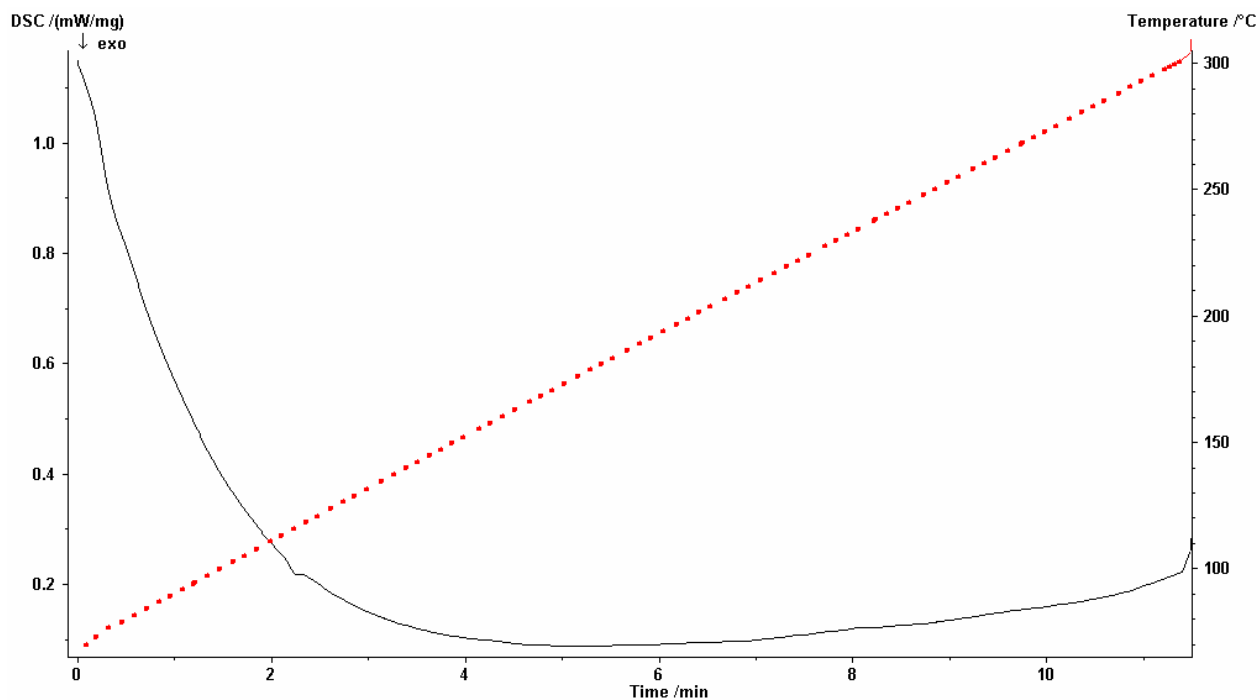
Figure 4.3.5. Differential Scanning Calorimetry graph of Cyclohexane held at $350^{o}C$ for 12 minutes which was stopped before first degradation of cyclohexane

The chemicals identified resulting from dehydrogenation reactions are presented in Table 4.4.1. GC-MS results showed that after the treatment of cyclohexane with 5%Pd-loaded CF at 350°C the presence of cyclohexene, 1-methyl-cyclopentene, 1,2-dimethylcyclohexene, 3-methylcyclohexene, 1-methyl-1,4-cyclo-hexadiene, 2,4-dimethyl-cyclopentanone, benzaldehyde. These results indicated that reforming of compounds due to dehydrogenation and oxidation reactions occurred on the Pd 5%-CF.

Cyclohexane (97% pure) was measured according to ratio of its peak area integration to all area due to total area of curve (Figure 4.3.6). There was significant increase in the intensity of peaks after heat treatment at 350°C for 15 minutes (Figure 4.3.7). Especially GC peaks observed retention times intensively relative to other chemicals at 13, 20.0, 21.5, 26.0, 27.5 minutes (Figure 4.3.7). Possible compounds for peaks are 2,4-dimethyl-cyclopentanone, phenylacethylene, benzaldehyde, 1-hydroxybutanone, fulfural. Oxidation and reforming of cyclohexane occurred during 15 minutes heating at 350°C (Table 4.3.1). TICs of dehydrogenation of cyclohexane showed almost same trend in terms of relative amount of obtained chemicals (Figure 4.3.6-11). Although GC analysis of two samples were stopped in 12 and 14 minutes (Figure 4.3.10-11) same TICs were obtained. It indicated reforming and dehydrogenation happened probably within first 10 minutes of heating applied to sample.
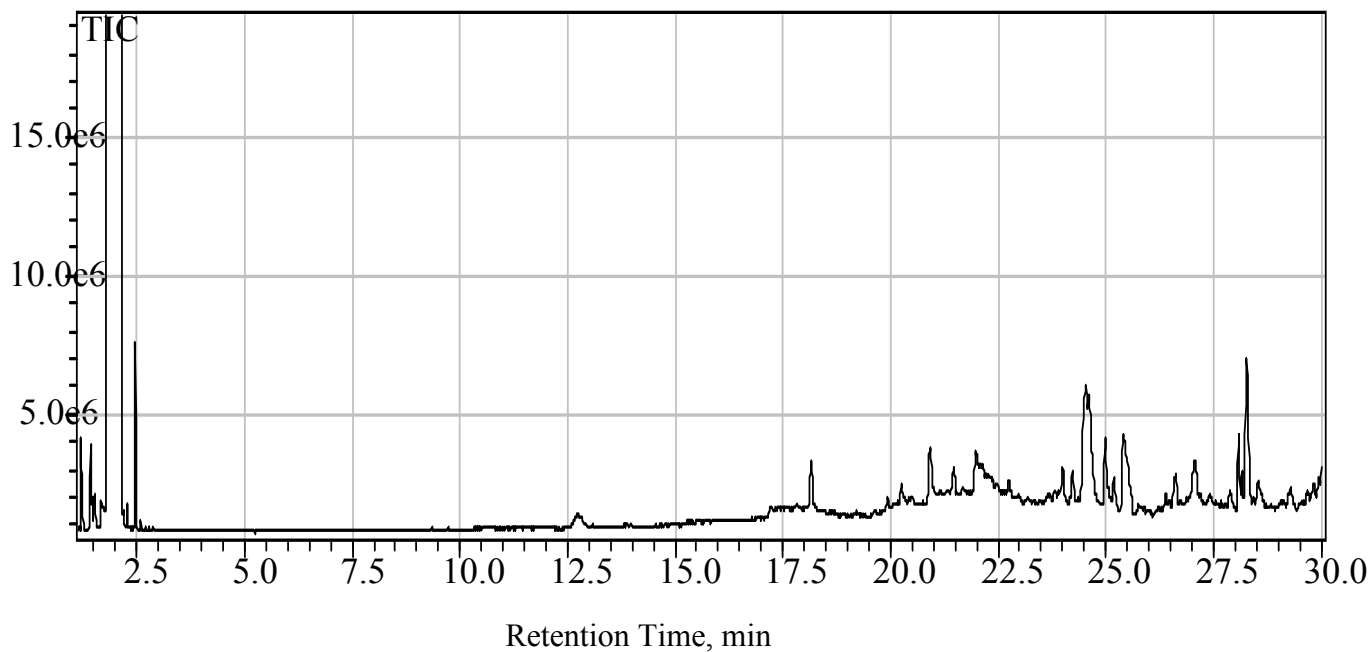
Figure 4.3.6. Total Ion Chromatogram of cyclohexane. Cyclohexane content was 97.51% in purity.
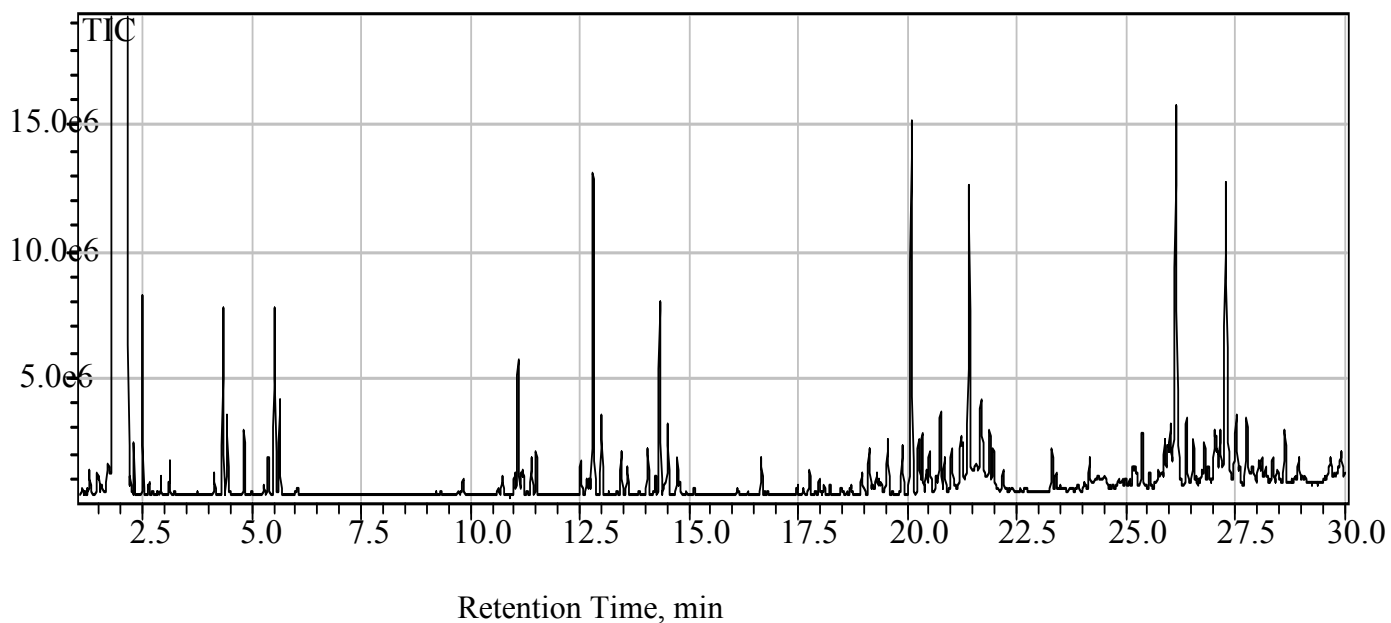
Figure 4.3.7. Total Ion Chromatogram of products after cyclohexane was treated in %5 Pd-loaded carbon fiber for 15 minutes at 350°C. Cyclohexane content decreased to 95.67%.
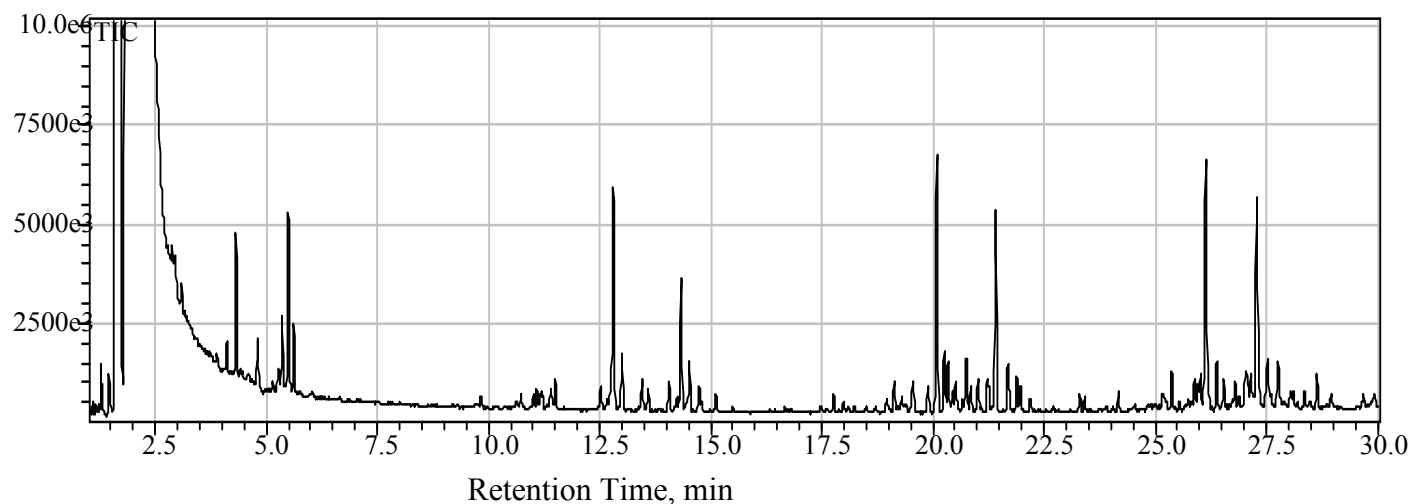
Figure 4.3.8. Total Ion Chromatogram of products after cyclohexane was treated in %5 Pd-loaded carbon fiber for 30 minutes at 350°C. Cyclohexane cocntent decreased to 94.33%.
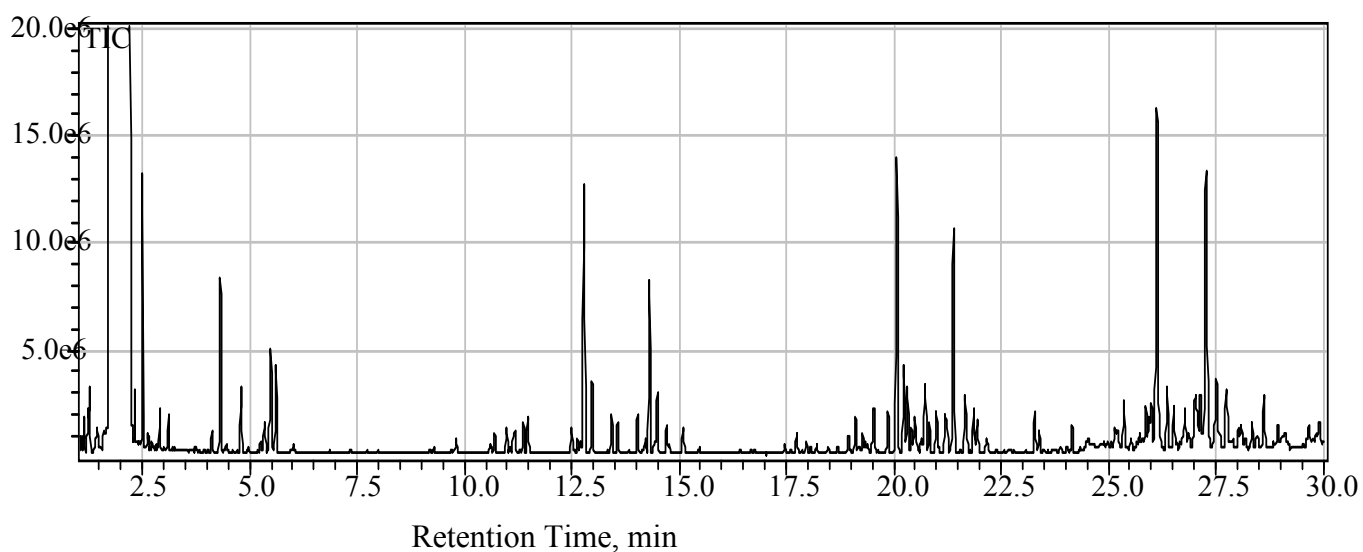
Figure 4.3.9. Total Ion Chromatogram of products after cyclohexane was treated in %5 Pd-loaded carbon fiber for 60 minutes at 350°C. Cyclohexane cocntent decreased to 89.10%.
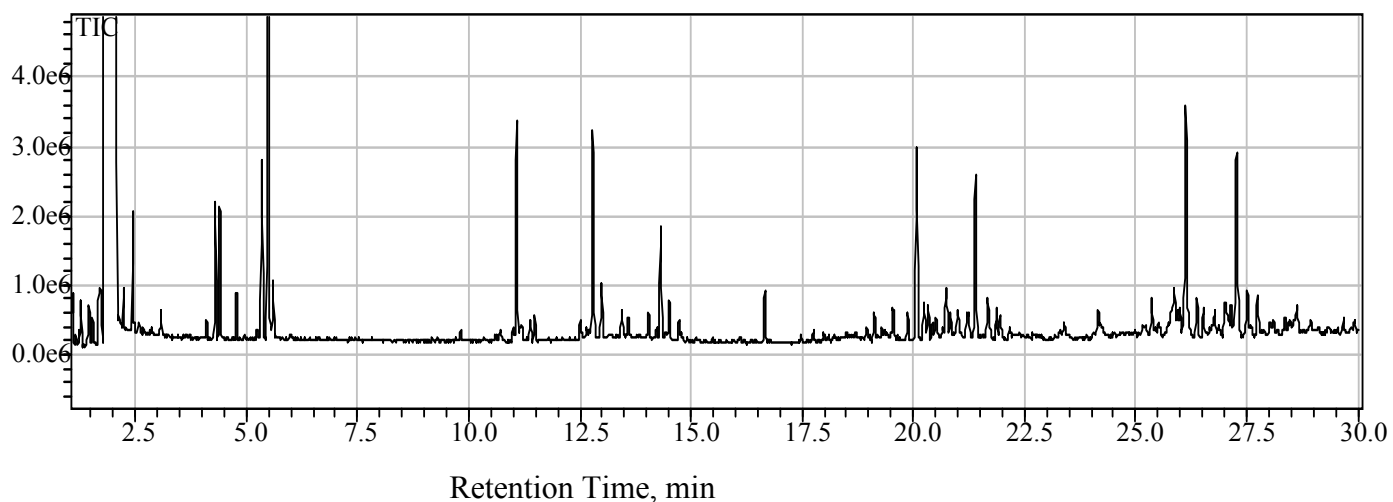
Figure 4.3.10. Total Ion Chromatogram of products after cyclohexane was treated in %5 Pd-loaded carbon fiber for 16 minutes at 350°C which reaction was stopped after first DSC peak obtained. Cyclohexane cocntent decreased to 96.65%.
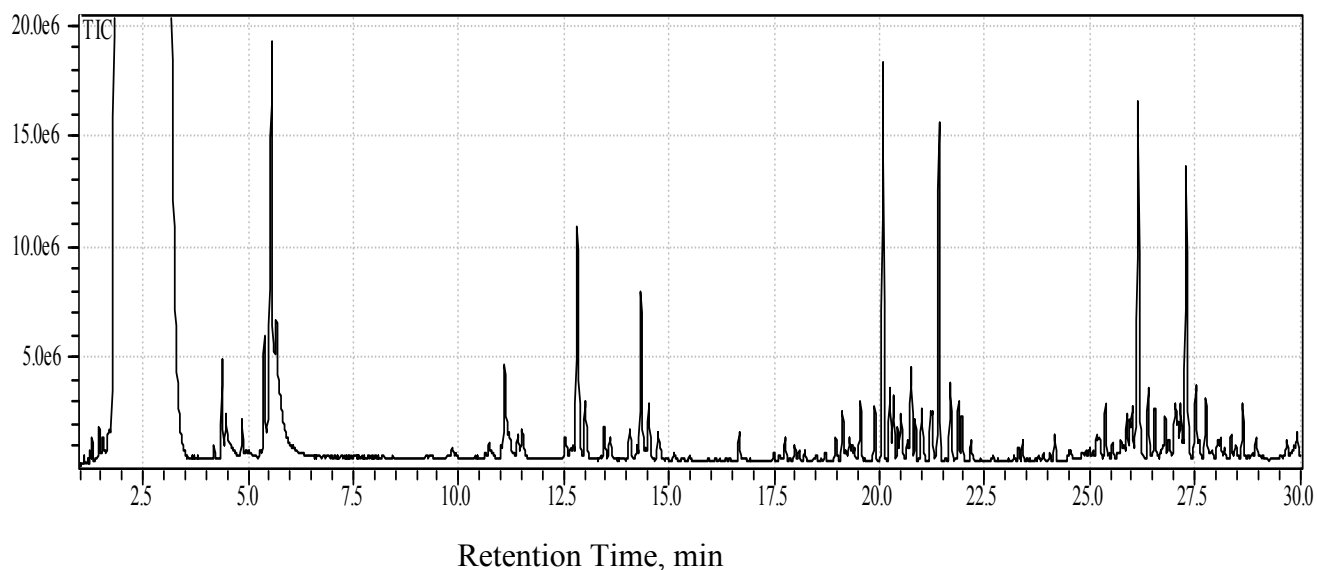
Figure 4.3.11. Total Ion Chromatogram of products after cyclohexane was treated in %5 Pd-loaded carbon fiber for 12 minutes at 350°C which reaction was stopped before first DSC peak obtained. Cyclohexane cocntent decreased to 96.12%.

Table 4.3.1. Retention times and possible compounds analyzed in GC-MS after treatment in micro-autoclave

Retention Times in GC(min)	Possible Compounds
1.5	Cyclohexene 2,3-dimethylbutene
1.9	1-methyl-cyclopentene Isoprene
2.1	1,2-dimethylcyclohexene 1,4-dimethylcyclohexene Methyl-cyclohexane
2.6	3-methylcyclohexene 2-methyl furan 1,2-dimethylcyclohexane
5.6	1-methyl-1,4-cyclohexadiene 2-ethylbutyral aldehyde
13	2,4-dimethyl-cyclopentanone 1-ethyl-4-methylbenzene 3-hexanol 5-hexen-1-ol 3-methylpentanol
14.5	1,3,5-trimethylbenzene styrene
20	Phenylacethylene 2-methyl-cyclopenten-2-one 1-hexanol
26	Fulfural 3,5-dimethyl-cyclopenten-2-one
20	Phenylacethylene 2-methyl-cyclopenten-2-one 1-hexanol
21.5	1-hydroxybutanone 2,6,6-trimethyl-cyclohex-2-en-1-one
26	Fulfural 3,5-dimethyl-cyclopenten-2-one
27.5	Benzaldehyde Benzyl propyl ether Camphor Decanal

CONCLUSIONS

1. Carbon fibers were produced at different temperatures from 500-1000°C which were also stabilized at 200 and 300°C under an air atmosphere in the first part of the study. Surface area of all carbon fibers was measured by BET method. Carbon fibers carbonized at 600-900°C and stabilized at 300°C for 1 hour had relatively larger surface area among 48 carbon fiber sample. Then pore distributions of these four carbon fibers were measured. Carbon fiber carbonized at 600°C that had the largest surface area had pore in 3nm.

2. FT-IR spectra of carbon fibers showed that carbon fibers had especially two main peaks at 1600 cm^{-1} and 1200 cm^{-1} due to aromatic $-C=C-$ and $=C-H$ bonds, respectively.

3. In the second part of the experiment, fibers were activated in a CO_2 atmosphere for 0.5, 1 hour at 800°C, 900°C for 1hour and finally activated by $AlCl_3$-Et_2O at 800°C. Then their pore distributions were measured. CF activated by carbon dioxide at 800°C for 1 hour and stabilized at 300°C had the largest surface area among all fibers including activated ones. This sample had 82 nm pores in diameter.

4. FT-IR spectra of many carbon fibers contained strong CO_2 peak, this indicated burned carbon fibers caused adsorption of these molecules.

5. Surface area of fibers activated at 900°C by CO_2 and 800°C by $AlCl_3$-Et_2O decreased.

6. In the second part of the study, 5%Pd in weight was loaded via $NaBH_4$ onto carbon fiber carbonized at 800°C and stabilized at 300°C for 1 hour. This fiber was chosen intentionally to observe change in surface characteristics after activation with CO_2. Higher temperatures like 800°C was required for activation.

7. Degradation of cyclohexane gave two main endothermic peaks near 290°C and 350°C in DSC analysis.

8. After dehydrogenating of cyclohexane over 5%Pd-loaded/CF, the compounds identified in the micro-autoclaves were cyclohexene, 1-methyl-cyclopentene, 1,3,5-trimethylbenzene, 3-methylcyclohexene , decanal, 1-hexanol.

REFERENCES

[1] Fitzer E. (1989). Carbon Fibres: Present State and Future Expectations. In Figueiredo J. L., Bernardo C. A., Baker R. T. K., & Hüttinger K. J.(Eds.), *Carbon Fiber Filaments and Composites (pp. 3-42).* Dordrecht: Kluwer Academic Publishers Group.

[2] Ryu Z., Zheng J. & Wang M. (1998). Porous Structure of PAN-Based Activated Carbon Fibers. *Carbon.* 36(4), 427-432..

[3] http://www.chem.wisc.edu/~newtrad/CurrRef/BDGTopic/BDGtext/BDGGraph.html

[4] Matatov-Meytal, Y., Sheintuch, M. (2002). Catalytic fibers and cloths. *App. Catal. A*. 231, 1–16.

[5] Park, S.J., Donnet, J.B., 1998. *J. Colloid Interface Sci*. 206, 29.

[6] Park, S.J., Jang, Y.S., 2002. *J. Colloid Interface Sci*. 249, 458.

[7] Park, S.J., Jung, W.Y. (2002). *J. Colloid Interface Sci*. 250, 196.

[8] Matatov-Meytal Yu. & Sheintuch M. (2002). Catalytic fibers and cloths. *Applied Catalysis A: General.* 231(1-2), 1-16.

[9] Kaneko K., Ishii C., Ruike M. & Kuwabara H. (1992). Origin superhigh surface area and microstalline graphitic structures fibers of activated carbons. *Carbon.* 30(7), 1075-1088.

[10] Littrell K.C., Khalili N.R., Campbell M., Sandı G. & Thiyagarajan P. (2002). Microstructural Analysis of Activated Carbons Prepared from Paper Mill Sludge by SANS and BET. *Chem. Mater.* 14(1), 327-333.

[11] Thwaites M.W., McEnaney B., Botha F.D. (1992). *Preprints Division of Fuel Chemistry of ACS*, 37(2), 497–504.

[12] Stoeckli F., Daguerre E., Guillot A. (1999). *Carbon.* 37, 2075–7.

[13] Dalton S., Heatley F. & Budd P. M. (1999). Thermal stabilization of polyacrylonitrile fibres. *Polymer*. 40(20), 5531–5543.

[14] Williams P. T. and Reed A. R. (2004). High grade activated carbon matting derived from the chemical activation and pyrolysis of natural fibre textile waste. *Journal of Analytical and Applied Pyrolysis*. 71(2), 971-986.

[15] Donnet B. & Bansal R. C. (1984). *Carbon Fibers*. New York: Marcel Dekker. Chap. 2.

[16] Yoon S. H., Korai Y., Mochida I. (1989). Carbon Fibers and Active Carbon Fibers. In Harry Marsh, Francisco Rodriguez-Reinoso (Eds.), *Sciences of carbon materials*. Publicaciones de la Universidad de Alicante, 2000. Spain (pp. 309).

[17] Brasquet C., Rousseau B., Estrade-Szwarckopf H. & Le Cloirec P. (2000). Observation of activated carbon fibres with SEM and AFM correlation with adsorption data in aqueous solution. *Carbon* 38(3), 407–422.

[18] Ryu Z., Rong H., Zheng J., Wang M. & Zhang B. (2002). Microstructure and chemical analysis of PAN-based activated carbon fibers prepared by different activation methods. *Carbon*. 40(7), 1131– 1150.

[19] Lozano-Castello D., Raymundo-Pinero E., Cazorla-Amorosa D., Linares-Solano A., Muller M. & Riekel C. (2002). Characterization of pore distribution in activated carbon fibers by microbeam small angle X-ray scattering. *Carbon* 40(14), 2727-2735.

[20] Landau M. V., Kogan S. B., Tavor D., Herskowitz M. & Koresh J. E. (1997). Selectivity in heterogeneous catalytic processes. *Catalysis Today*. 36(4), 497-510.

[21] Villar-Rodil S., Martínez-Alonso A., Tascón J. M. D. (2002). Carbon Molecular Sieves for Air Separation from Nomex Aramid Fibers *Journal of Colloid and Interface Science*. 254(2), 414-416.

[22] Rodriguez-Reinoso F. (1998). The role of carbon materials in heterogeneous catalysis. *Carbon*. 36(3), 159-175.

[23] Seaton, N. A.; Walton, J. P. R. B.; Quirke, N. (1989). A New Analysis Method for the Determination of the Pore Size Distribution of Porous Carbons from Nitrogen Adsorption Measurements. *Carbon*. 27, 853-861.

[24] Brennan J. K., Bandosz T. J., Thomson K. T. & Gubbins K. E. (2001). Water in porous carbons. *Colloids and Surfaces A: Physicochemical and Engineering Aspects.* 187–188, 539–568.

[25] Macia-Agullo J. A., Moore B. C., Cazorla-Amoros D. & Linares-Solano A. (2004). Activation of coal tar pitch carbon fibres: Physical activation vs. chemical activation *Carbon.* 42(7), 1367–1370.

[26] Fu R., Liu L., Zeng H. (2002). The Dynamic Adsorption of Benzene Vapor on the ACF Activated by Phosphoric Acid. *Journal of Applied Polymer Science.* 83(9), 1841-1847.

[27] Park S. J. & Kim K. D. (2001). Influence of activation temperature on adsorption characteristics of activated carbon fiber composites. *Carbon.* 39(11), 1741–1746.

[28] Suárez-García F., Martínez-Alonso A. and Tascón J. M. D. (2004). Activated carbon fibers from Nomex by chemical activation with phosphoric acid. *Carbon.* 42(8-9), 1419-1426

[29] Fu R., Liu L., Huang W., Sun P. (2003). Studies on the Structure of Activated Carbon Fibers Activated by Phosphoric Acid. *J. Appl. Pol. Sci.* 87, 2253–2261

[30] Yoon S. H., Lim S., Song Y., Ota Y., Qiao W., Tanaka A. & Mochida I. (2004). KOH activation of carbon nanofibers. *Carbon.* 42(8-9), 1723–1729.

[31] Suarez-Garcia F., Martınez-Alonso A., Tascon J. M. D. (2004). Nomex polyaramid as a precursor for activated carbon fibres by phosphoric acid activation. Temperature and time effects. *Microporous and Mesoporous Materials* 75 73–80

[32] Szabo T., Szeri A. & Dekany I. (2005). Composite graphitic nanolayers prepared by self-assembly between finely dispersed graphite oxide and a cationic polymer. *Carbon*. 43(1), 87-94.

[33] Mangun C.L., Benak K.R., Daley M.A. & Economy J. (1999). Oxidation of Activated Carbon Fibers: Effect on Pore Size, Surface Chemistry, and Adsorption Properties. *Chem. Mater.*, 11(12), 3476-3483.

[34] Wang F. L. & Hwang C. (2004). Promoted activated-carbon fibers used as a catalyst for propionitrile synthesis from methanol and acetonitrile. *Applied Catalysis A: General*. 276(1-2), 9–16.

[35] Wang Z. M., Yamashita N., Wang Z. X., Hoshinoo K. & Kanoh H. (2004). Air oxidation effects on microporosity, surface property, and CH_4 adsorptivity of pitch-based activated carbon fibers. *Journal of Colloid and Interface Science* 276(1), 151–158.

[36] Nabais J. V. M., Carrott P. J. M. & Carrott R. (2005). From commercial textile fibres to activated carbon fibres: Chemical transformations. *Materials Chemistry and Physics*. 93(1), 100-108.

[37] Pittman C. U., He G. R., Wub B. & Gardner S. D. (1997). Chemical Modification of Carbon Fiber Surfaces by Nitric Acid Oxidation Followed by Reaction with Tetraethylenepentamine. *Carbon* 35(3), 317-331.

[38] Saufi S.M. & Ismail A.F. (2002). Development and characterization of polyacrylonitrile (PAN) based carbon hollow fiber membrane. *Membrane Sci. &Tech*. 24(Suppl.), 843-854.

[39] Muniz J., Marban G. & Fuertes A.B. (2004). SO_2 Retention over Polyarylamide-Based Activated Carbon Fibers. *Environmental Progress,* 19(4), 246-254.

[40] Li L., Quinlivan P. A.& Knappe D. R. U. (2002). Effects of activated carbon surface chemistry and pore structure on the adsorption of organic contaminants from aqueous solution. *Carbon* 40(12), 2085–2100.

[41] Simonov P.A., Romanenko A.V., Prosvirin I.P., Moroz E.M., Boronin A.I., Chuvilin A.L. & Likholobov V. A. (1997). On the nature of the interaction of H_2PdCl_4 with the surface of graphite-like carbon materials. *Carbon* 35(1), 73-82

[42] Simonov P.A., Troitskii S.Y. and Likholobov V.A. (2000). Preparation of the Pd/C Catalysts: A Molecular-Level Study of Active Site Formation. *Kinet. Catal.* 41(2) 255-269.

[43] Toebes M. L., Dillen J. A. & Jong K. P. (2001). Synthesis of supported palladium catalysts. *Journal of Molecular Catalysis A: Chemical*. 173(1-2), 75–98.

[44] Weaver G.C., Norrod K. (1998). Surface-enhanced Raman spectroscopy - A novel physical chemistry experiment for the undergraduate laboratory . *J. Chem. Educ.,* 75, 621,

[45] Sing K. (2001). The use of nitrogen adsorption for the characterization of porous materials. *Colloids and Surfaces A: Physicochemical and Engineering Aspects*. 187–188, 3–9.

[46] Ho Y.S., Porter J.F., Mckay G (2002). Equilibrium Isotherm Studies for the Sorption of Divalent Metal Ions onto Peat: Copper, Nickel and Lead Single Component Systems. *Water,   Air, and Soil Pollution*. 141, 1–33,.

[47] Kowalczyk P., Gun'ko V. M., Terzyk A. P., Gauden P. A., Rong H., Ryu Z. & Do D. D. (2003). The comparative characterization of structural heterogeneity of mesoporous activated carbon fibers (ACFs). *Applied Surface Science*. 206(1-4), 67-77.

[48] Auer E., Freund A., Pietsch J. & Tacke T. (1998). Carbons as supports for industrial precious metal catalysts. *Applied Catalysis A: General*. 173(2), 259-271.

[49] Thomas J.M. & Thomas W.J. (1997). *Principles and Practice of Heterogeneous Catalysis*. New York: VCH

[50] Carnevillier C., Epron F. & Marecot P. (2004). Controlled preparation and characterization of plurimetallic Pt–Sn and Pt–Ir–Sn/Al2O3 reforming catalysts. *Applied Catalysis A: General*. 275(1-2), 25–33.

[51] Tien P.D., Satoh T., Miura M, & Nomura M. (2005). Efficient and Reusable Palladium Catalysts Supported on Activated Carbon Fibers for Dehydrogenation of Tetrahydronaphthalene. *Energy & Fuels*. 19(3), 731-735.

[52] Koel B. E., Blank D. A. & Carter E. A. (1998). Thermochemistry of the selective dehydrogenation of cyclohexane to benzene on Pt surfaces. *Journal of Molecular Catalysis A: Chemical*. 131(1-3), 39–53.

[53] Moreno-Castilla C., Alvarez-Merino M.A., Lopez-Ramon M.V. & Rivera-Utrilla J. (2004). Cadmium Ion Adsorption on Different Carbon Adsorbents from Aqueous Solutions. Effect of Surface Chemistry, Pore Texture, Ionic Strength, and Dissolved Natural Organic Matter. *Langmuir*. 20(19), 8142-8148.

[54] Mukhopadhyay S., Rothenberg G., Wiener H., Sasson Y., "Solid.solid palladium-catalysed water reduction with zinc : mechanisms of hydrogen generation and direct hydrogen transfer reactions" New J. Chem., 2000, 24, 305-308

[55] Kariya N., Fukuoka A., Utagawa T., Sakuramoto M., Goto Y. & Ichikawa M. (2003). Efficient hydrogen production using cyclohexane and decalin by pulse-spray mode reactor with Pt catalysts. *Appl. Catal. A: General*. 247(2), 247–259.

[56] Grant A. W., Ngo L. T., Stegelman K., & Campbell C. T. (2003). Cyclohexane Dehydrogenation and H2 Adsorption on Pt Particles on ZnO(0001)-O. *J. Phy. Chemistry B*. 107(5), 1180-1188.

[57] Ramos A. L. D., Alves P. S., Aranda D. A.G., Schmal M. (2004). Characterization of carbon supported palladium catalysts: inference of electronic and particle size effects using reaction probes. *Applied Catalysis A: General*. 277(1-8), 71–81.

[58] Gupta A., Harrison I.R. (1997). New Aspects in the Oxidative Stabilization of Pan-based Carbon Fibers: II. *Carbon.* 35(6), 809-818.

[59] Pamula E. & Rouxhet P. G. (2003). Bulk and surface chemical functionalities of type III PAN-based carbon fibres. *Carbon*. 41(10), 1905–1915.

[60] Deki S., Nabika H., Akamatsu K., Mizuhata M. & Kajinami A. (2001). Preparation and Characterization of Metal Nanoparticles Dispersed in Polyacrylonitrile Thin Film. *Scripta Materialia*. 44(8-9), 1879–1882.

[61] Edie D.D. (1998). The Effect of Processing on the Structure and Properties of Carbon Fibers. *Carbon*. 36(4), 345-362.

[62] Shevla G. (1976). Comprehensive Analytical Chem. *(pp. 343)*. Elsevier, Amsterdam.

[63] Ryu Z., Zheng J., Wang M., Zhang B. (2000) Nitrogen Adsorption Studies of PAN-Based Activated Carbon Fibers Prepared by Different Activation Methods. *J. Coll. Interface Sci.* 230, 312–319.